# The *Drosophila* Male Germline During DNA Damage and Aging

**by**

**Kevin L. Lu**

**A dissertation submitted in partial fulfillment**
**of the requirements for the degree of**
**Doctor of Philosophy**
**(Cellular and Molecular Biology)**
**in the University of Michigan**
**2017**

**Doctoral Committee:**

**Professor Yukiko Yamashita, Chair**
**Associate Professor Sundeep Kalantry**
**Associate Professor David Lombard**
**Assistant Professor Jacob L. Mueller**
**Professor Shawn Xu**

Kevin L. Lu

kevinlu@umich.edu

ORCID iD: 0000-0003-2677-9537

# Acknowledgements

To my family and friends who have been by my side during this time. Thank you for your support during the challenges and the victories. I thank my Ph.D. mentor, Yukiko Yamashita, for her guidance and example, whose uncompromising expectations have led to her challenging me and insisting upon my growth as a scientist and a person over the past few years. In addition, all the current and former members of the Yamashita laboratory who have served as the insightful colleagues, willing collaborators, and entertaining company that have made my time completing this dissertation so enjoyable. Lastly, I want to acknowledge all of the previous scientific mentors I have had that have led me to this point, starting from my first research laboratory experience well over a decade ago.

# Table of Contents

# List of Figures

# Abstract

Evolution is thought to drive the progression of populations, conferring advantages through alterations in structure and form. However, the corollary to this theory would dictate that the things that do not change, those which are evolutionarily conserved, would imply some importance to their existence. Though many examples of this type of conserved phenomena have been observed, the underlying purposes for their existence remain poorly explored or understood.

Two ubiquitous features of germ cells in nearly all metazoans are their development as a cyst of interconnected cells and the relative sensitivity of the germline to DNA damage. We show that in the *Drosophila* male germline, cysts of interconnected spermatogonia always die in unison even when only a subset of the cells within display cytologically detectable DNA damage. Our experiments showed that this all-or-none germ cell death depends upon the connectivity between members of a cyst, and is likely based on mitochondrial signals originating from the damaged cells. Interestingly, the relative sensitivity of spermatogonia at any given stage of development correlated to the number of interconnected germ cells contained within the cyst, suggesting that degree of connectivity dictates the robustness with which spermatogonia induce germ cell death in response to insult. This created a model where we propose that perhaps one reason germ cell connectivity has been so strongly conserved is to confer a robust quality control mechanism to germ cells, ensuring the fidelity of genomes that are passed on to the next generation.

Another general feature of nearly all eukaryotic genomes is the organization of the ribosomal RNA genes into highly-transcribed cistrons and large tandem arrays known as the rDNA. In yeast, instability of the rDNA due to its arrangement has been shown to play a central

role in replicative aging, but little was known about its role in higher eukaryotes. We speculated that if similar instability would manifest during aging of multicellular organisms, it would be likely to occur in long-lived, mitotically-active tissue stem cells. We show that germline stem cells exhibit ectopic activation of normally-silent rDNA loci during aging, and germ cells experience a dramatic reduction of rRNA gene copy number on the actively transcribed array. Furthermore, these phenotypes present in the old parents (from abnormal rDNA activation to reduced gene copy number) are heritable and able to be observed in the subsequent generation. Thus our work suggests that there may be a conserved role for dynamicity of the rDNA and rDNA instability during aging.

The work contained in this dissertation attempts to reconcile recurring themes observed in evolution by leveraging the powerful tools of the *Drosophila* model system. The results in the first part offer one possible explanation for why pre-meiotic germ cells are connected to one another, linking it to their well-documented sensitivity to DNA damage and speculating that the driving force behind it all is a desire to increase genomic quality control for gametes. The second half of this dissertation looks at a unique genomic element shared by most eukaryotes, the rDNA, and suggests that this remarkable conservation underlies a more fundamental role in replicative aging in multicellular organisms.

# Chapter 1

# Introduction

## 1.1 Germ cell development in the *Drosophila* testis

### 1.1.1 Germline stem cells

In males of many species (and non-mammalian females), adult gamete production is supported by a germline stem cell (GSC) population which is responsible for populating the germline[1,2]. These stem cell populations must balance self-renewal with differentiation; excessive self-renewal can result in tumorigenesis, whereas differentiation at the expense of self-renewal can result in stem cell depletion and manifest as tissue aging[3]. Most stem cells, including GSCs, reside in a specialized microenvironment (the stem cell niche) that provides extrinsic signals and supports stem cell division and self-renewal[4–6]. Because a combination of cell-intrinsic and cell-extrinsic (niche dependent) factors control stem cell differentiation and self-renewal, it is necessary to study stem cell biology *in situ* in the context of its native tissue.

One of the best-understood populations of stem cells are *Drosophila* adult GSCs, owing to the well-defined cell biology and strong genetic tools of the system. In the *Drosophila* testis, approximately 8-10 GSCs are known to reside in the apical tip adjacent to a cluster of somatic niche cells called the hub[1,2,7] (**Figure 1.1**). The hub provides a source of ligand for JAK-STAT and BMP signaling in GSCs, which are necessary for GSC self-renewal and maintenance[4,5,8]. *Drosophila* male GSCs divide in a characteristically asymmetric manner, where one product of cell division remains attached to the hub and retains its stem cell identity while the other daughter

cell is displaced away and proceeds to differentiate as a gonialblast (GB)[9]. This is achieved by a stereotypical orientation of the GSC centrosomes to a plane perpendicular to the hub during interphase, which results in assembly of the mitotic spindle in a similarly perpendicular plane[10,11].

Beyond their stereotypical asymmetric division, *Drosophila* GSCs also possess another unique feature: delayed cellular abscission. Following GSC mitosis, the GSC and GB remain connected through the next S-phase by a transient ring canal (midbody ring) generated from the contractile ring. A membranous, germline-specific aggregate of endoplasmic reticulum-like vesicles known as the spectrosome runs through this transient ring canal, physically connecting a GSC to its immediate daughter cell[12–16]. These two features of *Drosophila* male GSCs allow the *Drosophila* testis to be an ideal model system for studying the cell biology of stem cells and asymmetric stem cell division.

### 1.1.2 Spermatogonial divisions and spermatogenesis

Following displacement from the niche, the GB undergoes four more transit-amplifying mitoses to produce a 16-cell spermatogonia (SG) cyst (**Figure 1.1**). These transit-amplifying mitoses always occur in synchrony and, like the initial GSC division, results in incomplete cytokinesis[7]. However unlike during GSC division, cellular abscission is never completed and all SG within a cyst remain connected by cytoplasmic bridges throughout all gonial divisions. During these divisions, the spectrosome inherited in the GB proceeds to grow in size and runs through the ring canals of interconnected SG within a cyst, growing into a membranous germline-specific organelle known as the fusome[17].

As the SG divisions occur, growing SG cysts proceed down the length of the testes away from the apical tip[7,18]. What results is the organization of developing SG cysts in a spatiotemporal manner, with GBs the closest gonial cells to the somatic hub and the 16-SG cysts the furthest.

Developing spermatogonia are encapsulated by non-dividing somatic cyst cells, which expand with the growing cyst and provide a source of extrinsic signals that control germ cell differentiation and division[5,19,20]. The gonial divisions proceed at a consistent rate, and the process of SG transit-amplification takes approximately 4-5 days. Transit-amplifying divisions are eventually repressed by germ cell autonomous expression of the genes *bag-of-marbles* (*bam*) and *benign gonial cell neoplasm* (*bgcn*)[21].

Following the last transit-amplifying division, a 16-cell SG cyst is produced. Soon thereafter, the 16-cell SG cyst becomes primary spermatocytes (SCs), which are morphologically distinguishable by their larger size. Primary spermatocytes initiate an extended period of developmental growth and activation of the spermatocyte transcriptional program before eventually entering meiosis further down the length of the testis[7]. The morphological changes that occur from primary spermatocytes to mature spermatids involve dramatic cellular and nuclear remodeling and have been well-characterized at an ultrastructural and genetic level[7,18,22,23]. Taken together, the *Drosophila* testis provides a powerful and well-defined system for studying all stages of spermatogenesis and germ cell development, from germline stem cells to mature spermatids.

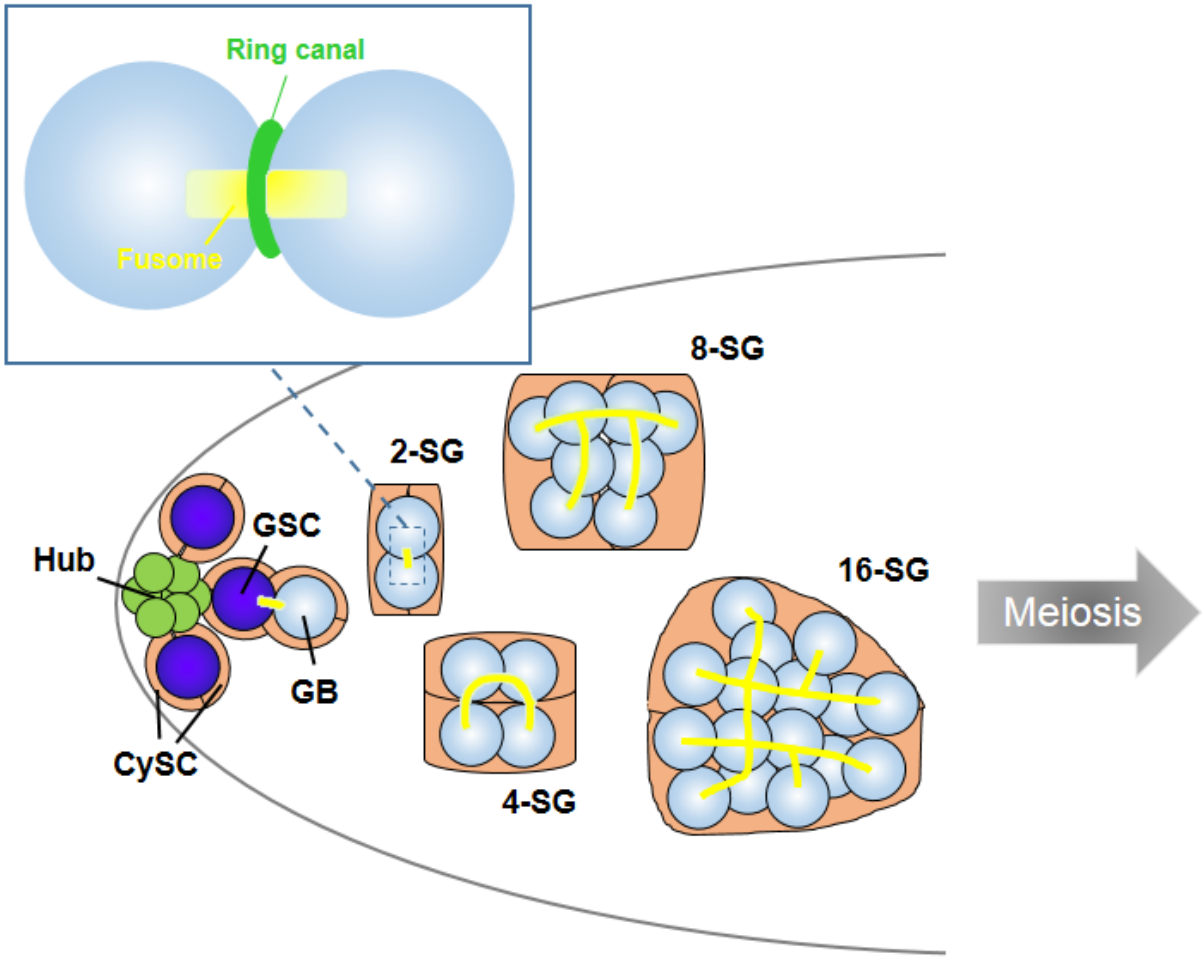


**Figure 1.1.** Model of *Drosophila* spermatogenesis. The apical tip of the testis contains the mitotic region of transit-amplifying germ cells. A germline stem cell (GSC) divides to produce a single-celled gonialblast (GB). The GB proceeds to undergo four more transit-amplifying divisions, finally resulting in a 16-cell spermatogonia cyst (16-SG). Two somatic cyst stem cells (CySC) encase each GSC and grow in size as germ cell cysts expand. The hub is a cluster of somatic cells that act as the stem cell niche, and provides a landmark for spatial identification of the GSCs, which are arranged in a rosette pattern around it.

## 1.2 Germ cell connectivity: a conserved phenomenon*

### 1.2.1 The structure of and mechanisms for achieving germ cell connectivity

As early as the 19th century, cysts of interconnected germ cells were described by biologists of the time including Sertoli (1877) and von Ebner (1878)[24]. Since then, it became evident that stable intercellular bridges connecting the cytoplasm of germ cells is a common feature of developing germ cells in both female and male metazoans[25–27]. The mechanisms that underlie the formation of interconnected germ cell cysts have been intensively investigated.

The structure of germ cell intercellular bridges has been best studied in the *Drosophila* female germline. Much like described in males in the previous section, asymmetric division of germline stem cells (GSCs) produces one self-renewing GSC and one cystoblast, the latter of which proceeds to differentiate. The cystoblast undergoes four mitotic divisions with incomplete cytokinesis, resulting in formation of a cyst with 16 interconnected germ cells[28]. During these mitotic divisions, the contractile ring is stabilized without completely pinching off sister cells. These stabilized contractile rings result in intercellular bridges referred to as ring canals. Ring canals are outlined by the actin cytoskeleton, which grow considerably in size from 0.5 μm to ~10 μm in diameter[29]. The first step in ring canal formation is the appearance of phospho-tyrosine residues along the contractile ring during mitosis[30,31]. The ring canal is initially composed of contractile ring components such as anillin, kinesin MKLP (Pavarotti) and myosin II. As ring canals grow, these initial components disappear, whereas the core components of mature ring canals, such as Hts-RC and Kelch, are loaded onto the ring canals[32–34]. The expansion of ring

*a part of this chapter is submitted for publication as
**Lu KL**, Jensen L, Lei L, Yamashita YM. 2017. Stay connected: A germ cell strategy. *Trends in Genetics.*

canals is critical for oocyte development by allowing for the intercellular transport of cytoplasmic materials.

In the *Drosophila* male germline, four gonial divisions with incomplete cytokinesis yields a cyst of 16 interconnected spermatogonia. Ring canals do not grow in size, likely reflecting the lack of need for the large scale cytoplasmic transport that is observed during oocyte development. Accordingly, male ring canals do not have Hts-RC or Kelch, a critical ring canal component in the female germline. Instead, male ring canals remain associated with contractile ring components such as anillin, septins (Peanut, Sep1, Sep2), and Pavarotti[17,35].

In mammals, germ cells also develop intercellular bridges during gametogenesis in males and females[24,26]. Germ cell intercellular bridges are observed in both fetal mouse ovaries and testes, forming germ cell cysts[24,36,37]. These cysts subsequently fragment in neonatal gonads, resulting in individual primary oocytes or prospermatogonia[38]. In adult testes, germ cells again undergo incomplete cytokinesis through spermatogonial and meiotic divisions, and these spermatogonial populations undergo repeated cycles of cyst fragmentation and branching[39]. The molecular composition of the intercellular bridges in adult testes was revealed by proteomic analysis. Several proteins that are involved in somatic cytokinesis, such as MKLP1, RacGap, SEPT2, SEPT7, SEPT9, and anillin were shown to localize to intercellular bridges in adult mouse testes[40]. Germline-specific components of intercellular bridges were also discovered, such as TEX14 and RBM44[41,42]. TEX14 was identified as a key protein that blocks the cytokinesis machinery containing CEP55, TSG101 and ALIX, thus leading to stable intercellular bridges generated from the contractile ring in germ cells in adult testes[41,43].

As mentioned earlier, in *Drosophila*, ring canals are filled with a membranous organelle called the fusome. The fusome, found in both males and females, is a germline-specific

membranous organelle that is considered to be a derivative of the endoplasmic reticulum[44]. The fusome adopts a branched morphology that runs through all germ cells within a cyst. The core fusome components are Hts-Fus/Adducin-like (a product of the *hu li tai shao* gene, which produces a peptide that is cleaved into Hts-Fus and Hts-RC, a component of ring canals as described above), α- and β-Spectrin, and Ankyrin[45–47].

Fusome-like structures have been observed in germ cells of multiple vertebrate systems, including the *Xenopus* ovary[48] and the dogfish testis[49], suggesting that ring canals and fusomes could be ubiquitous mechanisms for achieving germ cell connectivity. However, EM studies suggest that there may not be a spectrin-rich structure that would be equivalent to a fusome in mouse ovaries[37]. Regardless, it remains possible that germ cells across species utilize alternative means to supplement germ cell connectivity beyond actin-based ring canals/intercellular bridges, much like the role the fusome serves in *Drosophila* and other insects.

| Organism | Known protein components | Diameter | References |
|---|---|---|---|
| **Female Germline** | | | |
| Fruit fly (*Drosophila*) | Actin, Hts-RC, Kelch, Cheerio, Pav-MKLP, Tec29, mucin-D, myosin II, Cindr, Anillin | 0.5-10 μm (with an inner and outer rim) | 29–34,50–56 |
| Mouse (*Mus musculus*) | TEX14, MKLP1 | 0.5-1 μm | 37,57 |
| Frog (*Xenopus*) | Actin, Hts-RC, Kelch | 0.5-1 μm | 48 |
| Mammals (Humans, rabbits, rats, etc.) | Actin | 0.5-1 μm | 58,59 |
| **Male Germline** | | | |
| Fruit fly (*Drosophila*) | Anillin, Cindr, septins, Pav-MKLP, pTyr, mucin-D | 1-2 μm | 17,35,53,60–62 |
| Mouse (*Mus musculus*) | Actin, TEX14, MKLP1, CEP55, RBM44, Anillin, septins, RacGap | 1-2 μm | 24,26,40–43 |
| Mammals (Humans, rats, squirrels, etc.) | Actin | 1-2 μm | 25,63–66 |

**Table 1.1 Known components of germ cell intercellular bridges in various species.**

Provided above is a list of proteins known to be associated with germ cell intercellular bridges or involved in their formation. Species listed were selected based on amount of information available and potential interest in terms of biological relevance. Note that not much investigation has been done in human germ cells.

### 1.2.2 Functions of germ cell connectivity

The purpose for germ cell connectivity is best understood in meroistic ovaries where a subset of all germ cells are chosen to become oocytes while the remaining germ cells differentiate as supporting nurse cells. In the *Drosophila* ovary, following four mitotic divisions, only one germ cell develops as the oocyte whereas the remaining 15 germ cells become nurse cells. During and soon after the mitotic divisions, a polarity within connected germ cells is set up such that the oocyte can collect materials (e.g. mRNAs and organelles like mitochondria and centrosomes) from nurse cells[67,68]. This large-scale cytoplasmic trafficking into the oocyte is referred to as the "oocyte nursing mechanism," and depends upon the stable intercellular bridges between members of a germ cell cyst. Failure to set up this cyst polarity or in early transport of oocyte fate determinant(s) results in defective oocyte specification, leading to 16 nurse cells and no oocyte. Even if oocyte fate is correctly specified, later defects in transporting nurse cell contents into oocyte results in defective oocyte growth, leading to underdeveloped oocytes and thus sterility. Ring canals normally grow from <1 μm to 10 μm in preparation for oocyte nursing, and inhibition of the expansion of mature ring canals results in sterility[29].

Recent studies have demonstrated that fetal mouse ovaries also follow similar processes, where some germ cells function as nurse cells to donate their cytoplasm to their sister cells that will develop into oocytes[69]. The function of intercellular bridges in allowing cytoplasmic transport during mammalian oocyte differentiation was initially suggested by studies using EM. Organelles such as mitochondria, ER and free ribosomes were found within the bridge in rabbit and mouse fetal ovaries[37,58,70]. A recent study of lineage-labeled sister cyst cells further revealed that organelles (centrosomes, Golgi complexes and mitochondria) redistribute extensively within germline cysts during mouse oocyte differentiation. In the neonatal mouse ovary, cysts fragment

into individual germ cells after cytoplasmic transport/enrichment occurs and the individual cells that inherited a Balbiani body (B-body) become the primary oocytes. The germ cells that lack a B-body undergo apoptosis. When cytoplasmic transport was blocked by inhibitors of microtubule polymerization or dynein in in vitro cultured mouse fetal ovaries, primary oocytes contain less cytoplasm and are defective in their ability to develop into later stage oocytes[69].

The fusome in *Drosophila* and other insects connecting germ cells likely plays a different and complementary role to the connectivity achieved by ring canals. One likely function of the fusome is to facilitate and enhance communication among germ cells within a cyst, beyond what would be achieved through undirected cytoplasmic diffusion via ring canals. In the *Drosophila* ovary, the fusome is known to associate with cell cycle regulators (Cyclin A, B, E, Cdk1, and cyclin degradation factors)[71–74], and loss of the fusome results in disruption of the characteristic cell cycle synchronization within the cyst. These results show that the fusome plays a critical role in facilitating the sharing of specific information among the germ cells within a cyst. At the same time, the fusome likely also acts as a selective barrier that plugs the ring canals to prevent the ubiquitous sharing of cytoplasmic contents between germ cells, including organelles. For example, mitochondria and centrosomes move from nurse cells to the oocyte only after the fusome disintegrates[75,76]. Exactly what is shared between germ cells via ring canals as opposed to the fusome (and vice versa) has not been comprehensively established, and remains an intriguing topic of research.

Our knowledge regarding the function of germ cell connectivity has been framed around the idea of a "nursing mechanism" carried out by nurse cells to nurture developing oocytes. However, germ cell connectivity has been conserved in biological contexts where a nursing mechanism does not apply, like in panoistic ovaries (where all germ cells become oocytes without

the development of any nurse cells) or in the male germline (where all germ cells become mature sperm). In the male germline it has been proposed that germ cell connectivity allows for genotypically haploid post-meiotic spermatids to remain phenotypically diploid, particularly in the context of sex chromosome gene products[77]. Nevertheless, this does not explain the existence and conservation of extensive germ cell connectivity in pre-meiotic diploid spermatogonia.

### 1.2.3 The phylogenetic evolution of intercellular connectivity

As mentioned above, there are contexts in which germ cell connectivity exists where oocyte nursing is non-existent, suggesting that connectivity may have evolved for even more fundamental purposes. Primitive insects such as grasshoppers, cockroaches, and stoneflies have panoistic ovaries where all germ cells develop as oocytes without ever developing nurse cells. This implies that oocyte development does not always require intercellular bridges to aid cytoplasmic transport from nurse cells. Yet curiously, in several species with panoistic ovaries, mitotic germ cells are interconnected with cytoplasmic bridges, followed by separation of individual germ cells, each of which becomes an oocyte[78–80].

These observations clearly point to the possibility that germ cell cytoplasmic connectivity might have more functions beyond 'oocyte nursing'. Although no comprehensive effort has been made to determine when germ cell connectivity arose during evolution, there are several examples where researchers have described germ cell connectivity in diverse species, including early-diverging animals such as Cnidarians, Ctenophores, and Poriferans. In hydra (belonging to Cnidaria), germ cells are connected both in spermatogenesis and oogenesis, and the utilization of a nurse cell mechanism during oocyte development already makes an appearance[81,82]. In Poriferans (e.g. sponges, calcarea), germ cells are often generated from somatic cells. However, when they

undergo gametogenesis, it appears that post-meiotic spermatids are connected by cytoplasmic bridges without evidence for connectivity in earlier spermatogonial stages[83,84], an observation consistent with the hypothesis that male germ cells need to complement their haploid genome by connectivity[77].

Interestingly, evidence of mitotic cell interconnectivity goes back possibly before the emergence of metazoans. Choanoflagellates are believed to be the closest relative of animals, diverging over 760 million years ago[85]. During their life cycle, they alternate between a unicellular phase as swimming cells and a colony-forming phase. During the colony-forming phase of the choanoflagellate *S. rosetta*, a single cell undergoes multiple rounds of cell divisions with incomplete cytokinesis, leading to the formation of a colony of up to ~50 cells[86,87]. It was shown that cells within the colony are connected by intercellular bridges, although it remains entirely unknown what purposes these bridges may serve. However, this suggests that stable intercellular bridges connecting mitotic cells emerged fairly early during evolution, likely predating the emergence of metazoans and before the evolution of an oocyte nursing mechanism. This makes the near-ubiquitous evolutionary conservation of cellular connectivity in germ cells (but not most somatic cells) even more mysterious.

## 1.3 Ribosomal DNA: a unique genomic element

### 1.3.1 Structure and maintenance of the ribosomal DNA

Ribosomal RNA (rRNA) genes encode for the RNA component of mature ribosomes, and are present in hundreds of copies arranged in tandem arrays on the eukaryotic chromosome that can span megabases in length[88,89]. These arrays of rRNA genes are referred to collectively as the ribosomal DNA (rDNA), and its transcription is responsible for the organization of the nucleolus

where mature ribosomes are assembled within the nucleus[90–92]. The number of rDNA arrays and their chromosomal locations vary across species. For example, in humans the rDNA arrays are located on the short arms of all the acrocentric chromosomes[93,94], and in *Drosophila* they are found adjacent to the centromere on the sex chromosomes[95–97] (**Figure 1.2**). The presence of hundreds of copies of rRNA genes is thought to be reflective of the cellular requirement for rRNA and ribosome synthesis, reflecting over 50-80% of the cell's total transcription[98]. In *Saccharomyces cerevisiae*, a single rRNA gene unit consists of a cistronic 35S rRNA transcript transcribed by RNA polymerase I from which the 18S, 5.8S, and 28S rRNAs are processed and cleaved[99,100]. The arrangement of the rDNA into similar tandem cistrons is almost ubiquitously conserved in higher eukaryotes like *Drosophila* and mammals, where the 45S precursor rRNA is cleaved and processed into equivalent mature 18S, 5.8S, and 28S rRNAs[89,101]. In addition to the coding rRNA genes, the rDNA also contains various genomic spacers that may have non-ribosomal functions. Within an rRNA gene, the coding regions are separated by internal transcribed spacers (ITS) that separate the mature rRNA ORFs as well as external transcribed spacers (ETS) that contain the rRNA promoter. In addition, individual rRNA genes within the rDNA array are separated by intergenic spacers (IGS) that vary in length[88,102] (**Figure 1.2**).

The coding region of the mature rRNA genes demonstrate remarkable sequence conservation, with human and mouse 18S rRNA showing a divergence rate of only 0.1-1%[103]. This is thought to be a result of exceedingly high selective pressure on these coding regions relating to their roles in mature ribosomes bridging interactions with proteins, mRNA, and tRNA[102], though evolutionary studies have been understandably difficult. While the structure of the rDNA array and the coding regions are highly conserved across all eukaryotes, the noncoding portions of the rDNA (the IGS, ETSs, ITSs, and promoters) evolve and diverge rapidly. In fact, it has been shown

that mouse and human rDNA and Pol I transcriptional machinery are incompatible[104,105]. And even within closely related *Drosophila* species, spacer regions diverge greatly in sequence, size, and arrangement[106]. Recently, synthetic biology experiments have shown that replacing just the internal transcribed spacer (while leaving the original coding regions) of *S. cerevisiae* with that of two other yeast species, *Schizosaccharomyces pombe* or *Candida albicans*, is lethal[107]. All of this is suggestive of an essential and ubiquitous role for the genomic arrangement of the rDNA, and possible species-specific (or other as-yet-unknown) roles for the noncoding regions contained within.

In *S. cerevisiae*, replication of the rDNA array is tightly intertwined with its maintenance. Because the rRNA genes are among the most highly transcribed in the genome and are not shut off during S-phase, a replication fork block protein, Fob1, is critical for blocking expansion of a replication fork to prevent collision with oncoming transcriptional machinery[108,109]. In addition to acting to reduce replication-transcription conflicts by blocking bidirectional expansion of replication forks, Fob1 also plays an active role in maintenance of the rDNA array. Fob1 binding causes DNA double strand breaks at stalled replication forks, and are repaired by unequal sister chromatid exchange resulting in gene copy number expansion on one sister chromatid[110–113]. The evolutionarily-conserved *SIR2* was also shown to play a role in this process[114]. This mechanism is critical in yeast for rDNA amplification and maintenance over successive replicative cycles. Evidence for a replication fork barrier in rDNA was recently identified in human cells[115], suggesting the potential for conservation of this mode of rDNA maintenance and amplification in higher eukaryotes.

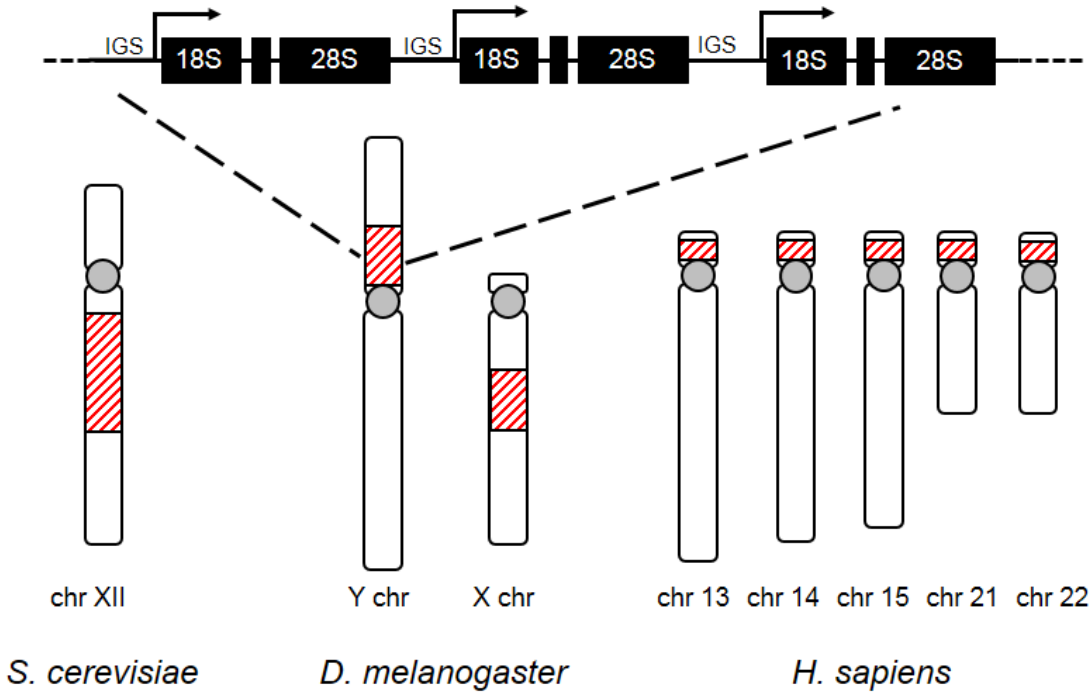


**Figure 1.2.** Diagram of the arrangement of the coding regions for the 45S rRNA genes and the intergenic spacers (IGS). Spacers can consist of duplications of various lengths, and can vary in total size between each rRNA gene repeat. Chromosomal locations of the rDNA arrays (red bands) in *S. cerevisiae*, *D. melanogaster*, and humans.

### 1.3.2 Silencing of rDNA and nucleolar dominance

The rDNA is typically present in excess numbers, and in fact it has been shown that usually less than half of the normal rRNA gene copy number is enough to support cell or organismal viability[116–118]. Because rRNA genes are typically present in hundreds of copies in the eukaryotic genome and make up the bulk of cellular transcription, some of the rDNA must be actively silenced to match the metabolic and translational demand of the cell[119]. In addition, its tandem repetitive arrangement makes the rDNA array an inherently unstable part of the genome[120–122], and because of this, proper repression of rRNA genes is thought to be important in maintaining the stability of the rDNA (detailed below).

In mammalian cells, rDNA is silenced by large-scale DNA methylation and heterochromatin-mediated repression by the nucleolar remodeling complex NoRC[123–126]. NoRC components act to recruit DNMT1, DNMT3b, and HDACs to rRNA genes targeted for silencing[125,126]. Intriguingly, the majority of epigenetic modifications for silencing mammalian rDNA is targeted to the promoter region, which is sufficient to repress expression[124]. Accordingly, DNA methylation and histone modification appear to be interdependent processes, where inhibition of histone deacetylation prevents efficient DNA methylation[127]. Deletion of a critical NoRC component in mammals results in loss of heterochromatin, rDNA stability, and premature cellular senescence[125,128]. In *Drosophila*, repression of rDNA is achieved by a combination of heterochromatin-mediated repression and RNA interference. Disruption of either results in rDNA instability and formation of extrachromosomal rDNA circles[129].

A special case of rDNA silencing is known as nucleolar dominance, where entire rDNA arrays on individual chromosomes are actively repressed (as opposed to the silencing which targets individual rRNA genes within an array). In this case, rDNA arrays on some chromosomes are

"dominant," actively transcribed and organizing the nucleolus, while rDNA on other chromosomes is repressed. The phenomenon was first observed almost a hundred years ago in interspecies plant hybrids, where rDNA arrays can contain thousands of rRNA genes and their active transcription appears as secondary constrictions on chromosome spreads. It was noted when crossing two closely-related species within a plant genus that the resulting hybrid progeny only contained secondary constrictions from one set of parental chromosomes[130]. Since then, nucleolar dominance has been described in interspecies hybrids of multiple plant species, where it has been best studied[131–133]. In plants, both nucleolar dominance between interspecies hybrids and control of normal rRNA transcription levels (in non-hybrids) are accomplished by extensions of the same mechanisms, extensive DNA methylation and HDAC-mediated histone modifications[133–136]. These observations demonstrated that a clear hierarchy for species-specific rDNA exists in hybrids, but what remains unknown is why this is the case or how such large-scale, selective chromosomal repression is achieved.

Nucleolar dominance between interspecies hybrids is not restricted to just plants, and appears to be the rule rather than the exception. In hybrid progeny from *Drosophila melanogaster* and *Drosophila simulans*, it was found that the *D. melanogaster* rDNA was always active while the *D. simulans* rDNA was silenced[137]. Likewise, interspecies hybrids of *Xenopus* also demonstrate nucleolar dominance[138]. Interspecies nucleolar dominance may also extend to hybrids from separate genuses as well, as human-mouse hybrid cell lines appear to express rRNA from only one species[139,140]. However, the meaning behind and/or purpose for interspecies nucleolar dominance is still mostly unclear, as it seems it may be dispensable without necessarily compromising hybrid viability. In *Drosophila* interspecies crosses, if the *D. melanogaster* rDNA was lost (along with

the chromosome containing it), then the normally-inactive *D. simulans* rDNA is able to begin expressing, suggesting that it can be used to support hybrid viability if needed[137].

Fascinatingly, even within a species, silencing of rDNA may extend beyond just the silencing of individual rRNA genes within an array to large-scale silencing of entire chromosomal arrays in a phenomenon that could be considered nucleolar dominance. It has long been documented in humans that different cell types have different numbers of nucleoli, which likely reflects their different translational demands. In fact, within each cell type, the number of rDNA arrays that appear transcriptionally active based on silver staining and secondary constrictions is variable, reflecting complete inactivation of arrays on specific chromosomes[141,142]. Whether or not a specific hierarchy of chromosomal rDNA arrays exists like in interspecies hybrids has not been determined. In *Drosophila melanogaster*, however, the hierarchy of nucleolar dominance has been easier to establish owing to the fact that only two rDNA arrays exist, one on each of the sex chromosomes[95–97]. Through cytogenetic mapping, transcription-dependent incorporation of H3.3, and assessment of relative transcript levels all in larval brains, it was shown that rDNA from the Y chromosome is active in males and the X chromosome is inactive[143,144].

### 1.3.3 Links between ribosomal DNA biology and aging

As mentioned above, disrupting repression of the rDNA and inducing array instability results in cellular senescence[125,128]. In fact, the highly repetitive, tandem arrangement of rRNA genes makes the rDNA array one of the most unstable regions in the genome, prone to homologous recombination and replication mishaps over time[121]. To this end, the links between the biology of rDNA and replicative aging (the number of divisions a cell has gone through) are strong, and were first established in the budding yeast *Saccharomyces cerevisiae*[145,146].

In budding yeast, cell division is asymmetric and characterized by a smaller daughter cell budding off of a larger mother cell. The mother cell's replicative lifespan is finite and results in only ~20-30 daughter cells, but the daughter cells generated from these mothers almost always begin with a renewed replicative lifespan[147,148]. It was initially shown that as mother cells advance in replicative age, their nucleoli undergo drastic morphological changes that reflect underlying instability in the rDNA, resulting in intrachromosomal recombination that generates extrachromosomal rDNA circles (ERCs)[149]. ERCs are asymmetrically retained in the mother cell in a septin/nuclear pore dependent manner, potentially explaining the asymmetric partitioning of replicative age between mother and daughter[149,150]. Importantly, introduction of an artificial ERC with an ARS significantly reduced replicative lifespan[149]. Following the initial discovery of ERCs in aging yeast, many studies of mutants have found a correlation between perturbation of nucleolar morphology, accumulation of ERCs, and replicative senescence[146,151,152]. Notably, these studies also resulted in the discovery of the role of the evolutionarily-conserved histone deacetylase *SIR2* in aging, which acts in part by repressing rDNA recombination, suppressing ERC formation, and extending replicative lifespan[153–155]. ERCs have also been detected in multiple higher eukaryotes including *Drosophila* and human cells, but their role in aging in those organisms has not been

carefully tested[156,157]. Nonetheless, these studies provided the basis for the "ERC theory of aging" in yeast as the rDNA-based determinant of lifespan, and suggested the potential for a universal link between rDNA and aging in other organisms.

An alternative theory, the "rDNA theory of aging," arose as an evolution of and alternative viewpoint to the "ERC theory of aging"[145]. It proposes that underlying instability of the rDNA itself is the source of replicative aging in yeast, and that ERCs are a consequence of that rather than causal. There are several lines of evidence that suggest this theory may more accurately reflect the underlying rDNA biology. First, some mutants that result in increased rDNA recombination and decreased lifespan do not produce an increase in ERCs, best exemplified by the RNA pol II complex *hpr1Δ* mutant[158]. Conversely, in yeast *sgs1* mutants that are known to result in perturbed nucleolar morphology, ERC formation, and reduced lifespan, expression of the human homolog *BLM* helicase gene restored lifespan without reducing ERC levels[159]. When the rDNA replication origin was mutated to impair initiation, ERC production was reduced but replicative lifespan was also reduced[160]. Lastly, elegant work by the Amon lab showed that activation of the meiotic program during sporulation resets replicative age, and that inducible expression of a meiotic transcription factor, Ndt80, could extend lifespan in both young and old vegetative cells[161]. However, ERC levels were the same in old cells with and without lifespan extension by *NDT80* expression, suggesting that merely the cellular presence of ERCs is not sufficient for inducing cellular senescence. Regardless of the "ERC theory" versus the "rDNA theory," the evidence for changes in rDNA playing a role in aging of yeast is unequivocal.

Additionally, evidence has emerged that links the rDNA to other well-studied and evolutionarily-conserved aging pathways, including dietary restriction and TOR signaling. It was noted that dietary restriction and rapamycin inhibition of the TOR pathway in yeast, both known

to extend lifespan, result in nucleolar changes[162,163]. Mechanistically, it was shown that dietary restriction and TOR inhibition acts at least partially through recruitment of Sir2 to the rDNA, decreasing rDNA instability[163–166]. Because the role that dietary restriction and TOR signaling play in aging has been conserved from yeast to higher eukaryotes[146,167,168], it stands to reason that some of the intertwined rDNA biology during aging may have been conserved as well.

## 1.4 Summary and aims of dissertation

The evolutionary conservation of a phenomenon implies a fundamental meaning for it that merits conservation in the first place. However, the underlying meanings of many such phenomena have remained poorly explored or understood. Outlined above are excellent examples of two such phenomena: evolutionary conservation of germ cell connectivity and the genomic organization of the rDNA.

The mechanisms by which germ cells are connected via stable intercellular bridges have been well-studied over the past five decades. We now know many of the molecular components of bridges in the *Drosophila* and mouse germlines, including a few germline-specific proteins and accessory means of achieving connectivity like the fusome. However, our understanding of why germ cell connectivity exists in the first place is framed around the idea of oocyte nursing, which is not applicable in females of some species or in all males. The first half of my thesis was motivated by a surprising discovery in the *Drosophila* male germline (detailed in subsequent chapters), and led to the hypothesis that germ cell connectivity might serve to enhance DNA damage sensitivity in the germline versus the soma.

The conservation of the arrangement of rRNA genes into similar cistronic units and on a larger scale into rDNA arrays is striking across almost all eukaryotic organisms. This structure and

its transcriptional activity is what leads to genomic instability in yeast, and I hypothesized that comparable challenges could be encountered in the rDNA of higher eukaryotes during aging. Specifically, my hypothesis was that male germline stem cells (GSCs) in *Drosophila*, which continuously divide asymmetrically, would undergo rDNA-related changes during aging like what was observed in asymmetrically-dividing budding yeast. The second goal of my thesis was to determine whether these changes occurred, and characterize them if they were.

Studies that aim to understand the underlying design of nature can be broadly separated into wanting to know "how" a phenomenon is achieved and "why" it exists in the first place. The former is descriptive and evidence is direct, whereas the latter is more difficult because evidence can be indirect and often must be inferred. The goal of the experiments in this dissertation sought to leverage the power of the *Drosophila* testis system to test the aforementioned hypotheses: 1) understand the sensitivity of the germline to direct DNA damage and if/how germ cell connectivity plays a role and 2) determine whether changes in rDNA occur during replicative aging of GSCs and the germ cells they produce. However, the overarching idea that ties together these distant topics is the act of attempting to understand the design of nature through the lens of evolutionary hints. Though conservation of the features of the rDNA between species is obvious, it was not known "how" (or if) rDNA is involved in aging of multicellular organisms. On the other hand, though much is known about "how" germ cell connectivity is achieved in many species, obvious gaps exist in our understanding of "why" this is in the first place. What resulted from this dissertation is, hopefully, a better understanding of what occurs in the germline in response to various insults, be it direct DNA damage or aging.

# Chapter 2

# Materials and Methods

This chapter provides information on the materials and methods used in chapters 3 and 4. Protocols are presented roughly in the order in which they will appear in later chapters.

## 2.1 Germ cell death protocols

**Fly husbandry and strains:**

All fly stocks were raised on standard Bloomington medium at 25°C, and young flies (0 to 2-day old adults) were used for all experiments unless otherwise noted. The following fly stocks were used: *hts*$^{01103}$ [14], *nos-gal4* [169], UAS-✔*-spectrin*$^{RNAi}$ (TRiP.HMC04371), *c587-gal4* [19], UAS-*Diap1, EndoG*$^{MB07150}$ [170] (obtained from the Bloomington Stock Center), *p53*$^{5A-1-4}$ [171,172], Df(2R)BSC26, Df(3R)ED6096, Df(2L)Exel7077, Df(3R)BSC699 (obtained from the Bloomington Stock Center), *p53RE-GFP-nls* reporter [173] (a gift of John Abrams, University of Texas Southwestern Medical Center), *Omi*$^{\Delta 1}$, *Omi*$^{Df1}$ [174,175] (a gift of Eli Arama, Weizmann Institute of Science), *mnk*$^{6006}$ [176] (a gift of William Theurkauf, University of Massachusetts Medical School), Ubi-Pavarotti-GFP [52] (a gift of David Glover, University of Cambridge).

**Immunofluorescence staining and microscopy:**

Immunofluorescence staining of testes was performed as described previously [177]. Briefly, testes were dissected in PBS, transferred to 4% formaldehyde in PBS and fixed for 30 minutes.

Testes were then washed in PBS-T (PBS containing 0.1% Triton-X) for at least 60 minutes, followed by incubation with primary antibody in 3% bovine serum albumin (BSA) in PBS-T at 4°C overnight. Samples were washed for 60 minutes (three 20-minute washes) in PBS-T, incubated with secondary antibody in 3% BSA in PBS-T at 4°C overnight, washed as above, and mounted in VECTASHIELD with DAPI (Vector Labs). The following primary antibodies were used: mouse anti-Adducin-like 1B1 (*hu-li tai shao* – Fly Base) [1:20; Developmental Studies Hybridoma Bank (DSHB); developed by H.D. Lipshitz]; mouse anti-alpha-spectrin 3A9 (1:20; DSHB; developed by R. Dubreuil, T. Byers); rat anti-vasa (1:50; DSHB; developed by A. Spradling), rabbit anti-vasa (1:200; d-26; Santa Cruz Biotechnology), mouse anti-Fasciclin III (1:200; DSHB; developed by C. Goodman), anti-LaminDm0 (1:200; DSHB; developed by P. A. Fisher), rabbit anti-γ-H2AvD pS137 (1:100;Rockland), rabbit anti-Mnk (1:100; courtesy of Saeko Takada), rabbit anti-Cleaved Drosophila Dcp-1 (Asp216) (1:200; Cell Signaling Technology). Images were taken using a Leica TCS SP8 confocal microscope with 63x oil-immersion objectives (NA=1.4) and processed using Adobe Photoshop software. For detection of germ cell death, testes were stained with Lysotracker Red DND-99 in PBS (1:1000) for 30 minutes prior to formaldehyde fixation. Stages (GB, 2-, 4-, 8-, and 16-SGs) of dying SGs were identified by counting the number of nuclei within the cyst visualized by Lamin Dm0 and DAPI [178]. Note that the number of 'stageable' dying SGs underrepresents the total population of dying SGs, because nuclear structures disintegrate during later phases of cell death, making it impossible to count the number of SGs within a dying cyst [178]. Such 'unstageable' SGs were not included in the scoring in this study.

For observation of unfixed samples, testes were dissected directly into PBS and incubated in the dark with the desired dyes for 5 minutes, mounted on slides with PBS and imaged within 10

minutes of dissection. The dyes used in live imaging are: Lysotracker Red DND-99 (1:200) or Lysotracker Green DND-26 (1:200) (Thermo Fisher Scientific), Hoechst 33342 (1:200), and FM4-64FX in PBS (1:200) (Thermo Fisher Scientific). SG stage (2-, 4-, 8-, or 16-SG) was assessed by number of Hoechst-stained nuclei. Note that the scoring of dying SGs is not directly comparable between fixed and unfixed samples (for example, results shown in Fig. 1 vs. Fig. 2), due to the difference in the method of SG staging and timing.

**Ionizing radiation**

For radiation doses of 25-250 rad, a $^{137}$Cs source was used with a dose rate of approximately 100 rad per minute. Additionally, for radiation doses 100 rad and above, a Philips RT250 model or Kimtron Medical IC-320 orthovoltage unit was used (dose rates of 200 and 400 rad per minute respectively). Dosimetry was carried out using an ionization chamber connected to an electrometer system directly traceable to National Institute of Standards and Technology calibration. The relative biological effectiveness of $^{137}$Cs and x-ray sources is comparable at lower doses [179], and experiments were repeated with both sources for 100-250 rad, which yielded essentially the same results irrespective of radiation source.

**TUNEL Assay**

Larval heads with imaginal discs attached were dissected from third instar larvae into PBS, then fixed in 4% formaldehyde in PBS for 30 minutes. Samples were then washed in PBS-T (PBS containing 0.1% Triton-X) for at least 20 minutes, transferred to 100% methanol for 6 minutes with rocking, and washed again for at least 20 minutes in PBS-T. TUNEL assay was then carried out according to manufacturer's instructions using a Millipore ApopTag Red *In Situ* Apoptosis

Detection Kit (S7165). Following washes with PBS-T for 20 minutes, wing imaginal discs were dissected from larval heads and mounted in VECTASHIELD with DAPI (Vector Labs).

**Dose-response best fit regressions**

Best fit functions and lines for radiation dose-cell death response curves were generated by using GraphPad Prism 7 and the means-only values at all doses. Non-linear regressions were determined using a four-parameter logistic curve with no constraints on bottom, top, or hillslope and >1500 iterations. Standard linear regression was performed using cell death as a function of radiation dose. Goodness of fit, unadjusted $R^2$ value, was determined by 1.0 less the ratio of the regression sum of squares to the total sum of squares, $1 - SS_{reg}/SS_{tot.}$

**Statistics for comparison of 16-SG death distributions**

Distribution of number of dying SGs per 16-SG cyst between mutant and control conditions at every dose of radiation were compared using a 2x3 Pearson's chi-squared test. Data were transformed into three categories: 0 SGs dying, all 16 SGs dying, or 1-15 (partial cyst) SGs dying.

## 2.2 rDNA and nucleolar fragmentation protocols

**Fly husbandry and strains:**

All fly stocks were raised on standard Bloomington medium at 25°C. Unless otherwise stated, flies used for wild-type experiments were the standard lab wild-type strain *yw* ($y^1$ $w^1$). C(1)RM/C(1;Y)6, $y^1w^1f^1$/0 (Bloomington Stock Center, #9460), FM6/C(1)DX, $y^*f^1$ (Bloomington Stock Center, #784)[180], Df(YS)*bb*/$w^1sn^1bb^*$/C(1)RM, $y^1v^1f^1$ (Bloomington Stock Center, #4491). Nopp140-GFP[181] (a gift of Pat DiMario, Louisiana State University).

**Immunofluorescence staining and microscopy:**

Immunofluorescence staining of testes was performed as described previously [177]. Briefly, testes were dissected in PBS, transferred to 4% formaldehyde in PBS and fixed for 30 minutes. Testes were then washed in PBS-T (PBS containing 0.1% Triton-X) for at least 60 minutes, followed by incubation with primary antibody in 3% bovine serum albumin (BSA) in PBS-T at 4°C overnight. Samples were washed for 60 minutes (three 20-minute washes) in PBS-T, incubated with secondary antibody in 3% BSA in PBS-T at 4°C overnight, washed as above, and mounted in VECTASHIELD with DAPI (Vector Labs). The following primary antibodies were used: mouse anti-Adducin-like 1B1 (*hu-li tai shao* – Fly Base) [1:20; Developmental Studies Hybridoma Bank (DSHB); developed by H.D. Lipshitz]; rat anti-vasa (1:20; DSHB; developed by A. Spradling), rabbit anti-vasa (1:200; d-26; Santa Cruz Biotechnology), mouse anti-Fasciclin III (1:200; DSHB; developed by C. Goodman), rabbit anti-fibrillarin (1:200; Abcam ab5821), mouse anti-fibrillarin (1:200; Abcam [38F3] ab4566), rabbit anti-H3K9 dimethyl (1:100; Abcam [Y49] ab32521). Images were taken using a Leica TCS SP8 confocal microscope with 63x oil-immersion objectives (NA=1.4) and processed using Adobe Photoshop software.

**DNA fluorescence *in situ* hybridization**

Testes were prepared as in above, and optional immunofluorescence staining protocol was carried out first. Subsequently, fixed samples were incubated with 2 mg/ml RNase A solution at 37°C for 10 minutes, then subsequently washed with PBS-T+1mM EDTA. Subsequently, samples were washed in 2xSSC-T (2xSSC containing 0.1% Tween-20) containing increasing formamide concentrations (20%, 40%, then 50% formamide) for 15 minutes apiece. Hybridization buffer (50% formamide, 10% dextran sulfate, 2x SSC, 1mM EDTA, 1 μM probe) was added to washed samples, denatured at 91°C for 2 minutes, then incubated overnight at 37°C. Probes used included

$(AATAAAC)_6$-Cy5 for detection of the Y chromosome and CCACATTTTGCAAATTTTGATGACCCCCCTCCTTACAAAAAATGCG-Cy3 for detection of the X chromosome.

**Determination of X and Y chromosome SNPs**

The X chromosome was isolated by crossing experimental XY males with C(1)RM females, generating X/O males lacking the Y chromosome (and the Y rDNA). The Y chromosome rDNA was isolated by crossing experimental XY males with C(1)DX/Y females, which generated C(1)DX/Y females containing our experimental Y (and no rDNA on the compound X chromosome). 45S rRNA genes were sequenced using the following primers to identify single nucleotide variants between the two consensus sequences:

| **Name** | **5'-Sequence-3'** |
|---|---|
| ITS sequencing-F | CTTGCGTGTTACGGTTGTTTC |
| ITS sequencing-R | ACAGCATGGACTGCGATATG |
| 18S sequencing-F | GAAACGGCTACCACATCTAAGG |
| 18S sequencing-R | GGACCTCTCGGTCTAGGAAATA |
| 28S sequencing-F | AGCCCGATGAACCTGAATATC |
| 28S sequencing-R | CATGCTCTTCTAGCCCATCTAC |

Sequence alignment was done using ClustalW2.

**RNA fluorescence *in situ* hybridization**

For RNA FISH, all solutions used are RNase-free. Testes were collected in PBS and fixed in 4% formaldehyde in PBS for 30 minutes. Then testes were washed briefly in PBS, and permeabilized in 70% ethanol overnight at 4°C. Following overnight permeabilization, testes were briefly rinsed in 2xSSC with 10% formamide. Hybridization buffer (prepared according to protocol by LGB Biosearch for Stellaris probes) was prepared with probe (50 nM final concentration) and incubated overnight at 37°C. Following hybridization, samples were washed

twice in 2x SSC with 10% formamide for 30 minutes each and mounted in VECTASHIELD with DAPI (Vector Labs). Sequences of Stellaris probe sets used to detect R1 and R2 retrotransposons are below:

| **R1 probe#** | **5'-Sequence-3'-570** | **R2 probe #** | **5'-Sequence-3'-670** |
|---|---|---|---|
| 1 | cagatggcttcctgatgatc | 1 | cgcttcagtgatggaatctc |
| 2 | accagacatacgccataatc | 2 | gcagtgaagttgatgcctaa |
| 3 | tgcatcgaactggcagtatg | 3 | cctttgtcaatctttgtagc |
| 4 | atgtaccggaggtacggttc | 4 | aacaacctctgttgtggttt |
| 5 | acatgggggacactgcattc | 5 | gataaggacagtccgaaggg |
| 6 | gctctgtgattatcgaacgt | 6 | ctaacttgtggtagagctgt |
| 7 | cattgacgattgtcacgtcg | 7 | tttttcttaggacgcctatc |
| 8 | atatgtggcccacatagatg | 8 | gccatcttcgcacataatat |
| 9 | gatgttgtggtcactcaatt | 9 | aatgctatcggcacatccag |
| 10 | acaggagctatgctctcaac | 10 | acttttgggggtgcatgaa |
| 11 | aaagttttccggaagttcgg | 11 | acccatcttagtgatggaat |
| 12 | tatgtactatactgcgcagg | 12 | gtcttagccttaacattgga |
| 13 | cgatcgagtcaacttccttc | 13 | ggtgaggccatttaatgtta |
| 14 | cgacgaagtcttcggacttc | 14 | gtttttcggcttcgaggaaa |
| 15 | gaccactacaagctctacag | 15 | ctaataatctatctcgggcc |
| 16 | acgaagcgtttccagtcatc | 16 | cggacgcgataacagttcat |
| 17 | tcggcaaatcttgtagacgc | 17 | ttgttcgcccaatatttttc |
| 18 | aaattgcggaggagcactcg | 18 | accatcaactgagaggtaca |
| 19 | aacctcgaatacttcgaggg | 19 | aaacgcgtgggttgactaac |
| 20 | tgcagatagtgccattgatg | 20 | catatattcctttcctgtta |
| 21 | caatcggatgcatcgggaaa | 21 | tttatccgcagacgaatacc |
| 22 | ctcacacttgtccttatctg | 22 | tacgagactttgtgggtagg |
| 23 | aaattgccatctgcagcctt | 23 | acgacactgtcgttccaatt |
| 24 | cacatcgtccttggcgaaat | 24 | ttgtttcgggagcatcacat |
| 25 | caacactgctcttcacgtgc | 25 | gcatttttgcattatgtggt |
| 26 | tccattcgacgttgtcgaat | 26 | ccgcttgattcgatttacta |
| 27 | ggaactgcttcggatcactg | 27 | gttcaacaatgaccacgcag |
| 28 | tatgcactcagctggcaata | 28 | ccaggtctggtttattaagg |
| 29 | tcgacgagaagcagcaagtc | 29 | atgtgattttgtcgtagtgc |

| | | | |
|---|---|---|---|
| 30 | tagcacagctcgggaatttc | 30 | ctgtcacaatttgtgtgtcg |
| 31 | cacgtttctacgatggacat | 31 | cgcatcatccatagagtgtc |
| 32 | catgattaccgtcttgctgg | 32 | ggtctgtcgtatctattgat |
| 33 | gaaggttcgctccagcaaac | 33 | aatctgcgacgcaattcagt |
| 34 | tgatgccaaggtaccgacag | 34 | cagggtggcagaatggaatt |
| 35 | aggaatttcattccttcact | 35 | tttaacggattgaccactcc |
| 36 | atgagtccgtcatatatggt | 36 | tcatatttgctgaggagacc |
| 37 | caccaaacagcacacaaggt | 37 | cctggacgctaatgatatga |
| 38 | caagcaggattagcctctgg | 38 | aaaacaaccgagactgcctc |
| 39 | actgttcggcataccgaaag | 39 | cgctcaggtacatgaactgt |
| 40 | cgctaataacttagcagcca | 40 | ttagctaagtccaatctcgg |
| 41 | attaaacactcctctaggcg | 41 | gatgttatgccaagacagca |
| 42 | gacgtatgggataaacctat | 42 | ttgcgatgtttatgccttta |
| 43 | gtcctcatcgagaatccaaa | 43 | catcctcatagccatttaat |
| 44 | aatgcattgaacgacccgtg | 44 | cgcaacgcctacgtactaaa |
| 45 | caagcagtggtatcgctgag | 45 | atgcacgattcattgctcta |
| 46 | ctcatatggatctccacatg | 46 | actgtgtgtggtcagttttc |
| 47 | aagatccagttttcgccaag | 47 | gaaagatactaggtctgcca |
| 48 | cgttgagtcttctcttgatc | 48 | tcgcggaggtatggaaatct |

**SNP-FISH**

The protocol for RNA FISH was followed exactly as written above, except for probe concentrations. Final concentration of each SNP probe was 100 nM, and each mask oligo was 300 nM. Sequences of SNP probes and oligos are below:

| **Probe Set** | **5'-Sequence-3'-Quasar 570/670** |
|---|---|
| X SNP1 | AAAAAATACAAGTATTTAATCACATA |
| Y SNP1 | AAAAGATACAAGTATTTAATCACATA |
| SNP1 Mask | TATGTGATTAAATACT |

| | |
|---|---|
| X SNP2 | GTTTCTTCGATTTTCATGTTCGAAAC |
| Y SNP2 | GTTTTTTCGATTTTCATGTTCGAAAC |
| SNP2 Mask | GTTTCGAACATGAAAA |

| | |
|---|---|
| X SNP3 | AAATATTTATTAACGGTAAGGATATT |

| | |
|---|---|
| Y SNP3 | AAATGTTTATTAACGGTAAGGATATT |
| SNP3 Mask | AATATCCTTACCGTTA |

| | |
|---|---|
| X SNP4 | TTAGGCATTTTTGTTTTACTTGAAAA |
| Y SNP4 | TTAGCCATTTTTGTTTTACTTGAAAA |
| SNP4 Mask | TTTTCAAGTAAAACAA |

**EdU incorporation and staining**

Testes were dissected into room temperature Schneider's media for insect cell culture containing 10 nM EdU and incubated for 45 minutes with rocking. Then testes were rinsed with PBS and fixed in 4% formaldehyde for 15 minutes, and afterwards washed 3x with PBS-T for 15 minutes. Primary antibody incubation was carried out as normal. Following overnight antibody incubation, EdU fluorophore conjugation was carried out according to Click-iT Plus EdU imaging kit protocol (Invitrogen, C10640). After EdU fluorophore conjugation, secondary antibody staining was carried out as described earlier.

**qPCR**

Quantitative PCR was carried out using cycling conditions previously described[182] and *Power* SYBR Green reagent (Applied Biosystems). All numbers were normalized to tRNA-K-CTT, a multicopy tRNA gene known to be interspersed throughout the genome, and Gapdh. Primers used are listed below:

| **Primer Name** | **5'-Sequence-3'** | **Reference** |
|---|---|---|
| tRNA-K-CTT-qF | CTAGCTCAGTCGGTAGAGCATGA | [183,184] |
| tRNA-K-CTT-qR | CCAACGTGGGGCTCGAAC | |
| 18S-qF | AGCCTGAGAAACGGCTACCA | [183,184] |
| 18S-qR | AGCTGGGAGTGGGTAATTTACG | |
| 28S-qF | AATGGATGTGATGCCAATGTA | [144] |
| 28S-qR | TTCAGTGGATCGCAGTATGG | |
| 5.8S-qF | GCTCATGGGTCGATGAAGAA | |
| 5.8S-qR | GGACTGCGATATGCGTTCA | |
| Gapdh-qF | TAAATTCGACTCGACTCACGGT | DRSC FlyPrimerBank |

| | | |
|---|---|---|
| Gapdh-qR | CTCCACCACATACTCGGCTC | DRSC FlyPrimerBank |
| R1 qPCR2 fw | TAGAGCTTGTAGTGGTCGAG | |
| R1 qPCR2 rv | ATGGGTCGTCGGCATGATCT | |
| R2 qPCR fw | ATGAACTGTTATCGCGTCCG | |
| R2 qPCR rv | AAACGCGTGGGTTGACTAAC | |

**Mitotic chromosome spreads and fluorescence quantification**

Testes were squashed according to previously described methods[185]. Briefly, testes were dissected into 0.5% sodium citrate for 5-10 minutes and fixed in 45% acetic acid/2.2% formaldehyde for 4-5 minutes. Fixed tissues were firmly squashed with a cover slip then slides were submerged in liquid nitrogen. Following liquid nitrogen, slides were dehydrated in 100% ethanol for at least 5 minutes. Slides were then treated with 0.1 µg/ml RNase A for 1 hour at room temperature, then dehydrated in 100% ethanol again. Hybridization mix (50% formamide, 2x SSC, 10% dextran sulfate) with 100 ng each probe was applied directly to the slide and allowed to hybridize overnight at room temperature. Then slides were washed 3x for 15 minutes in 0.2x SSC, and mounted with VECTASHIELD with DAPI (Vector Labs). Sequences for probes used are below:

| **Probe Target** | **5'-Sequence-3'** |
|---|---|
| Y chromosome | $(AATAAAC)_6$-Cy5 |
| 240-bp IGS | TCCATTCACTAAAATGGCTTTTCTCTATAATACTTA GAGAATATGGGAATATTTCAACATTTTTCACT-Alexa488 |

| **18S rDNA Probe#** | **5'-Sequence-3'-Quasar 570** |
|---|---|
| 1 | tataactactggcaggatcaac |
| 2 | catggcttaatctttgagacaa |
| 3 | tcacttttaattcgtgtgtact |
| 4 | actgatataatgagccttttgc |
| 5 | ctgttaacgatctaaggaacca |

| | |
|---|---|
| 6 | agaattaccacagttatccaag |
| 7 | aggttcatgttttaattgcatg |
| 8 | tagcctaataaaagcacacgtc |
| 9 | aatataacgatcttgcgatcgc |
| 10 | atacgatctgcatgttatctag |
| 11 | acatttgaaagatctgtcgtcg |
| 12 | gtcctagatactaccatcaaaa |
| 13 | gatatgagtcctgtattgttat |
| 14 | agtgtactcattccaattacag |
| 15 | caattggtccttgttaaaggat |
| 16 | ccgcaacaactttaatatacgc |
| 17 | agcacaagttcaactacgaacg |
| 18 | acaattgtaagttgtactaccc |
| 19 | atataagaactccaccggtaat |
| 20 | tgcaggtttttaaataggagga |
| 21 | cccacaataacactcgtttaag |
| 22 | tgctttaagcactctaatttgt |
| 23 | cacagaatattcaggcatttga |
| 24 | cagaacagaggtcttatttcat |
| 25 | cctcttgatctgaaaaccaatg |
| 26 | ccaaactgcttctattaatcat |
| 27 | ttaagttagtcttacgacggtc |
| 28 | aacatctttggcaaatgctttc |
| 29 | ctctaactttcgttcttgatta |
| 30 | tcgtttatggttagaactaggg |
| 31 | gagagagccataaaagtagcta |
| 32 | aattcctttaagtttcagcttt |
| 33 | aatctgtcttacacacttatgt |
| 34 | ccatagattcgagaaagagcta |
| 35 | atcactccacgaactaagaacg |
| 36 | ttcgttatcggaattaaccaga |
| 37 | caccataatcctgaagatatct |
| 38 | gaatgaaggctacataagcttc |
| 39 | acacaataagcattttactgcc |
| 40 | gctccacttacataaacacatt |
| 41 | gtgtccttataatgggacaaac |
| 42 | gcaatttgtccatttaagaagc |
| 43 | ctgttattgctcaatctcatta |
| 44 | ggtctaggaaatacacgttgat |
| 45 | ttcacaatcccaagcatgaaag |
| 46 | gaattccaagttcatcgtgaac |

| | |
|---|---|
| 47 | caatgcgagttaatgactcaca |
| 48 | taattcaatcggtagtagcgac |

Fluorescence quantification was done on merged z-stacks using ImageJ using the Maximum Entropy plugin for automatic thresholding based on the histogram to automatically determine real signal from noise. Using this method, fluorescent probe signal was measured as Integrated Density and compared between the X and Y chromosomes.

**Statistical analysis**

For comparison of nucleolar morphologies, significance was determined by chi-squared test using a 2x3 contingency table (Normal; Deformed; Fragmented). For GSC-GB nucleolar morphologies, a 2x4 contingency table was used (four possible conformations in **Figure 4.2A-D**). For X rDNA activation by SNP-FISH, because X-only transcription was virtually never detected we simplified the comparison to Y-only rRNA vs both X&Y-rRNA and performed t-tests.

# Chapter 3

# Germ Cell Connectivity Enhances Cell Death in Response to DNA Damage in the *Drosophila* Testis*

## 3.1 Abstract

Two broadly known characteristics of germ cells in many organisms are their development as a 'cyst' of interconnected cells and their high sensitivity to DNA damage. Here we provide evidence that in the *Drosophila* testis, connectivity serves as a mechanism that confers to spermatogonia a high sensitivity to DNA damage. We show that all spermatogonia within a cyst die synchronously even when only a subset of them exhibit detectable DNA damage. Mutants of the fusome, an organelle known to facilitate intracyst communication, compromise synchronous spermatogonial death and reduces overall germ cell death following DNA damage. Our data indicate that a death-promoting signal is shared within the cyst, leading to death of the entire cyst. Taken together, we propose that intercellular connectivity supported by the fusome uniquely increases the sensitivity of the germline to DNA damage, thereby protecting the integrity of gamete genomes that are passed on to the next generation.

*this chapter appears in publication as
**Lu KL**, Yamashita YM. 2017. Germ cell connectivity enhances cell death in response to DNA damage in the *Drosophila* testis. *eLife.*

## 3.2 Introduction

A prevalent feature of germ cell development across species is their proliferation as an interconnected cluster of cells, widely known as a germ cell cyst. In many organisms from insects to humans, germ cells divide with incomplete cytokinesis that results in interconnected cells with shared cytoplasm, leading to cyst formation[24,26,186]. During oogenesis of many species from flies to mammals, this intercellular connectivity is critical for the process of oocyte specification, allowing only some of the developing germ cells to become oocytes while the others adopt a supportive role[69,186,187]. For example, in the *Drosophila* ovary, four rounds of germ cell divisions with incomplete cytokinesis results in a cyst of 16 interconnected germ cells, where only one becomes an oocyte while the remaining 15 germ cells become nurse cells. During this process, nurse cells support oocyte development by providing their cytoplasmic contents to oocytes via intercellular trafficking[75,187,188]. In contrast to oogenesis, where cytoplasmic connectivity has a clear developmental role in oocyte development, spermatogenesis is a process where all germ cells within a cyst are considered to be equivalent and become mature gametes[7,189]. Despite the lack of a 'nursing mechanism' during spermatogenesis, intercellular connectivity is widely observed in spermatogenesis in a broad range of organisms[24,189]. While a function for this connectivity has been proposed in post-meiotic spermatids[77], the biological significance of male germ cell connectivity during pre-meiotic stages of spermatogenesis remains unknown.

Another well-known characteristic of the germline is its extreme sensitivity to DNA damage compared to the soma, with clinical interventions such as radiation or chemotherapy often resulting in impaired fertility[190–192]. It has been postulated that the high sensitivity of the germline to DNA damage is part of a quality control mechanism for the germ cell genome, which is passed

onto the next generation[193]. However, the means by which the germline achieves such a high sensitivity to DNA damage remains unclear.

Here we provide evidence that germ cell connectivity serves as a mechanism to sensitize the spermatogonia (SGs) to DNA damage in the *Drosophila* testis. We show that an entire SG cyst undergoes synchronized cell death as a unit even when only a subset of SGs within the cyst exhibit detectable DNA damage. Disruption of the fusome, a germline-specific organelle that facilitates communication amongst germ cells within a cyst, compromises synchronized germ cell death within a cyst in response to DNA damage. The sensitivity of a germ cell cyst to DNA damage increases as the number of interconnected germ cells within increases, demonstrating that connectivity serves as a mechanism to confer higher sensitivity to DNA damage. Taken together, we propose that germ cell cyst formation serves as a mechanism to increase the sensitivity of genome surveillance, ensuring the quality of the genome that is passed onto the next generation.

## 3.3 Results

### 3.3.1 Ionizing radiation induces spermatogonial death preferentially at the 16-cell stage

The *Drosophila* testis serves as an excellent model to study germ cell development owing to its well-defined spatiotemporal organization, with spermatogenesis proceeding from the apical tip down the length of the testis. Germline stem cells (GSCs) divide to produce gonialblasts (GBs), which undergo transit-amplifying divisions to become a cyst of 16 interconnected spermatogonia (16-SG) before entering the meiotic program as spermatocytes (**Figure 3.1A**). In our previous study we showed that protein starvation induces SG death, predominantly at the early stages (~4-SG stage) of SG development[194] (**Figure 3.1A**). Starvation-induced SG death is mediated by apoptosis of somatic cyst cells encapsulating the SGs[194], which breaks the 'blood-testis-barrier'

and leads to SG death[195,196]. Though we also noted significant SG death at the 16-SG stage in the course of our previous work, it was independent of nutrient conditions and thus was not the focus of the study[194].

In search of the cause of this 16-SG death, we discovered that it can be induced by ionizing radiation. When adult flies were exposed to ionizing radiation that causes DNA double strand breaks (DSBs), a dramatic induction of SG death was observed (**Figure 3.1B** and **3.1C**). Dying SGs induced by ionizing radiation were detected by Lysotracker staining as described by previous studies, showing characteristic acidification of the entire cell[175,178,194]. SG death in control and irradiated flies proceeded in the same manner, where all of the SGs within a cyst die simultaneously by becoming Lysotracker-positive (**Figure 3.1B**). Importantly, in contrast to starvation-induced SG death which was dependent on somatic cyst cell apoptosis, radiation-induced SG death was not suppressed by inhibiting cyst cell apoptosis (**Figure 3.2**), suggesting that radiation-induced SG death is a germ cell-intrinsic response.

The frequency of dying SG cysts peaked around 3 to 6 hours after irradiation and decreased by 24 hours post-irradiation (**Figure 3.1C**). Interestingly, we found that ionizing radiation robustly induces cell death at the 16-SG stage, although death of other stages (2-, 4-, 8-cell SGs) was also induced (**Figure 3.1C**). This pattern of SG death held true regardless of the ionizing radiation dose (**Figure 3.3**). While testing multiple doses of ionizing radiation, we noticed that exposure to even a very low dose of ionizing radiation could dramatically induce death of 16-SGs. By measuring dose-dependent death of 16-SGs at six hours post-irradiation, we found that the 16-SG death induced by increasing radiation was a distinctly non-linear response, quickly reaching a plateau of ~3 dying 16-SG cysts per testis (**Figure 3.1D**). In comparison, cell death in a defined area of the irradiated wing imaginal disc (a mitotically-active somatic tissue with unconnected cells) followed

a linear dose-response relationship where an increase in radiation resulted in a proportional increase in cell death (**Figure 3.1D**). These results demonstrate a remarkable sensitivity of 16-SGs to ionizing radiation compared to somatic cells.

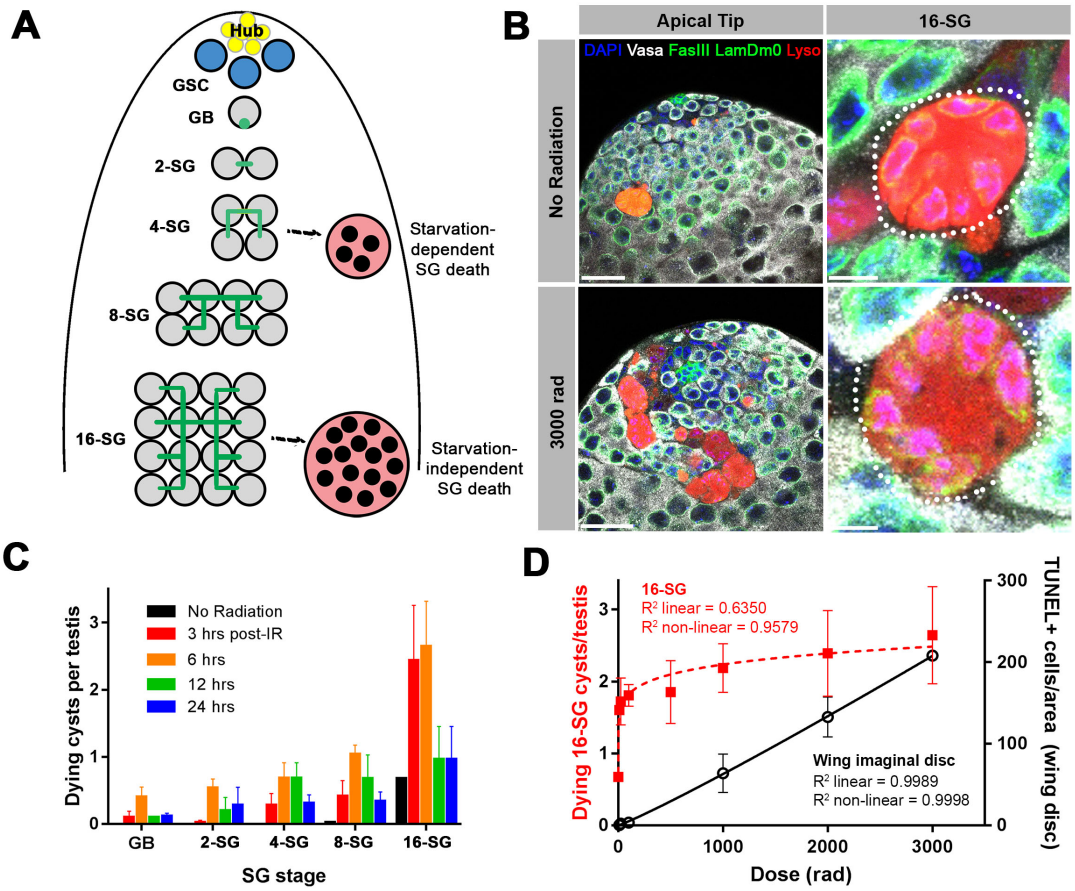


**Figure 3.1. A high level of SG death in response to ionizing radiation.**
**(A)** Illustration of SG development and germ cell death in the *Drosophila* testis. **(B)** An example of the testis apical tip (left panels) with dying SGs marked by Lysotracker staining in control and irradiated flies. High magnification images of dying 16-SGs (dotted outline) are shown in right panels. Lysotracker (red), Vasa (white), FasIII and Lamin Dm0 (green), and DAPI (blue). Bars: 25µm (left panels), 5 µm (right panels). **(C)** Quantification of dying SG cysts by stage from 3 to 24 hours after 3000 rad (Mean ± SD). n ≥ 17 testes, repeated in triplicate. It should be noted that the SG death frequency was scored as 'number of dying SG cysts at each stage per testis'. We have shown that the number of SG cysts is consistently ~5-6 cysts per stage per testis [194], justifying the use of 'number of dying SG cysts/testis' as a proxy for frequency of SG cyst death. **(D)** Number of Lysotracker-positive 16-SG cysts (red) and TUNEL-positive wing imaginal disc cells (black) 6 hours post-irradiation as a function of radiation dose (Mean ± SD). n ≥ 17 testes, and n ≥ 3 wing discs, repeated in triplicate. Best fit lines shown determined by non-linear regression.

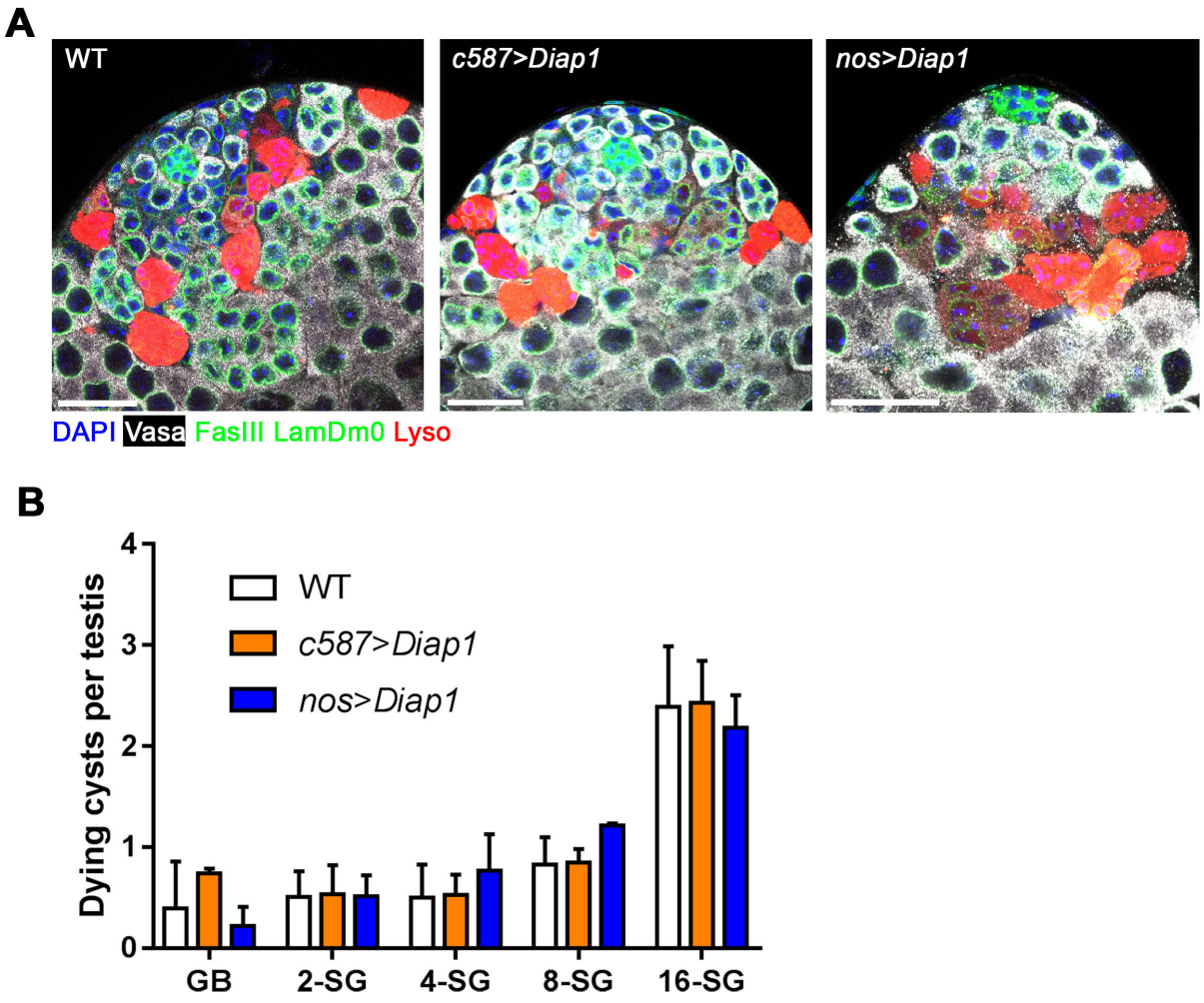


**Figure 3.2. Radiation-induced SG cyst death is independent of somatic cyst cell apoptosis.** **(A)** Representative images of testes apical tips from wild type, *c587-gal4*>UAS-*Diap1*, and *nos-gal4*>UAS-*Diap1* expressing flies (suppressing apoptosis in somatic and germ cells respectively) six hours after 2000 rad. Lysotracker (red), Vasa (white), FasIII and Lamin Dm0 (green), DAPI (blue). Bars: 25 µm. **(B)** Quantification of dying SG cysts by stage from above (Mean ± SD). No significant differences at any SG stage between WT vs. *c587>Diap1* or *nos>Diap1* (p-value * <0.05 t-test).

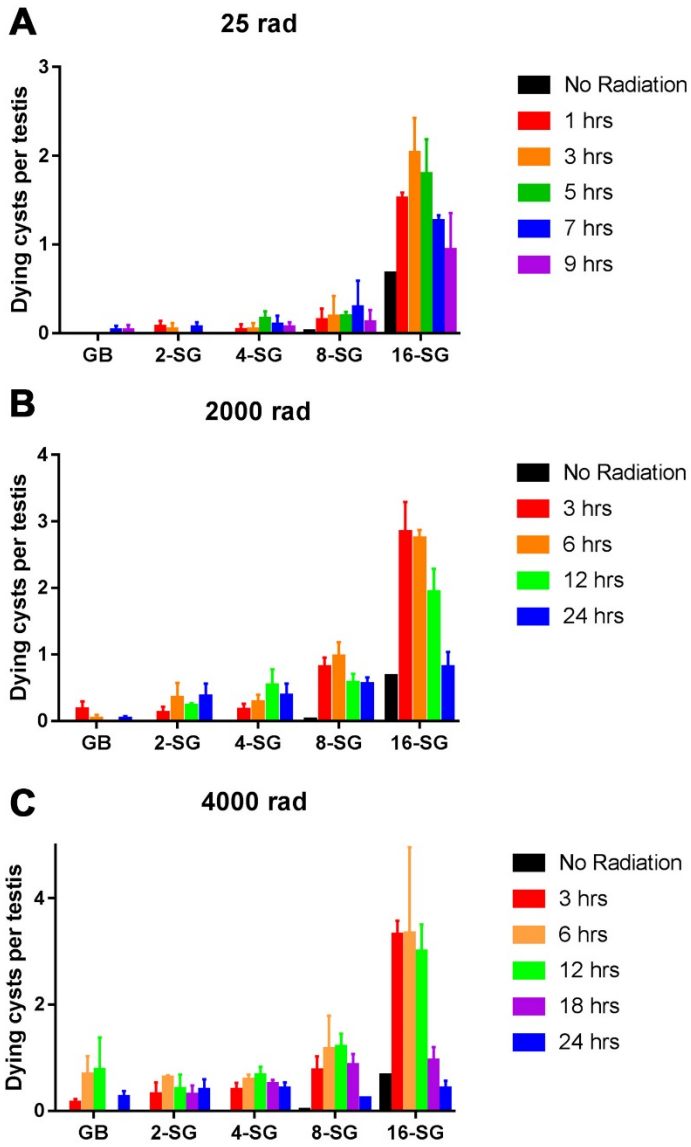


**Figure 3.3. SG death in response to ionizing radiation.**
Quantification of SG death by stage and time following varying doses of ionizing radiation. **(A)** 25 rad (n = 66 testes), **(B)** 2000 rad (n = 84 testes), **(C)** 4000 rad (n = 68 testes).

### 3.3.2 All SGs within a cyst die even when only a subset of cells exhibit detectable DNA damage

To gain insight into the cause of the unusual sensitivity of 16-SGs to DNA damage, we evaluated the response of SGs to ionizing radiation at a cell biological level. DSBs result in phosphorylation of the histone H2A variant (γ-H2Av), the Drosophila equivalent of mammalian γ-H2AX, reflecting the very early cellular response to DSBs[197]. Using an anti-γ-H2Av antibody (pS137), we confirmed that γ-H2Av can be robustly detected in SGs following a high dose of ionizing radiation (**Figure 3.4A**). When a low dose of ionizing radiation was used (≤100 rad), we frequently observed 16-SG cysts in which only a subset of cells within the cyst exhibited detectable γ-H2Av signal but all 16 cells were Lysotracker-positive and dying (**Figure 3.4B**).

The fraction of γ-H2Av-positive SGs within each cyst increased gradually with increasing radiation dose irrespective of SG stage (**Figure 3.4C** and **Figure 3.5**), consistent with the linear nature in which ionizing radiation damages DNA molecules[198]. However, Lysotracker staining showed that SGs within a cyst were always either all Lysotracker-positive or -negative (**Figure 3.4D**). These results suggest that while DNA damage is induced in individual SGs within a cyst proportional to the dose of radiation, cell death is induced in all of the SGs within the entire cyst, leading to elevated SG death that follows a non-linear response with increasing dose.

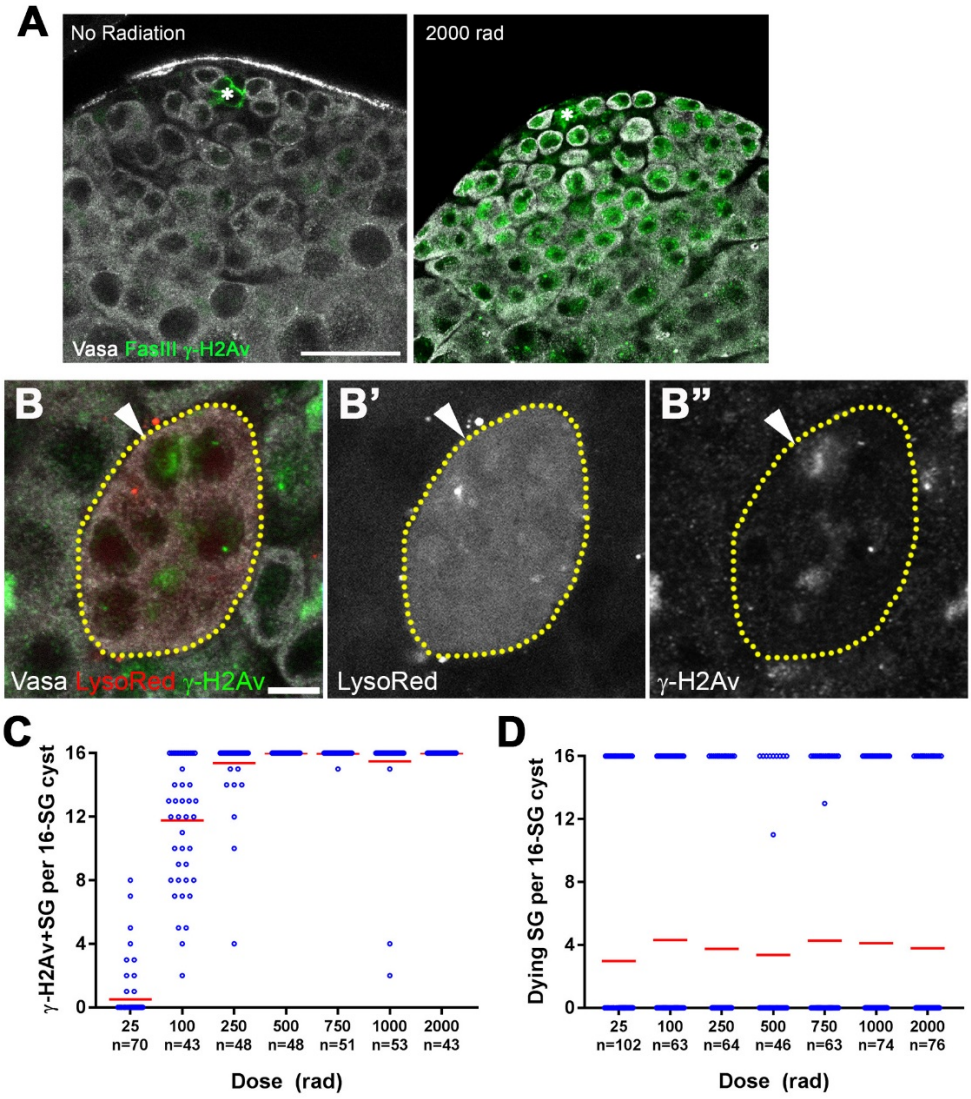


**Figure 3.4. All SGs within a cyst die even when only a fraction of cells exhibit detectable DNA damage.**

**(A)** Representative images of testes apical tips from unirradiated and irradiated flies. Vasa (white), FasIII and γ-H2Av (green). Bar: 25 µm. **(B)** An example of a dying 16-SG cyst (yellow dotted outline) with only a subset of SGs containing detectable DNA damage (arrowhead). γ-H2Av (green), Lysotracker (red), Vasa (white). Bar: 5 µm. **(C)** Number of γ-H2Av-positive cells within each 16-SG cyst at various radiation doses. Blue circles, individual data points. Red line, mean. n = number of 16-SG cysts scored. **(D)** Number of Lysotracker-positive cells within each 16-SG cyst. Blue circles, individual data points. Red line, mean. n = number of 16-SG cysts scored.

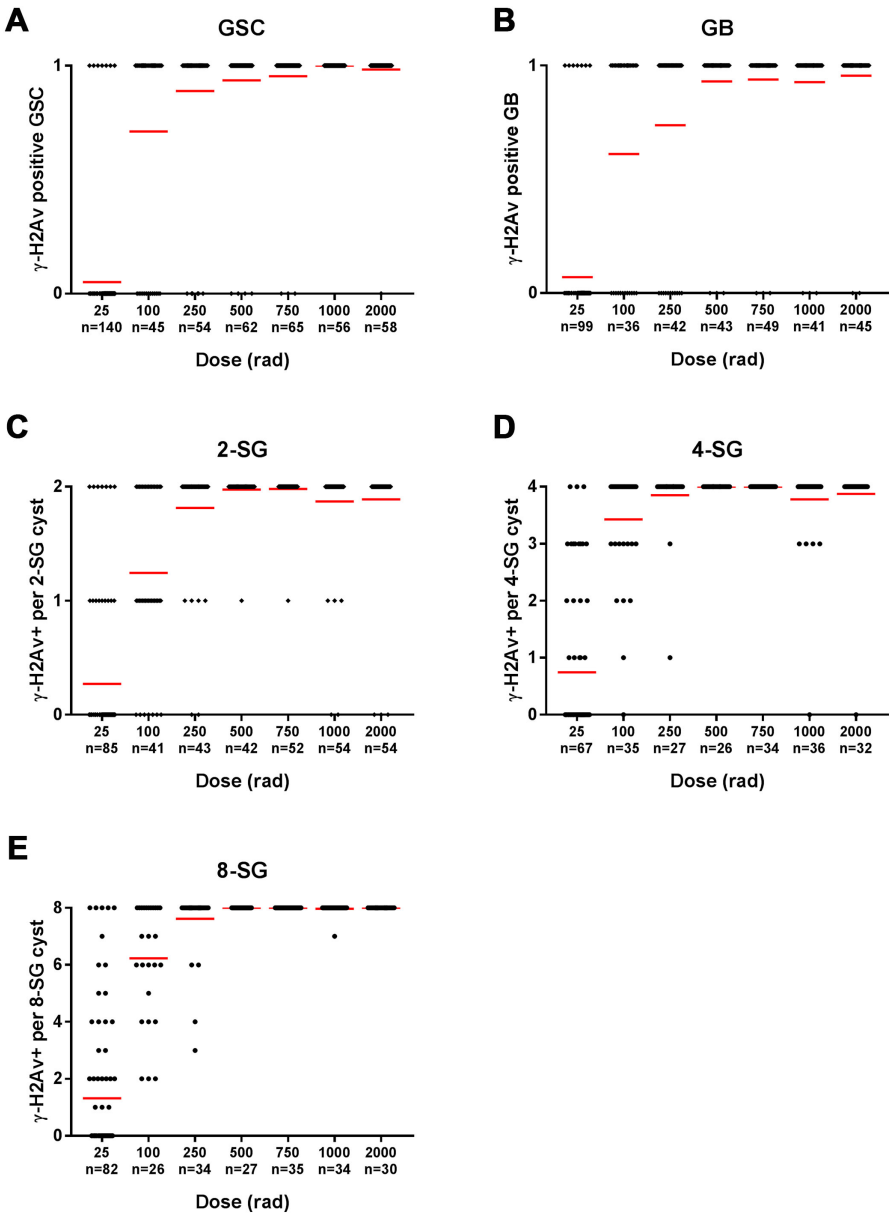


**Figure 3.5. All SG stages show gradual accumulation of γ-H2Av-positive cells with increasing radiation.**
Number of γ-H2Av-positive cells per cyst at increasing radiation doses in **(A)** germline stem cells **(B)** gonialblasts **(C)** 2-SG **(D)** 4-SG **(E)** 8-SG. Red line, mean.

### 3.3.3 The fusome is required for synchronized all-or-none SG death within the cysts

The above results led us to hypothesize that all SGs within a cyst might be triggered to die together even when only a subset of SGs within the cyst have detectable DNA damage, explaining the extremely high sensitivity of the germline to DNA damage. In *Drosophila* and other insects, the fusome is a germline-specific membranous organelle that connects the cytoplasm of germ cells within a cyst and mediates intracyst signaling amongst germ cells [45,71]. We speculated that if germ cell cysts undergo synchronized cell death by sharing the decision to die, the fusome might mediate the 'all-or-none' mode of SG death upon DNA damage.

To examine the role of the fusome in all-or-none SG death upon irradiation, we used RNAi-mediated knockdown of *α-spectrin* and a mutant of *hts*, core components of the fusome [17,45–47,71] (**Figure 3.6**). Mutant and control flies were irradiated and their testes were stained with Lysotracker to identify dying SGs in combination with the lipophilic dye FM 4-64 to mark cyst cell membranes, demarcating the boundaries of SG cysts[178]. In control testes, 16-SG cysts were almost always found to be either completely Lysotracker-positive or -negative under all conditions tested as described above, indicating that 16-SG cysts make an all-or-none death decision (**Figure 3.7A, B, E, F**). Of particular importance, even at a lower dose of radiation (e.g. 100 rad) where only a subset of germ cells exhibit visible γ-H2Av staining, the 16-SG cyst was either entirely Lysotracker-negative or -positive. In contrast, *α-spectrin* RNAi and *hts* mutant testes frequently contained 16-SG cysts with a mixture of individual Lysotracker-positive and -negative SGs (**Figure 3.7C, D, G, H**), suggesting that the all-or-none mode of SG death was compromised. Importantly, the mean fraction of 16-SG that died in response to radiation exposure at any dose was reduced when the fusome was disrupted (**Figure 3.7B, D, F, H**). These data show that the fusome is required for the coordinated death of all SGs within a cyst, and suggests that the intracyst

communication increases overall SG death in response to radiation-induced DNA damage. Moreover, the fact that loss of germ cell communication in fusome mutants allows for the survival of some SGs strongly argues against the possibility that SGs without cytologically detectable γ-H2Av are sufficiently damaged to trigger cell death on their own, and that SGs are individually dying. Instead, the death of SGs without detectable γ-H2Av in wild type/control can likely be attributed to a shared death signal from other cells, as blockade of intercellular communication in fusome mutants allows for their survival.

It should be noted that the fusome mutants appeared to maintain ring canals, as evidenced by the intact ring shape of Pavarotti-GFP, a marker for ring canals[52] (**Figure 3.8**). Therefore, intracyst communication triggering SG death is likely mediated by the fusome, rather than physical openings between SGs within the cyst (see Discussion). Consistent with this idea, somatic follicle cells of the egg chamber, which are known to be connected by ring canals but without a fusome[199], were observed to die individually by becoming positive for cleaved caspase (Dcp-1) (**Figure 3.9A**). Additionally, these cells did not exhibit acute sensitivity to low doses of radiation like interconnected SG do and displayed an essentially linear dose-response (**Figure 3.9B, C**).

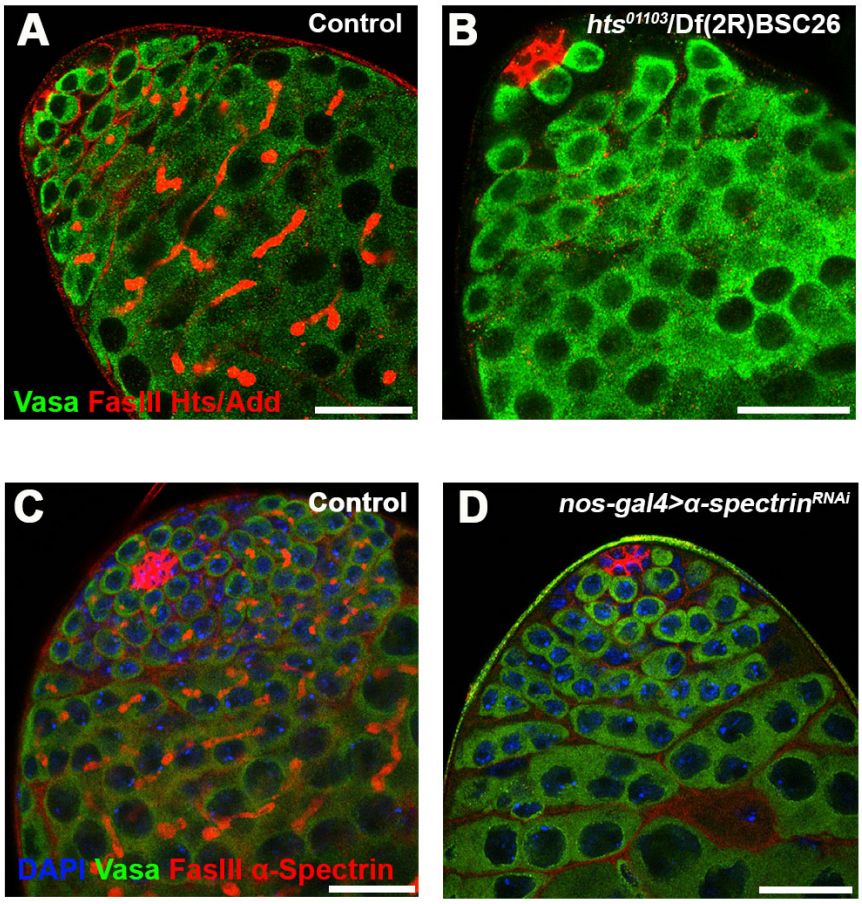


**Figure 3.6. Validation of fusome elimination in *hts* mutant and *α-spectrin*$^{RNAi}$ testes.**
**(A, B)** Hts/Adducin staining (red) in control (A) and *hts*$^{01103}$/Df(2R)BSC26 mutant (B) testes. Red: Hts/Add and FasIII. Green: Vasa (germ cells). Bars: 25 µm. Note that *hts* mutation eliminates fusome staining (leaving FasIII staining of the hub cells).
**(C, D)** ✔-Spectrin staining (red) in control (C) and *nos-gal4>UAS-spectrin*$^{RNAi}$ (D) testes. α-Spectrin and FasIII (red), Vasas (green), DAPI (blue).

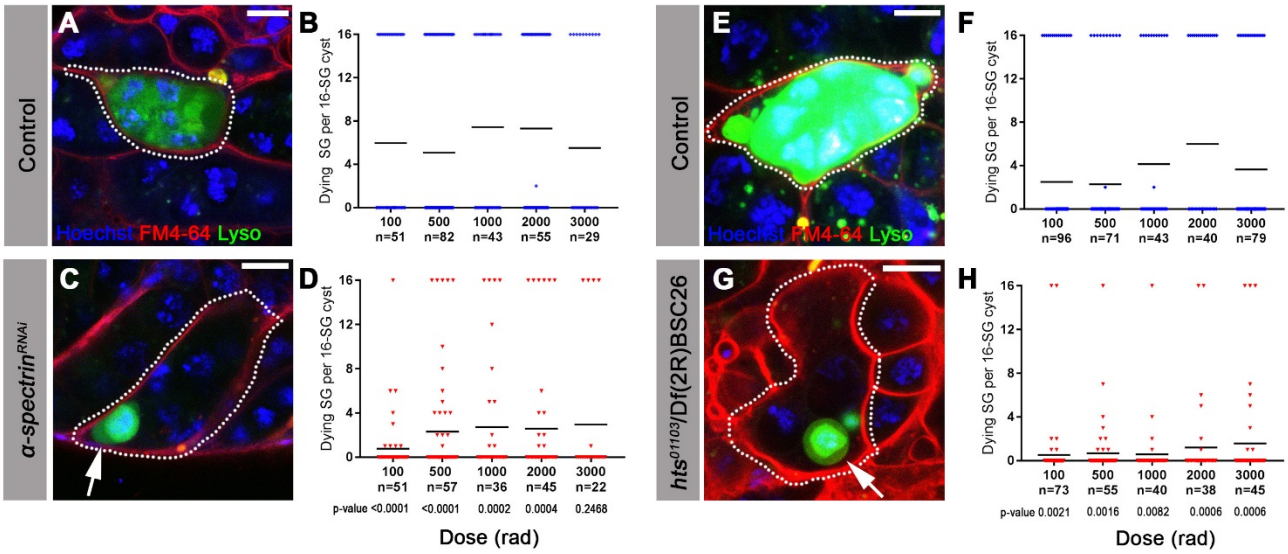


**Figure 3.7. The fusome is required for synchronized all-or-none SG death within a cyst.** **(A)** A Lysotracker-positive 16-SG cyst (green, dotted outline) in unfixed control testes, with cyst borders marked by FM 4-64 (red) and SG nuclei marked by Hoechst 33342 (blue). Bar: 7.5 µm. **(B)** Number of Lysotracker-positive cells within each 16-SG cyst of control testes at varying radiation doses. Black line, mean. n = number of 16-SG cysts scored. **(C)** A 16-SG cyst (dotted outline) in *nos-gal4*>UAS-*α-spectrin*$^{RNAi}$ testes containing a single Lysotracker-positive SG (arrowhead). Bar: 10 µm. **(D)** Number of Lysotracker-positive cells within each 16-SG cyst of *nos-gal4*>UAS-*α-spectrin*$^{RNAi}$ testes at varying radiation doses. Black line, mean. n = number of 16-SG cysts scored. P-values (comparing the corresponding radiation doses between control and mutant) determined by chi-squared test (See methods). **(E, F)** *hts*$^{01103}$/+ control testes. Bar: 5 µm. **(G, H)** *hts*$^{01103}$/Df(2R)BSC26 mutant testes. Bar: 7.5 µm.

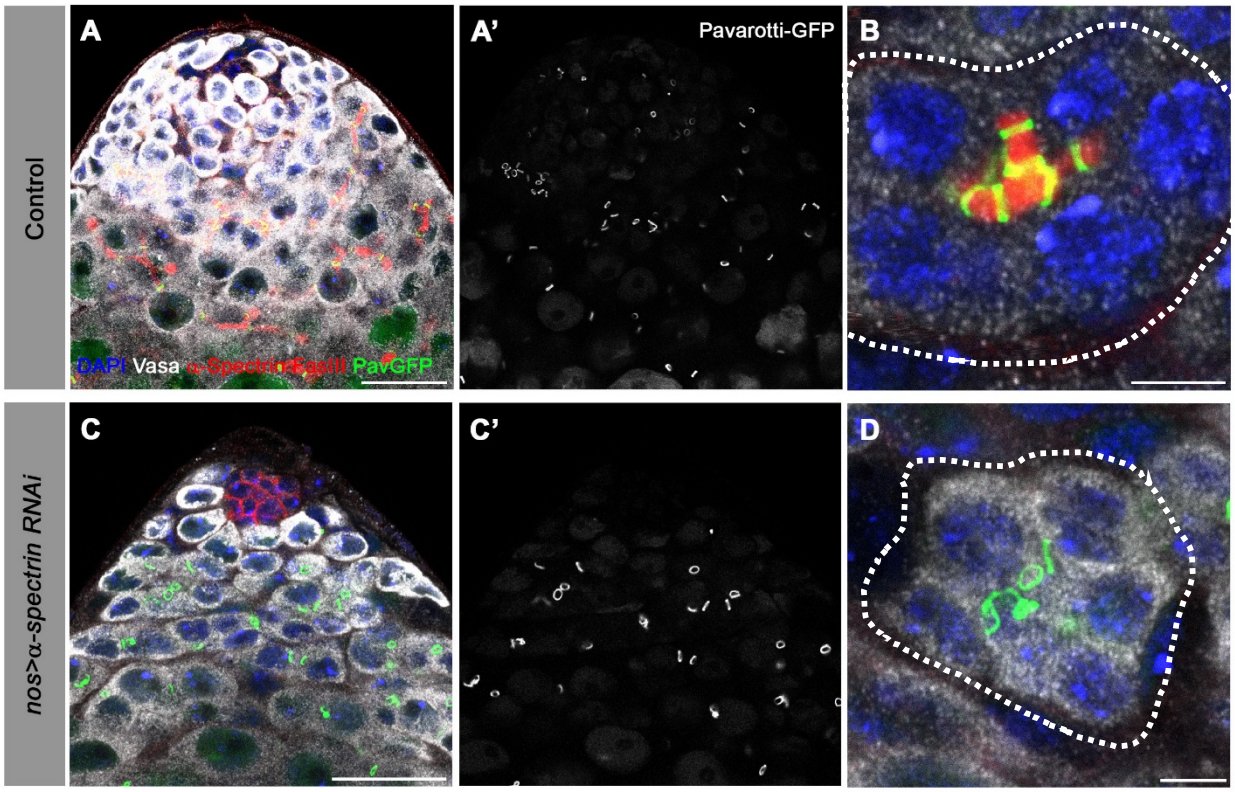


**Figure 3.8. SG ring canals are maintained in fusome mutants.**
Apical tip of testes from **(A)** control and **(C)** *nos-gal4>UAS-α-spectrin*$^{RNAi}$ flies stained for DAPI (blue), Vasa (white), FasIII and α-Spectrin (red), and Pavarotti-GFP (green). Bars: 25 µm. SG cysts (outlined) from **(B)** control and **(D)** *nos-gal4>UAS-α-spectrin*$^{RNAi}$ flies. Bars: 5 µm.

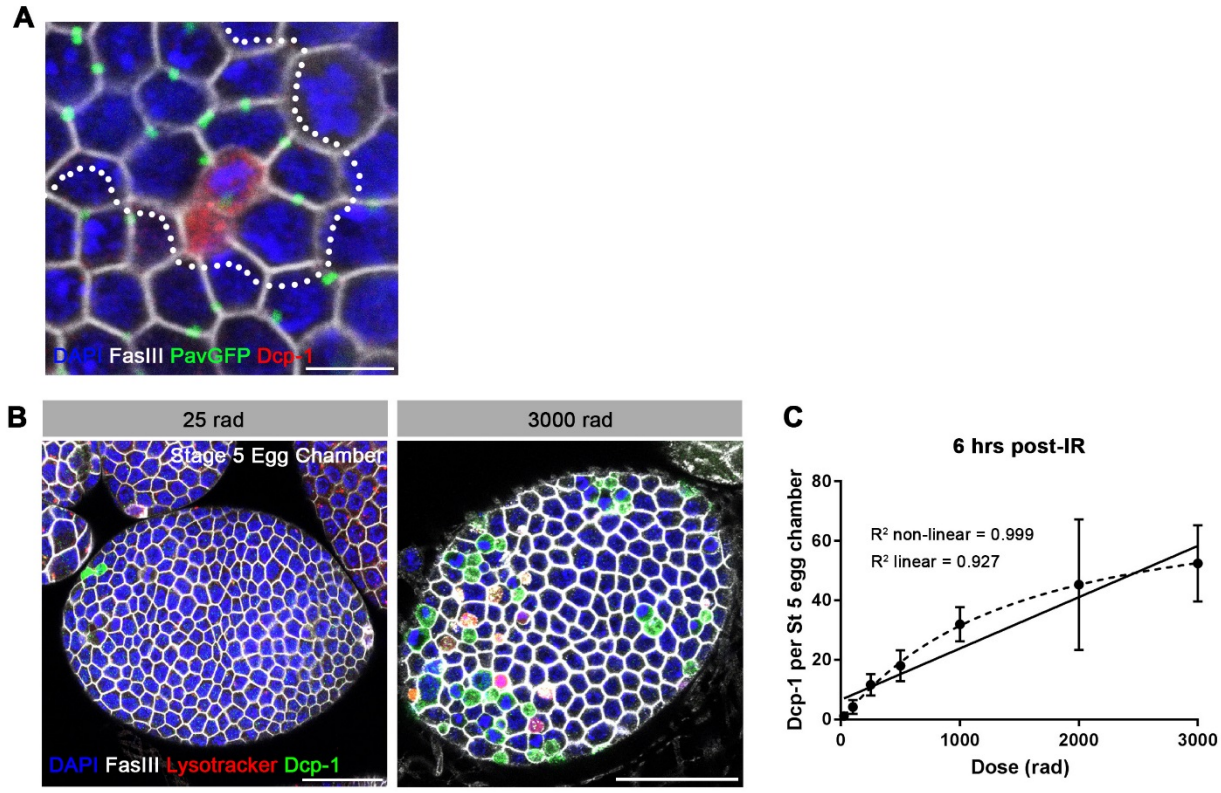


**Figure 3.9. Follicle cell death in response to ionizing radiation exposure.**
**(A)** Dcp-1 staining (red) in interconnected 'clone' of follicle cells (dotted outline). The boundary of follicle cell clone was determined by following the connectivity visualized by Pavarotti-GFP[199] (green). DAPI (blue), FasIII (white). Bar: 5 μm. **(B)** Cleaved caspase Dcp-1 staining (green) in stage 5 egg chambers at 6 hours following low or high dose radiation. Lysotracker (red), DAPI (blue), FasIII (white). Bars: 25 μm. Note that follicle cells die via apoptosis, exhibiting cleaved caspase signal. Lysotoracker did not overlap with cleaved caspase, and was not distributed evenly in the cytoplasm as is the case for germ cell death. Thus, Lysotracker signal in follicle cells might represent phagocytosis to engulf dead follicle cells. **(C)** Number of Dcp-1-positive follicle cells in stage 5 egg chambers 6 hours post-irradiation as a function of radiation dose (Mean ± SD). n ≥ 6 egg chambers, repeated in triplicate. Although the data fits a non-linear regression ($R^2$=0.999) slightly better than a linear regression ($R^2$=0.927), follicle cell death does not exhibit a steep increase in cell death at low doses (≤100 rad) as in SG.

### 3.3.4 The mitochondrial proteins HtrA2/Omi and Endonuclease G are required for all-or-none SG death

The above results suggest that intercellular communication mediated by the fusome plays a critical role in allowing for all-or-none commitment of SGs to death or survival. Based on these results, we hypothesized that a signal to promote cell death exists that is rapidly transmitted from damaged SGs to others via their intercellular connections.

It has previously been shown that germ cell death in the *Drosophila* testis depends on mitochondria-associated factors rather than effector caspases[175]. The *Drosophila* homolog of the mitochondrial serine protease HtrA2/Omi is cleaved and released from the mitochondrial compartment as part of the mitochondria-associated death pathway to promote cell death in response to nuclear DNA damage[174,200–202]. The catalytic function of released HtrA2/Omi is known to control the death of SGs in the testis in a non-apoptotic pathway. Yacobi-Sharon et al. further showed that Endonuclease G (EndoG) is also involved in germ cell death[175]. EndoG normally resides in mitochondria but is released to promote degradation of nuclear chromatin and induce cell death[203].

In *HtrA2/Omi* mutant flies, we frequently observed a mix of Lysotracker-positive and -negative SGs within a single cyst, similar to what was seen in fusome mutants (**Figure 3.10A**). Disruption of the all-or-none mode of SG death within the cyst was observed at any dose of radiation tested (**Figure 3.10B**). Disrupted all-or-none SG death occurred in both heterozygous ($Omi^{\Delta 1}$/+) and transheterozygous ($Omi^{\Delta 1}/Omi^{Df1}$) conditions, consistent with the previous report that heterozygous conditions exhibit haploinsufficiency in inducing SG death [175]. In contrast, wild type control 16-SG cysts maintained their all-or-none mode of SG death (**Figure 3.10B**). Likewise, a loss-of-function $EndoG^{MB07150}$ mutant allele[170] also showed disruption of all-or-none SG death

in both heterozygous (*EndoG*$^{MB07150}$/+) and transheterozygous (*EndoG*$^{MB07150}$/Df(3R)BSC699) conditions (**Figure 3.10C, D**). Taken together, these data show the involvement of mitochondrial cell death pathway components HtrA2/Omi and EndoG in the all-or-none mode of SG death. Considering that these proteins are released from mitochondria to induce cell death, it is tempting to speculate that these proteins (or their downstream molecules/signals) are shared among SGs via the fusome to trigger synchronized SG death.

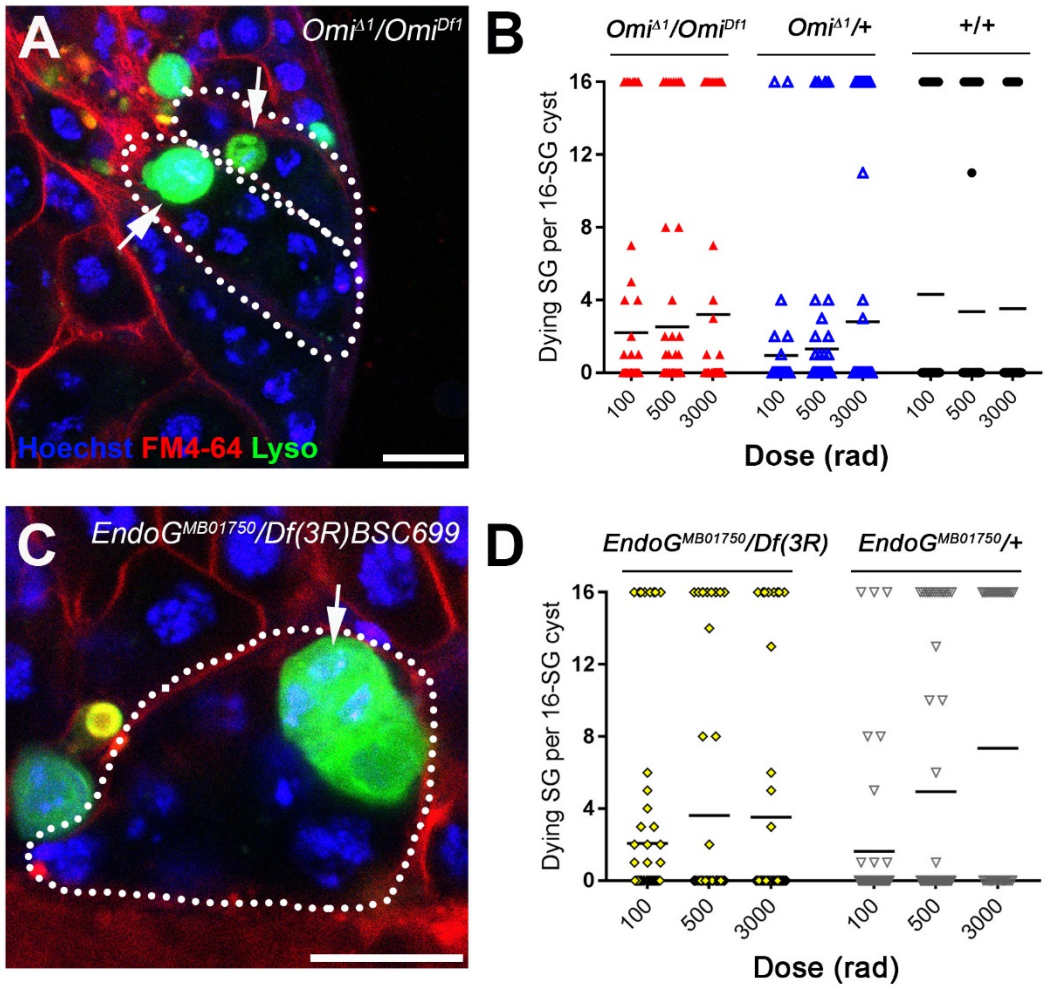


**Figure 3.10. The mitochondrial proteins HtrA2/Omi and Endonuclease G are required for all-or-none SG death.**
**(A)** SG cysts (dotted outlines) in $Omi^{\Delta 1}/Omi^{Df1}$ mutant testes containing individual Lysotracker-positive SGs (arrows). Hoechst 33342 (blue), FM 4-64 (red), Lysotracker (green). Bar: 10 µm. **(B)** Number of Lysotracker-positive SGs in each 16-SG cyst in $Omi^{\Delta 1}/Omi^{Df1}$, $Omi^{\Delta 1}/+$, and wild type testes. Black line, mean. n ≥43 cysts per dose. **(C)** 16-SG cyst (dotted outline) in $EndoG^{MB07150}$/Df(3R)BSC699 testes containing individual Lysotracker-positive SGs. Hoechst 33342 (blue), FM 4-64 (red), Lysotracker (green). Bar: 10 µm. **(D)** Number of Lysotracker-positive SGs in each 16-SG cyst in $EndoG^{MB07150}$/Df(3R)BSC699 and $EndoG^{MB07150}$/+ testes. Black line, mean. n ≥37 cysts per dose.

### 3.3.5 The DNA damage response pathway proteins *p53* and *mnk/chk2* do not regulate the all-or-none mode of SG death

The DNA damage response is a highly conserved pathway controlling cell death and DNA repair[204,205]. We thus examined the potential involvement in radiation-induced SG death of the universal DNA damage response pathway components, *mnk/chk2* and *p53,* whose conserved function in DNA damage response in *Drosophila* has been shown[206,207]. By using well-characterized loss-of-function alleles ($mnk^{6006}$ and $p53^{5A\text{-}1\text{-}4}$)[171,172,176], we found that these mutants broadly suppress SG death at high and low doses of radiation (**Figure 3.11D**). However, SG death in these mutants maintained an all-or-none pattern (**Figure 3.11A-C, E**). These results suggest that while *p53* and *mnk/chk2* may contribute to SG death via their general role in controlling the DNA damage response as has been described in somatic cells, they do not play a role in mediating the all-or-none pattern of SG death within a cyst that is unique to interconnected germ cells.

Consistent with the idea that neither *mnk/chk2* nor *p53* is responsible for a germline-specific all-or-none mode of cell death in response to DNA damage, Mnk/Chk2 or p53 was barely upregulated in the germline in response to a low dose of radiation (100 rad), which is sufficient to induce robust SG death. Using a polyclonal anti-Mnk/Chk2 antibody[208], we barely detected any signal in germ cells, although some level of signal was seen in the surrounding somatic cyst cells (**Figure 3.12**). Likewise, a p53 transcriptional reporter [173] showed only a slight increase in the signal in response to a low dose of radiation (**Figure 3.13**). Even at a high dose, robust expression of the reporter was observed only at 24 hours after irradiation, much later than the peak of SG death, which typically happens within a few hours. Collectively, these data (i.e. *mnk/chk2* and *p53* mutants maintaining all-or-none cell death and the lack of robust Mnk/Chk2 and p53 expression

in response to DNA damage) indicate that expression of p53 or Mnk/Chk2 in SGs is unlikely to account for the all-or-none mode of germ cell death in response to DNA damage.

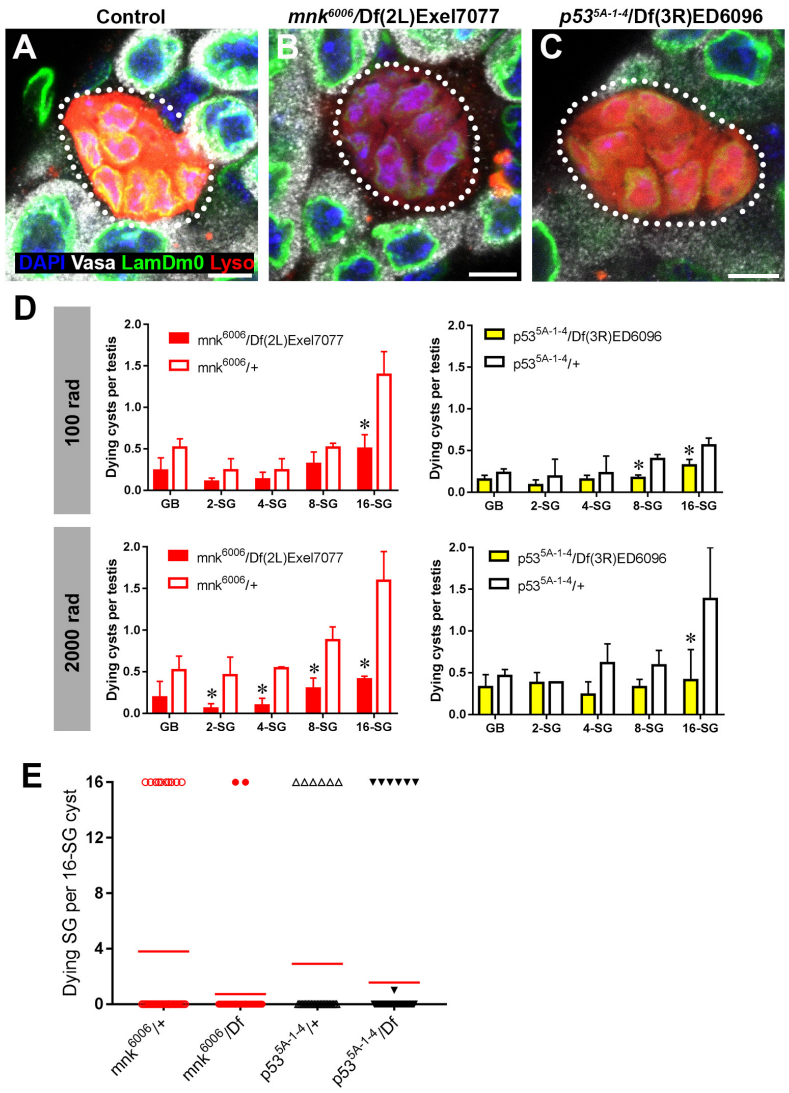


**Figure 3.11. *p53* and *Chk2/mnk* suppress SG death but do not regulate the all-or-none mode of SG death.**

(**A-C**) Examples of dying 16-SGs (dotted outline) in wild-type (A), *mnk*$^{6006}$/Df(2L)Exel7077 mutant (B), and *p53*$^{5A-1-4}$/Df(3R)ED6096 mutant (C) testes. Lysotracker (red), Lamin Dm0 (green), DAPI (blue) and Vasa (white). Bars: 5 µm. (**D**) SG cyst death by stage in *mnk/chk2* and *p53* mutants 6 hours after irradiation with 100 rad and 2000 rad (Mean ± SD, p-value * <0.05 t-test). Fixed, stained samples were used for scoring. Testes sample n ≥ 11 for each genotype, repeated in triplicate. **(E)** Number of Lysotracker-positive SG per 16-SG cyst in *mnk/chk2* and *p53* mutants following 100 rad. Red line, mean. Unfixed samples stained with Lysotracker, FM 4-64, and Hoechst 33342 were used for scoring.

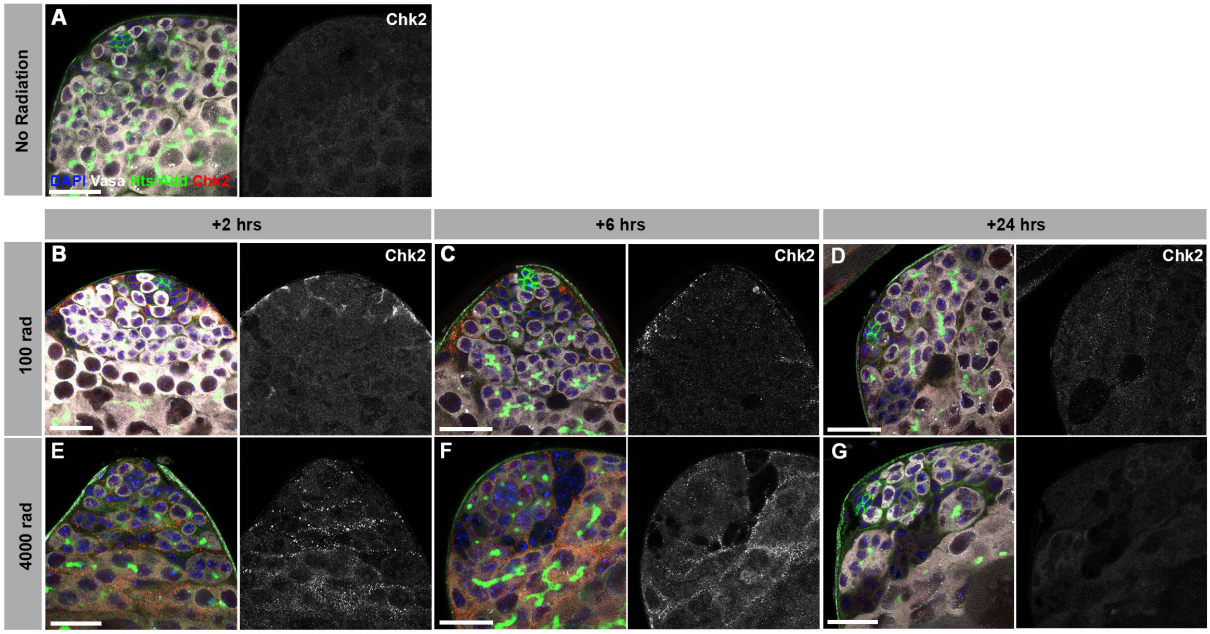


**Figure 3.12. Expression of Mnk/Chk2 in response to ionizing radiation.**
Testes from unirradiated flies **(A)**, flies irradiated with 100 rad **(B-D)**, or with 4000 rad **(E-G)**, stained for Mnk/Chk2 (red), Vasa (white), Hts (green), and DAPI (blue). Bars: 25 µm. Mnk/Chk2 was detected only after a high dose of radiation, predominantly in the somatic cyst cells surrounding the Vasa-positive germ cells.

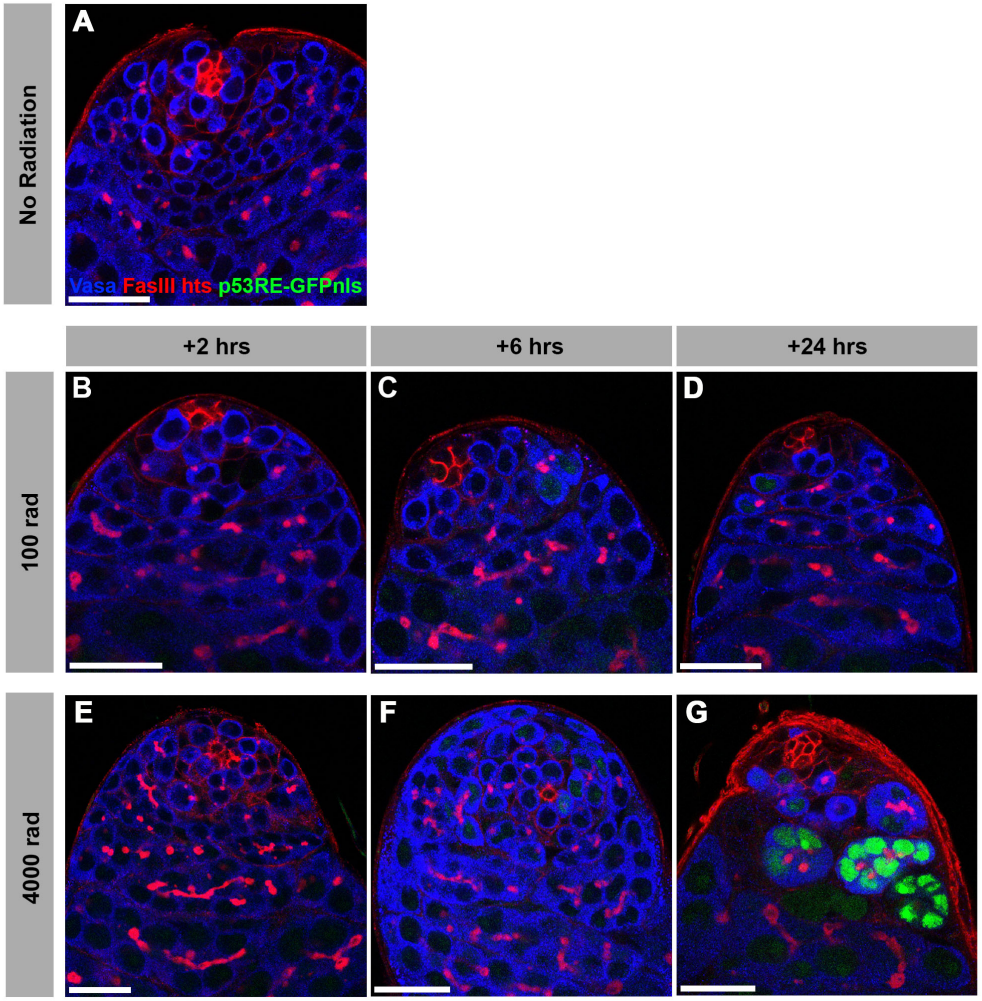


**Figure 3.13. Expression of p53 reporter in response to ionizing radiation.**
Testes from unirradiated flies **(A)**, flies irradiated with 100 rad **(B-D)**, or with 4000 rad **(E-G)**, stained for p53RE-GFPnls (green), Vasa (blue), Hts/Adducin and FasIII (red). Bars: 25 µm. p53RE-GFPnls was only detectable 24 hours following irradiation at a high dose (4000 rad).

### 3.3.6 Increasing connectivity of SGs increases sensitivity to DNA damage

The above results suggest that the ability of SGs to trigger cell death in response to DNA damage is facilitated by the sharing of death-promoting signals amongst SGs within a cyst, killing SGs that are not sufficiently damaged to commit to cell death on their own. This sharing of death-promoting signals is mediated by and dependent on the fusome, which facilitates intracyst communication. If this is the case, it would be predicted that increasing the connectivity of a SG cyst (the number of interconnected SGs within the cyst) would increase its sensitivity to DNA damage, because increased SG number per cyst will increase the probability of any cells being sufficiently damaged to trigger death. Indeed, as mentioned above, we observed a trend of 16-SG cysts dying more frequently than 2-, 4-, or 8-SGs (**Figure 3.1** and **Figure 3.3**). By plotting cell death frequency of all SG stages as a function of increasing radiation dose (**Figure 3.14**), it becomes clear that the sensitivity of SG cysts correlates with their connectivity, where 8-SGs are less sensitive than 16-SGs but more sensitive than 4-SGs and so on. Interestingly, single-celled GBs, the immediate daughter of GSCs that have not formed any intercellular connections, exhibited an essentially linear increase in death in response to radiation dose, which is reminiscent of somatic imaginal disc cells (**Figure 3.1D**). These results support the idea that germ cell connectivity plays a key role in increasing the sensitivity of the germline to DNA damage.

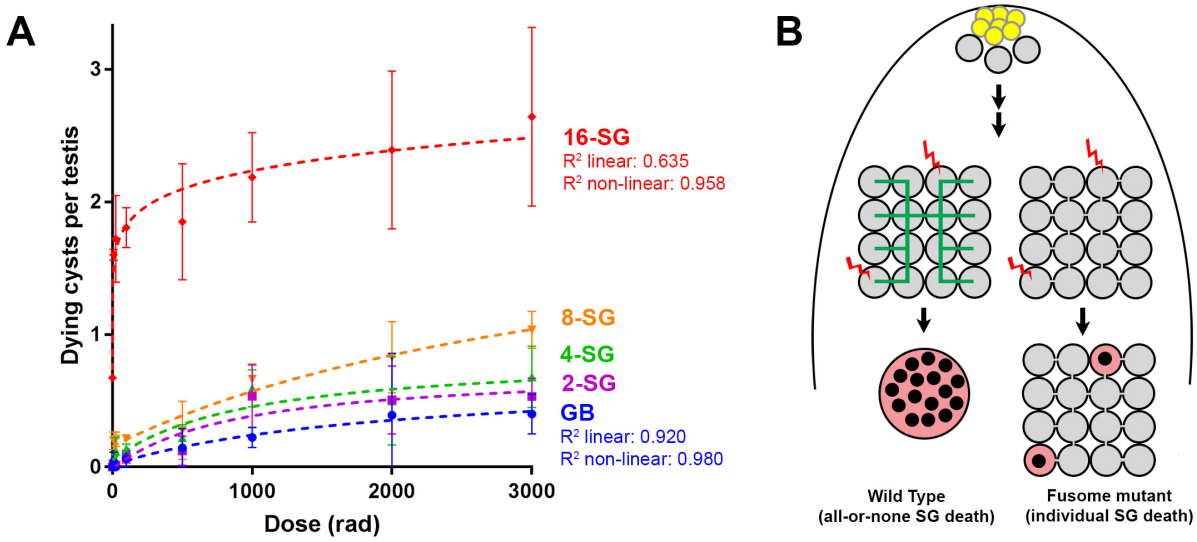


**Figure 3.14. Increasing connectivity confers higher sensitivity to DNA damage**
**(A)** Dose-dependent SG death in 2-, 4-, 8-, and 16-SG cysts (Mean ± SD). Best fit lines shown determined by non-linear regression. n ≥ 17 testes, repeated in triplicate. **(B)** Model of SG death enhanced by connectivity.

## 3.4 Discussion

Our present study may provide a link between two long-standing observations in germ cell biology: 1) the broad conservation of intercellular connectivity (cyst formation) of germ cells and 2) the sensitivity of the germline to DNA damage. The purpose for germ cell cyst formation outside of the meroistic ovary (i.e. the oocyte nursing mechanism) remained unclear. Our study shows that the connectivity of germ cells can serve as a key mechanism for their ability to robustly induce cell death, providing an explanation for cyst formation outside of the oocyte nursing mechanism. However, there are many cell types that are known to be connected to sibling cells, where synchronized cell death among the connected cells is not observed or does not make any biological sense. For example, early-stage embryos of *Drosophila* develop as syncytia, where the embryo could be considered a single cell with multiple nuclei (before cellularization occurs to separate nuclei into individual cells). The *C. elegans* germline is topologically similar to *Drosophila* early embryos in that all cells share the same cytoplasm. In these two examples, damaged nuclei die individually and synchronized cell death is not observed[176,209]. In *Drosophila* oogenesis, 16 interconnected cystocytes have distinct fates (one oocyte and 15 nurse cells), and it would not be beneficial to kill the oocyte when just one dispensable nurse cell is damaged. Moreover, nurse cells undergo programmed apoptosis later in oogenesis to finalize the cytoplasmic transport into the oocyte, yet this apoptosis does not kill oocytes. These examples have two important implications. First, openness via ring canals/intercellular bridges alone is likely insufficient to mediate synchronized cell death. Second, there are likely additional purposes for intercellular connectivity to be discovered other than the sharing of death-promoting signals.

Regarding the first point that physical openness alone is likely insufficient to induce cell death in undamaged sibling cells, we speculate that the fusome plays a key role in facilitating

intercellular communication of death-promoting signals. Because fusome mutants apparently maintain cytoplasmic openings (ring canals) between SGs (**Figure 3.8**), it suggests that the intercellular bridges/openings are not sufficient to allow intracyst communication of death-promoting signals. Consistent with this idea, we found that follicle cells of the egg chamber do not exhibit synchronized cell death in response to irradiation (**Figure 3.9**), even though these cells are known to maintain intercellular bridges/ring canals among multiple sibling cells, through which proteins (e.g. GFP) can be transported[199]. The lack of synchronized cell death in the follicle cells coincided with a proportional/linear increase in cell death with the increasing dose of radiation. Therefore, we propose that the fusome functions to transmit the death-triggering signals, similar to its known role in cell cycle synchronization within the germ cell cyst [71].

We imagine two possibilities to explain how the signals are shared within a cyst, leading to cell death: when one SG within a cyst decides to die, this 'decision of death' might be sent to all the other SGs within the cyst, leading to all-or-none SG death. Alternatively, the signal shared among SGs may be 'additive' in nature. In such a scenario, even when none of the individual SGs have sufficient DNA damage to trigger cell death on its own, addition of all damage signaling within the cyst might reach a level sufficient to induce cell death. Either way, such responses would effectively lower the threshold of DNA damage per cell needed to trigger germ cell death. Consequently, the sharing of signals between SGs through intercellular connections increases their likelihood to die following DNA damage, explaining the unusually high sensitivity of the germline to DNA damage.

According to this model, higher connectivity would confer higher sensitivity to DNA damage: as the connectivity increases, more cells would contribute to detecting any DNA damage the germline may be experiencing. Indeed, our data show a positive correlation between sensitivity

to radiation and the increasing connectivity of SG cysts (**Figure 3.14**). Remarkably, the fact that single-celled, unconnected GBs exhibit an essentially linear death response to increasing radiation suggests that individual germ cells do not necessarily have an intrinsically different DNA damage response that accounts for their high sensitivity to DNA damage.

A connectivity-based increase in sensitivity to DNA damage also has an important implication in the development of multicellular organisms. To pass on genomes to the next generation, it is critically important for germ cells to have the most stringent mechanisms to prevent deleterious mutations. However, as genome size increases in multicellular organisms, ubiquitously increasing the stringency of genome quality control could result in a high rate of cell death in all tissues, which could compromise the development or survival of organisms. Thus, a multicellular organism may require differential sensitivities to DNA damage between the soma and the germline: a more sensitive genome surveillance mechanism to protect the germline, whereas the priority of the soma shifting toward survival to support development/maintenance of somatic organs. A connectivity-based increase in sensitivity to DNA damage might be a simple method for multicellular organisms to achieve drastically different sensitivities to DNA damage between the soma and germline without having to alter intrinsic damage response pathways, although additional germline-specific DNA damage response mechanisms cannot be excluded. We speculate that one reason germ cell connectivity has arisen during evolution and been so widely conserved might be to confer higher sensitivity to DNA damage specifically in the germline. It awaits future studies to understand whether germ cells from other organisms exhibit high sensitivity to DNA damage in a manner dependent on intracyst communication.

# Chapter 4

# Dynamic Changes in the rDNA During Aging in the *Drosophila* Male Germline

## 4.1 Abstract

The repetitive ribosomal DNA (rDNA) is a unique genomic element whose biology has been implicated in aging-related changes and heterochromatin biology across species, but has never been comprehensively studied in the context of adult stem cells or across generations. To gain insight into these questions, we adapted a technique for RNA fluorescence in situ hybridization with single nucleotide polymorphisms (SNP-FISH) to distinguish rRNA transcripts from different chromosomal arrays within a single cell. We discovered that *Drosophila* male germline stem cells (GSCs), which contain rDNA arrays on the X and Y chromosomes, normally transcribe only from the Y chromosome and suppress the array on the X chromosome. However, the X chromosome rDNA becomes progressively activated during aging and we present evidence that suggests this is secondary to the age-related destabilization and loss of gene copy number in the Y rDNA array. Functionally, X rDNA activation is associated with perturbations in GSC cell cycle and activation of normally-repressed genomic elements that may be harmful to the cell. A strong transgenerational effect is also observed where male progeny bred from older parents with GSCs exhibiting X rDNA activation have an increased rate of GSC X rDNA activation at an early age and reduced ribosomal gene copy number in germ cells. Our work suggests that the rDNA is

a dynamic genomic element in germline stem cells that undergoes previously uncharacterized changes during aging, which has genetic and epigenetic implications for subsequent generations.

## 4.2 Introduction

The ribosomal DNA (rDNA) consists of tandem repetitive arrays of tens to hundreds of copies of the rRNA genes, which code for the mature RNA components of ribosomes (see Chapter 1.3.1 for an in-depth description). In *S. cerevisiae*, it is known that the rDNA is one of the most unstable parts of the genome, prone to intrachromosomal recombination and replication conflicts that can result in gene copy number loss[110,111,114,117,149,160] (**Figure 4.1B**). Accordingly, many mechanisms have evolved to stabilize the rDNA and linked to these events an ability to amplify gene copy number following loss[108,112,113,154,210–214]. What results is the picture of the yeast rDNA locus as an extremely dynamic genomic element that can contract and expand with time.

Numerous links have been drawn between changes in the rDNA during aging and perturbed morphology of the nucleolus, a subnuclear organelle organized by active transcription of the rRNA genes. Initially, changes in nucleolar morphology were observed in old yeast mother cells, manifesting as progressive fragmentation or expansion of the nucleolus thought to be reflective of destabilization and intrachromosomal recombination ("looping out") of the rDNA[149,152]. These changes in nucleolar morphology presage replicative senescence, and subsequently many mutants were identified that perturbed nucleolar morphology and resulted in accelerated aging[146,151,152]. A similar correlation between altered nucleolar morphology and senescence has also been observed in mammalian cells[215].

The structure of the individual rRNA genes and their arrangement into large rDNA arrays has been exceptionally conserved from yeast to higher eukaryotes, but direct studies of the age-

related changes of the rDNA in multicellular organisms have been limited. It remains unclear whether analogous rDNA instability occurs with time. One line of evidence that suggests higher eukaryotes experience similar challenges in dealing with the dynamic plasticity of the rDNA is that significant copy number variation has been observed within species[216,217] and even from cells within individual organisms[218]. If changes in the rDNA govern replicative age in multicellular organisms like it does in yeast, it stands to reason that the longest-living mitotically active populations of cells would be the strongest candidate to manifest these changes. To this end, we directed our studies towards *Drosophila* male germline stem cells (GSCs), which are known to be highly mitotically active throughout the lifespan of the adult fruit fly and are responsible for continuously repopulating the testis.

## 4.3 Results

Note that all experiments were carried out with the standard lab wild-type strain *yw* ($y^1$ $w^1$) unless otherwise noted. See methods (Chapter 2) for more details.

### 4.3.1 *Drosophila* male GSCs show perturbations in nucleolar morphology with age

In *Drosophila melanogaster*, the rDNA is known to be organized into arrays found on the sex chromosomes, each of which spans approximately 2-3 Mb[95–97] (**Figure 4.1A**). First, we carried out immunofluorescence staining in whole-mount adult testes from wild-type flies for fibrillarin, an evolutionarily-conserved component of the nucleolus responsible for processing pre-rRNA[92,219,220], to assess nucleolar morphology in GSCs. In most of the cells in the testis, the appearance of the nucleolus was of a single round, compact structure within the nucleus. Specifically in GSCs, the nucleolus in the majority of cells was a single round structure that was approximately ≤2 μm in diameter (**Figure 4.1C**). This morphology was as expected per previous

descriptions of the nucleolus in other *Drosophila* tissues[129], and was considered "Normal." However, other abnormal nucleolar morphologies also appeared to be present in a small number of GSCs: nucleoli were "Fragmented" when more than one fibrillarin focus could be observed, or "Deformed" when nucleolar morphology was grossly abnormal in size or shape but ectopic fibrillarin foci could not be distinguished (**Figure 4.1C**).

When nucleolar morphology was scored, it was found that 89.2% of total GSCs in newly-eclosed flies possessed normal nucleoli. Strikingly, the percentage of GSCs with normal nucleoli gradually dropped to 64.1% as flies aged to 40 days (**Figure 4.1D**). The distribution of nucleolar morphology in GSCs showed a significant accumulation of abnormal nucleoli at every age point, with the most significant increases at later ages). The average number of GSCs per testis also dropped from 9.27±1.23 at 0-1 days old to 6.24±1.56 at 40 days. Reports of the median lifespan of male *Drosophila* vary from 30 to 50 days depending on their genetic background and the conditions they are maintained in[221–223], but we were confident that 40 days was a time point of sufficiently advanced experimental age.

In *S. cerevisiae*, cell division is asymmetric and produces a mother and a daughter cell, where mother cells preferentially accumulate abnormal nucleoli while their daughter cells inherit normal nucleoli[149,161]. *Drosophila* male GSCs also divide in a characteristically asymmetric manner, where one daughter cell remains attached to the hub and retains its stem cell identity while the other daughter cell is displaced away and proceeds to differentiate as a gonialblast (GB)[9]. The GSC and GB remain transiently connected via the spectrosome, marked by the Hts/Adducin-like protein[14–16] (see Chapter 3 for more detail), and GSC-GB pairs can be readily identified reflecting the direct products of an asymmetric GSC division. To determine whether age-associated changes in GSC nucleolar morphology are reflected in their daughter cells, we performed fibrillarin

staining on GSC-GB pairs. With two cells (GSC and GB) and two possible nucleolar morphologies (normal and abnormal/fragmented), four possible GSC-GB configurations can be observed (**Figure 4.2A-D**). In newly-eclosed flies (0-1 days old), 82.5% of GSC-GB pairs were symmetrically normal in nucleolar morphology, decreasing to 56.8% by 40 days old (**Figure 4.2A, E**). This was mostly accounted for by an increase in GSCs with abnormal nucleoli paired with GBs that retained normal nucleoli, from 12.9% to 30.9% (**Figure 4.2B, E**). However, GBs with abnormal nucleoli did also increase in frequency with age, though to a lesser degree than GSCs (**Figure 4.2C, D, E**). These results demonstrate that a clear perturbation of nucleolar morphology occurs in GSCs with age, and appears to preferentially affect GSCs before their daughter cells.

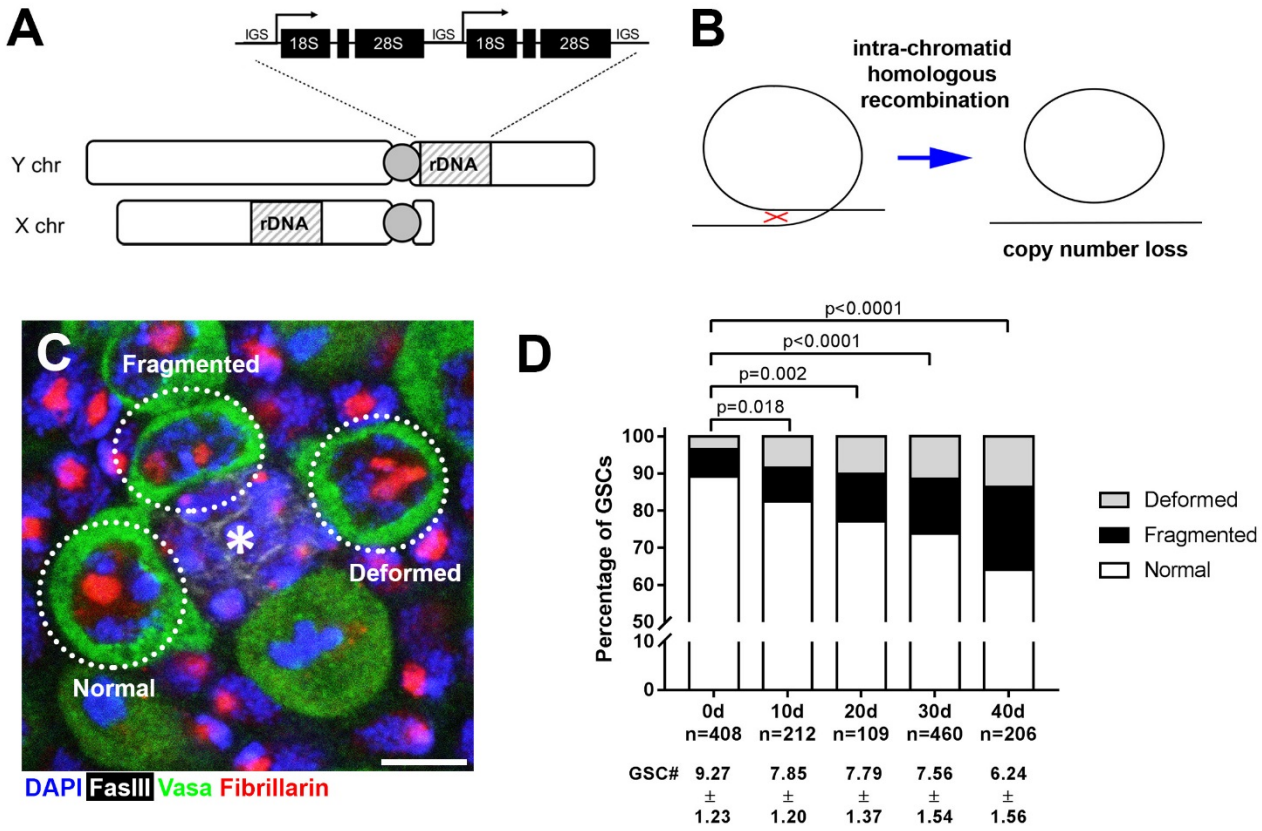


**Figure 4.1. *Drosophila* male GSCs show perturbations in nucleolar morphology with age**
**(A)** Graphical representation of the arrangement of *Drosophila* rRNA genes and the location of the rDNA on the sex chromosomes. **(B)** A model for how intra-chromatid homologous recombination (because GSCs spend the majority of their cell cycle in G2) can potentially result in endogenous copy number loss as well as generation of extrachromosomal circles.
**(C)** Immunofluorescence staining in whole-mount testes for the nucleolus in GSCs, marked by Fibrillarin (red). DAPI (blue), Vasa (green), FasIII (white). The hub is denoted by (*). GSCs with representative nucleolar morphologies are outlined. Bar: 5 μm. **(D)** Distribution of GSC nucleolar morphology during aging, graphed as a percentage of total GSCs scored (n listed underneath time point). For purposes of statistical analysis, values within the distribution were retained as whole counts to compare by chi-squared test (see methods), p-values listed.

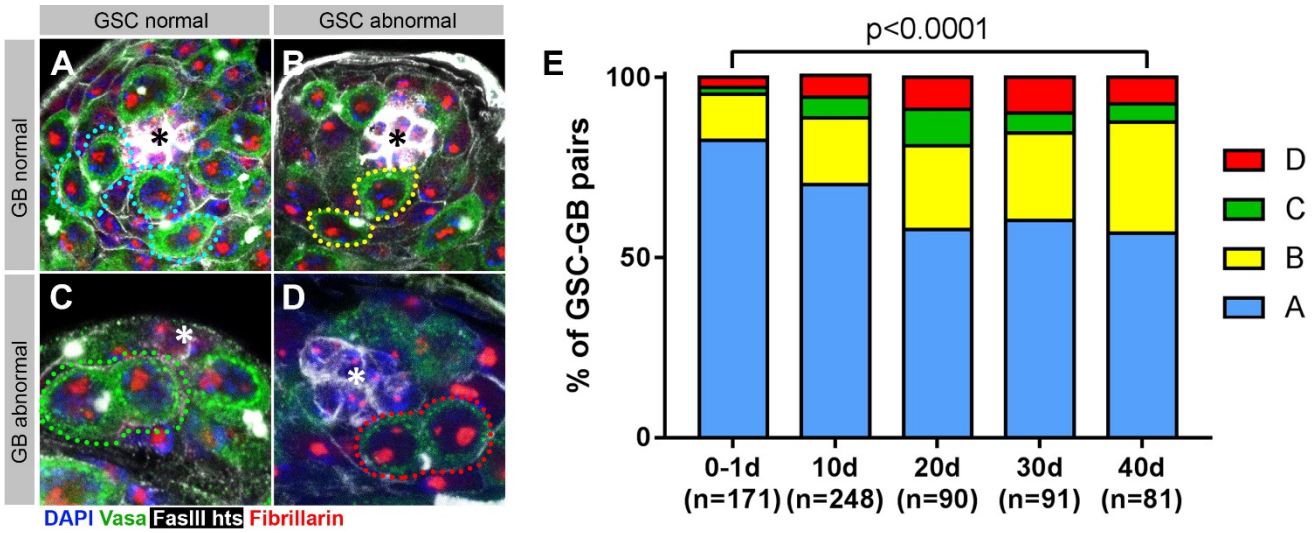


**Figure 4.2. GSCs with fragmented nucleoli accumulate before their daughter GBs**
**(A-D)** Representative images of all possible nucleolar morphologies for GSC-GB pairs (dotted outlines), identified by the presence of the bridging spectrosome (Hts/Adducin-like, white). DAPI (blue), Vasa (green), FasIII (also white), Fibrillarin (red). The hub is denoted by (*). **(E)** Distribution of GSC-GB nucleolar morphologies corresponding to the categories shown in A-D, graphed as percentage of total GSC-GBs scored (n listed underneath time point). For purposes of statistical analysis, values within the distribution were retained as whole counts to compare by chi-squared test (see methods), p-values listed.

### 4.3.2 Nucleolar fragmentation in GSCs reflects activation of X chromosome rDNA

The rDNA is also referred to as the nucleolar organizer region (NOR) because it was originally observed that within a cell, specific chromosomal regions were always associated with the nucleolus[90]. Eventually the identity of the NORs was discovered to be the rDNA arrays[97], and specifically the actively transcribed ones. A special type of rDNA silencing referred to as "nucleolar dominance" is known to occur, where entire chromosomal rDNA arrays are inactive and have no nucleolar organizing capability[105]. Typically in *Drosophila melanogaster* males, nucleolar dominance occurs where the Y chromosome rDNA is active and the X chromosome is inactive[143,144].

To examine the location of the NORs relative to the nucleolus, we carried out DNA fluorescence in situ hybridization combined with IF staining in whole-mount testes with probes complementary to unique satellite repeats known to be directly adjacent to the X and Y chromosome rDNA (**Figure 4.3A**). The 1.669 satellite consists of a simple $(AATAAAC)_n$ repeat specific to the Y chromosome, and the 1.688 satellite consists of a 359-bp sequence repeat unique to the X chromosome[224]. In GSCs with normal nucleoli, regardless of age, we observed a tight association of the Y chromosome with the nucleolus, with the X chromosome freely occupying nuclear territory near or away from the nucleolus (**Figure 4.3B**). This is consistent with the previously-published idea that the Y chromosome rDNA exerts nucleolar dominance over the X chromosome, and is solely responsible for rRNA transcription and for organizing the nucleolus in *Drosophila* male cells. However, in GSCs with nucleolar fragmentation, ectopic nucleoli were tightly associated with the X chromosome in 46/46 GSCs from 0-1 day old flies and 46/47 GSCs from 40 day old flies, suggesting that in these cases the X chromosome has gained some nucleolar organizing activity.

To directly test for rRNA transcription from the X chromosome, we genetically isolated the rDNA arrays from the X and Y chromosomes and identified four single nucleotide variants in their consensus coding and ITS sequences (see methods). From these, we generated pairs of fluorescently-labeled probes with all four variants and adapted a technique for detection of chromosome-specific rRNA *in situ* that we call SNP-FISH (single nucleotide polymorphism RNA fluorescence *in situ* hybridization) (**Figure 4.4A**). A variation of this technique has been used to detect SNVs from maternal versus paternal chromosomes in human cell culture[225]. In testes from X/O males that contain only the X rDNA, transcription of X rRNA is robustly detected and minimal cross-hybridization is observed from the probes designed to detect Y rRNA. Likewise in ovarioles from C(1)Dx/Y females that contain only the Y rDNA, Y rRNA is robustly detected but not X rRNA (**Figure 4.4B**). These experiments show that SNP-FISH has incredible specificity for detecting rRNA transcribed from the X versus Y chromosomes.

In order to directly assess rRNA transcription in GSCs with nucleolar fragmentation, we combined SNP-FISH with a fluorescent nucleolar marker, Nopp140-GFP, that co-localizes with fibrillarin and is possibly involved in pre-rRNA transcription or processing[181,226]. We found that in GSCs with normal nucleolar morphology as determined by Nopp140-GFP, the only detectable rRNA was from the Y chromosome. However in GSCs with fragmented nucleoli, one Nopp140-GFP focus was derived from the transcription of Y rRNA while the secondary Nopp140-GFP focus was composed entirely of X rRNA (**Figure 4.5A**). This clearly shows that nucleolar fragmentation in GSCs reflects activation of the X chromosome rDNA, which is normally repressed. The percentage of GSCs with active X and Y rRNA transcription also increased with age in a pattern that corresponds to the observed changes in GSC nucleolar morphology (**Figure 4.5B, C**). Note that GSCs with only X rRNA transcription were never observed, so for purposes

of statistical analysis only the categories of Y-only and XY-both transcription were considered. What these results show is that GSC nucleolar fragmentation reflects X rDNA activation on top of standard Y rDNA transcription, which occurs progressively in GSCs with age.

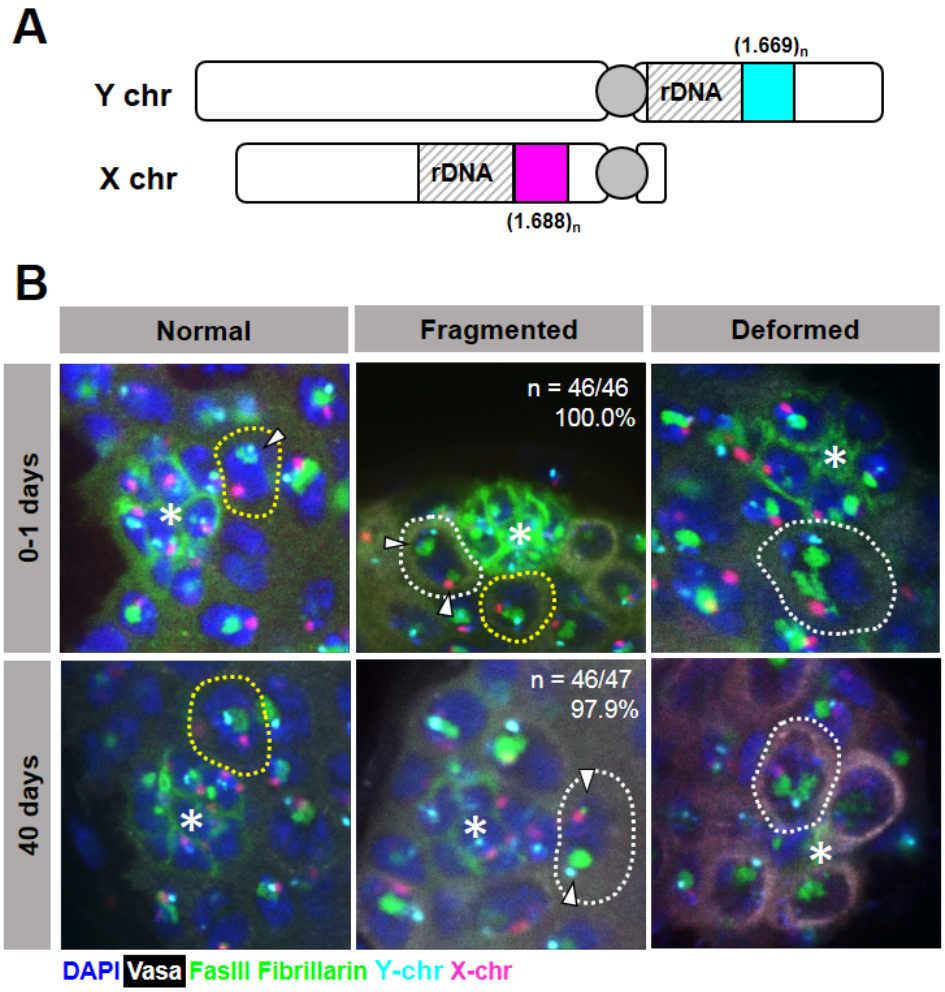


**Figure 4.3. Association of ectopic nucleoli with the X chromosome**
**(A)** Illustration of the location of the *Drosophila melanogaster* rDNA arrays on the sex chromosomes, with the adjacent chromosome-specific satellites. **(B)** DNA FISH for the X and Y chromosome and IF staining for nucleolar morphology in whole mount testes. GSCs with normal nucleoli (yellow outlines) and abnormal nucleoli (white outlines). Primary and ectopic nucleoli in fragmented GSCs (arrowheads). DAPI (blue), Vasa (white), FasIII and Fibrillarin (green), Y chromosome [1.669 satellite $(AATAAAC)_n$] (cyan), and X chromosome (1.688 satellite) (pink). The hub is denoted by (*).

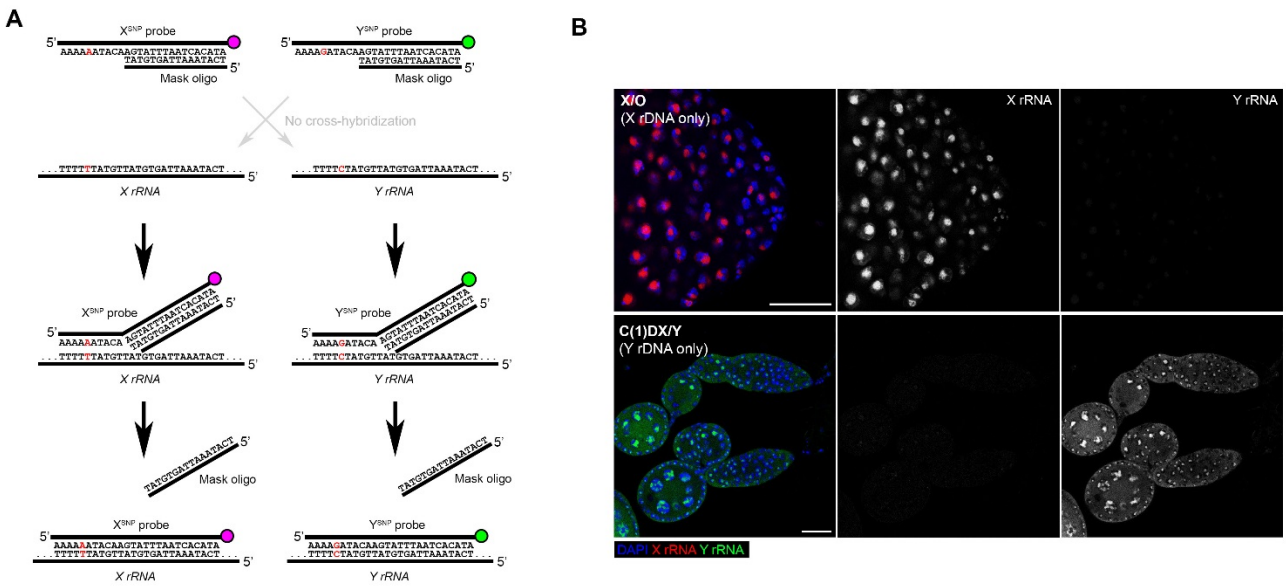


**Figure 4.4. SNP-FISH is highly specific for rRNA transcribed from the Y vs. X chromosomes**

**(A)** Schematic of the principle behind SNP-FISH for detecting rRNA transcripts. Shown as an example is a SNV in the 18S coding region of the X and Y rDNA. **(B)** Detection of X and Y rRNA using SNP-FISH in X/O and C(1)Dx/Y flies shows minimal cross-hybridization between probes. DAPI (blue), Y rRNA (green), X rRNA (red). Bars: 25 μm.

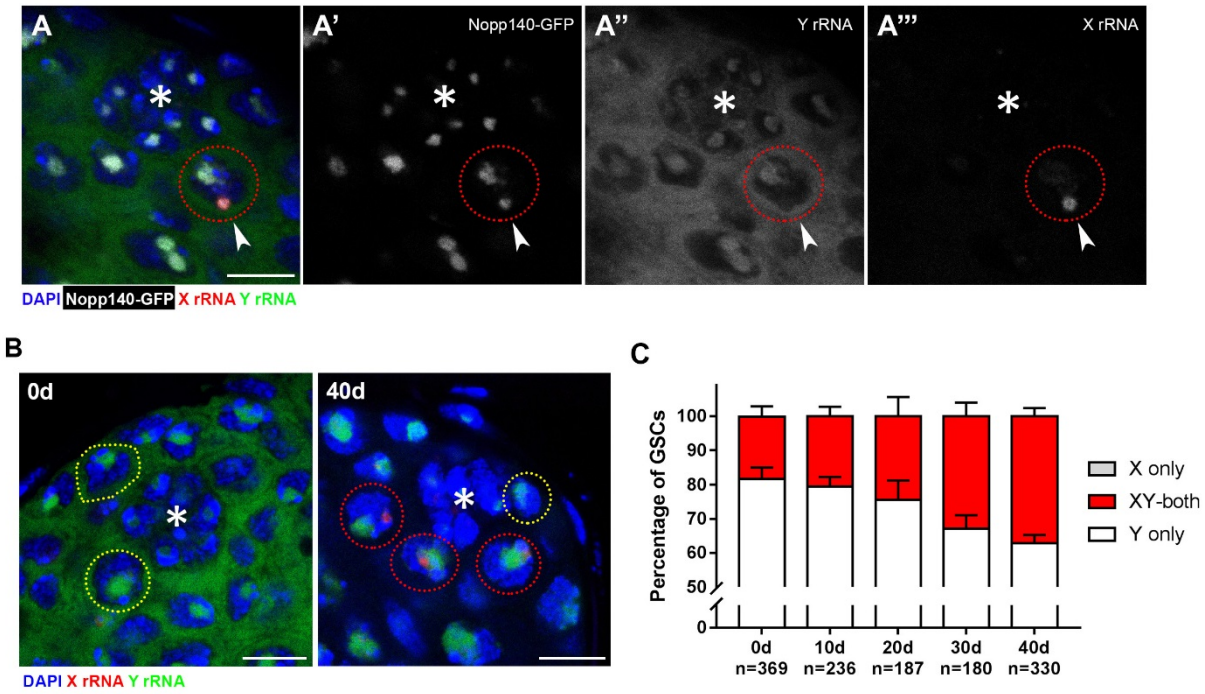


**Figure 4.5. Fragmented nucleoli in GSCs reflects activation of X chromosome rDNA**
**(A)** SNP-FISH with Nopp140-GFP, a fluorescent marker for the nucleolus. GSC with fragmented nucleolus (red outline), active X rRNA transcription (arrowhead). DAPI (blue), Nopp140-GFP (white), Y rRNA (green), X rRNA (red). The hub is denoted by (*). Bar: 7.5 µm. **(B)** SNP-FISH in GSCs from testes of flies at 0 and 40 days. GSCs transcribing Y rRNA (yellow outlines), GSCs transcribing both X and Y rRNA (red outlines). DAPI (blue), Y rRNA (green), X rRNA (red). The hub is denoted by (*). Bars: 7.5 µm. **(C)** GSC rRNA transcription during aging. Note that X-only transcription is never observed.

### 4.3.3 Transposon activation and replication delay in GSCs with activated X rDNA

While X chromosome rDNA activation in GSCs is clearly an age-associated phenotype, the biological implication was still unclear. Furthermore, the reason for nucleolar dominance of the Y rDNA and repression of the X rDNA in the first place was unknown. We hypothesized that the preference for the Y rDNA might reflect some detrimental effect of X rDNA transcription.

It is known that two retrotransposable elements, R1 and R2, selectively integrate into the rDNA[227–229]. While the rDNA arrays on the X and Y chromosomes are thought to be genetically identical, it was shown that the retrotransposable elements are eliminated more slowly from the X chromosome rDNA and as a result a greater fraction of the X rDNA is believed to be inserted[230–232]. We confirmed in our stocks by qPCR that the rate of R1 element insertion was approximately ten times higher in X rDNA than the Y rDNA (**Figure 4.7A**). We performed RNA fluorescence *in situ* hybridization to detect expression of R1 and R2 elements in GSCs, combined with Nopp140-GFP to determine nucleolar morphology (**Figure 4.6A**). GSCs with fragmented nucleoli were frequently found to have cytologically detectable expression of R1 and R2 retrotransposons; compared to GSCs with normal nucleoli, the rate of R1 and R2 expression in fragmented GSCs was approximately 3 and 5 times higher respectively (**Figure 4.6B**). These results show that X rDNA-activated GSCs also activate retrotransposable elements. Based on this, it is tempting to speculate that the nucleolar dominance of Y rDNA might reflect the preference of GSCs to first transcribe uninserted copies of rRNA genes found on the Y chromosome.

Assessing stem cell function can be broadly broken into determining their abilities to divide, self-renew, and differentiate. To determine whether nucleolar fragmentation/X rDNA activation affect the ability of GSCs to divide, we pulsed testes *ex vivo* with EdU to assess S-phase index. EdU is a thymidine analog incorporated into newly-replicated DNA[233,234] and, depending

on the length and beginning/end of the pulse relative to the total length of S-phase in a cell, can reflect the portions of the cell's genome that were successfully replicated during the pulse (see methods). An interesting observation was that during S-phase in GSCs, the heterochromatin, marked by H3K9 dimethylation, clusters around the nucleolus. Because of this discrete organization during replication and since our EdU pulse was significantly shorter than the duration of S-phase, the completion of distinct phases of euchromatin and heterochromatin replication could be observed (**Figure 4.6C**). It is generally accepted that euchromatin is replicated during early S-phase and the genomic heterochromatin, including the inactive rDNA, is replicated during late S-phase[235–237]. Thus a temporal order of genome replication in GSCs can be tentatively inferred, where completion of early S-phase euchromatin replication is reflected by a lack of EdU on the H3K9 dimethyl (H3K9me2 EdU-), late S-phase heterochromatin replication completion is reflected by presence of EdU only on the H3K9 dimethyl (H3K9me2 EdU+), and the successful transition between early and late S-phase is seen in GSCs where the entire nucleus is EdU-positive (All EdU+). In GSCs with fragmented nucleoli, an accumulation of GSCs was observed where euchromatin replication was occurring but heterochromatin replication had not begun (**Figure 4.6D**). This suggests that in GSCs that display nucleolar fragmentation and X rDNA activation, an underlying event is causing either an extension of euchromatin replication or a significant delay in the initiation of heterochromatin replication. From these data it is difficult to determine what that insult is, but it does suggest the occurrence of large-scale genomic changes that affect the timing of replication. One possible link is that the rDNA has been shown to influence global chromatin states across the genome, with rDNA deletion resulting in loss of heterochromatin-mediated gene silencing at distant loci[183]. Thus it is conceivable that what we observe as alterations

in genome replication in X rDNA-activated GSCs reflects rDNA disruption that affect the balance between heterochromatin and euchromatin in the nucleus.

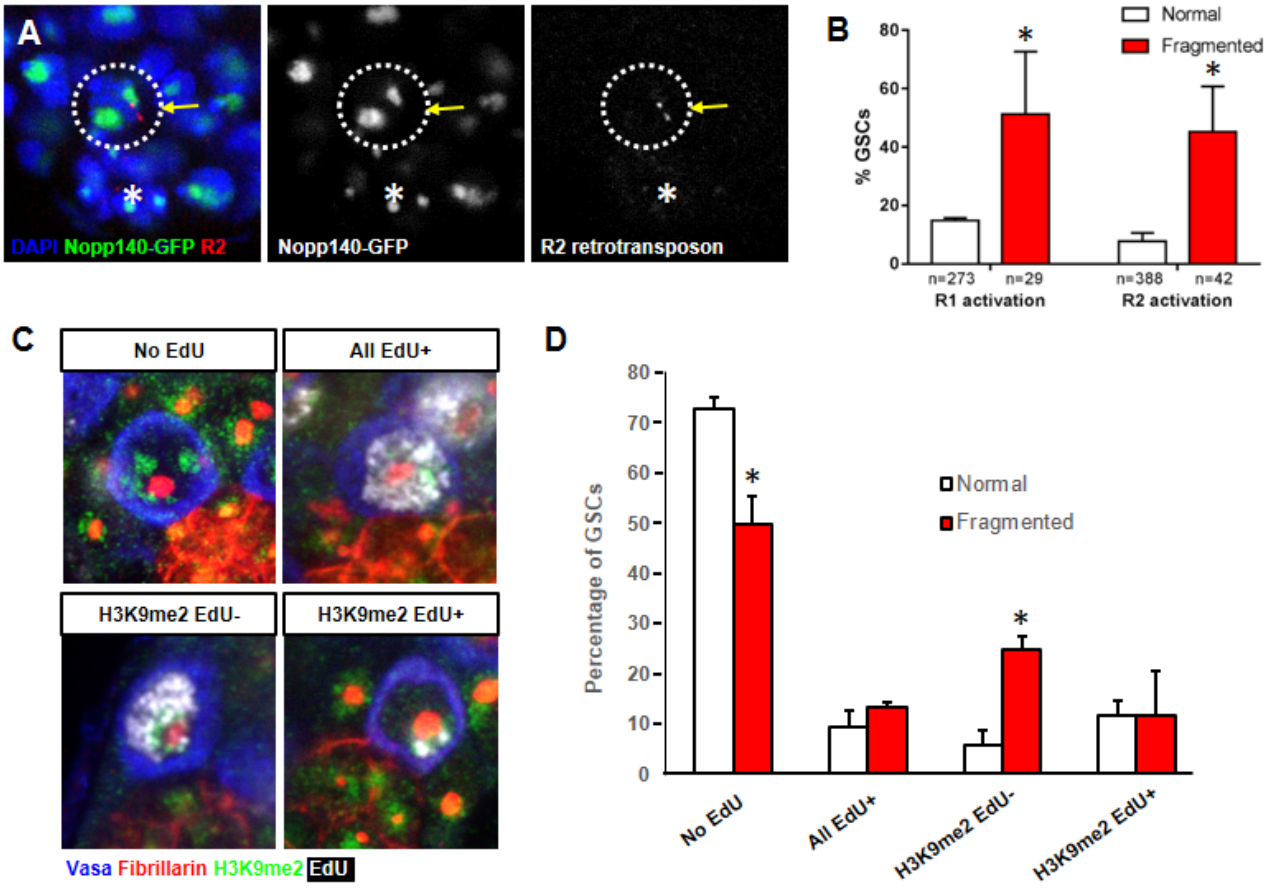


**Figure 4.6. Transposon activation and replication delay in GSCs with activated X rDNA**
**(A)** Detection of R2 retrotransposon expression by RNA FISH. GSC with fragmented nucleolus (dotted outline), R2 transcript (arrow). DAPI (blue), Nopp140-GFP (green), R2 (red). The hub is noted by the (*). **(B)** R1 and R2 retrotransposon activation in GSCs with normal and fragmented nucleoli (Mean ± SD, p-value * ≤0.05 t-test). **(C)** EdU staining can visualize the completion of early and late S-phase in GSCs. EdU (white), Vasa (blue), Fibrillarin and FasIII (red), H3K9 dimethyl (green). **(D)** Distribution of time within S-phase in GSCs with normal and fragmented nucleoli (Mean ± SD, p-value * ≤0.05 t-test).

### 4.3.4 rRNA gene copy number is lost in germ cells during aging

In *Drosophila*, individual rRNA genes that are inserted with R1/R2 elements are typically repressed when there are an excess number of functional gene copies, but it is thought that if the uninserted gene copies are somehow unable to produce sufficient rRNA, the R1/R2 inserted copies must be activated[238]. It has been extensively shown in yeast that stability of the rDNA is compromised during aging, with increased rates of recombination that likely produces loss of rDNA on the endogenous chromosome as well as extrachromosomal rDNA circles[120,121,145]. As a result, rDNA instability can manifest as variation in gene copy number and rDNA array size. In yeast, it was shown by pulsed field gel electrophoresis that chromosome XII size varied greatly between old mothers and young daughters, the size variation of which is mostly due to changes in the length of the rDNA array present on that chromosome[160]. Thus, we hypothesized that similar rDNA instability may occur in GSCs during aging, and that activation of the normally-repressed X rDNA is a compensatory response to this instability in the active rDNA.

First, we again genetically isolated the X and Y chromosome to compare their rDNA arrays. Using a previously published qPCR-based method for quantifying repetitive sequences and rRNA gene copy number[182,184], we found that the distribution of the rRNA genes was comparable between the X and Y chromosomes, as expected (**Figure 4.7A**). The Y chromosome contains a slightly higher relative copy number of rRNA genes. An approximately 10x greater rate of R1 element insertion in the X rDNA was also observed, consistent with previous reports[230,231]. Surprisingly, we found an unequal distribution in the 240-bp intergenic spacer (240-IGS) that is in between the individual rRNA genes within the rDNA array. As a control for whether successful isolation of the sex chromosomes had occurred, we used the 359-bp repeating 1.688 satellite which

is present only on the X chromosome and in small quantities on the compound X used to isolate the Y chromosome[224].

A significant reduction in rRNA gene copy number was observed by qPCR when comparing whole testes genomic DNA from 0-1 day and 40 day old flies (**Figure 4.7B**). This copy number loss was observed across all the mature rRNA genes encoded for in the 45S cistron, suggesting that the loss of rDNA in germ cells occurs in whole gene units rather than selectively in certain segments. Interestingly, the copy number of R1 and R2 retrotransposable elements was not seen to decrease with age, suggesting that the rDNA copy number loss primarily occurs in uninserted, actively-transcribed rRNA genes (**Figure 4.7B**). While this quantification data was from bulk germ cells, we attempted to improve our resolution by measuring relative rDNA quantity on the Y and X chromosomes from individual germ cells. Using DNA FISH on chromosome spreads from mitotic spermatogonia and meiotic spermatocytes (identified based on chromosome condensation patterns), we were able to clearly distinguish the rDNA arrays from the Y versus the X chromosome (**Figure 4.7C**). Quantification of fluorescence signal (see methods) revealed that at 0 days, the ratio of Y:X 18S rDNA was 1.38 ± 0.35 but this ratio dropped to 0.70 ± 0.25 by 40 days (**Figure 4.7D**). The Ybb- chromosome, a variant Y chromosome with a known partial rDNA deletion, was crossed with our X chromosome to serve as a positive control (mean Ybb-:X rDNA ratio 0.46 ± 0.08). Signal intensity for the 240-IGS was also quantified, and at 0 days showed a Y:X ratio of 2.83 ± 0.63 (**Figure 4.7E**), a result that corresponded remarkably well to the quantification by qPCR (**Figure 4.7A**). Unfortunately, we were only capable of achieving single cell rDNA quantification in spermatogonia, and not their progenitor GSCs.

These data demonstrate a remarkable loss of rRNA gene copy number in *Drosophila* male germ cells during aging, and specifically reduction of Y chromosome rDNA can be seen in

individual spermatogonia. In addition, we see that this loss likely involves only the rRNA gene copies that are not inserted by R1 or R2 elements. Thus, we propose that the age-associated activation of X rDNA in GSCs likely represents an attempt to compensate for the loss of functional rDNA on the Y chromosome due to rDNA instability in the active array.

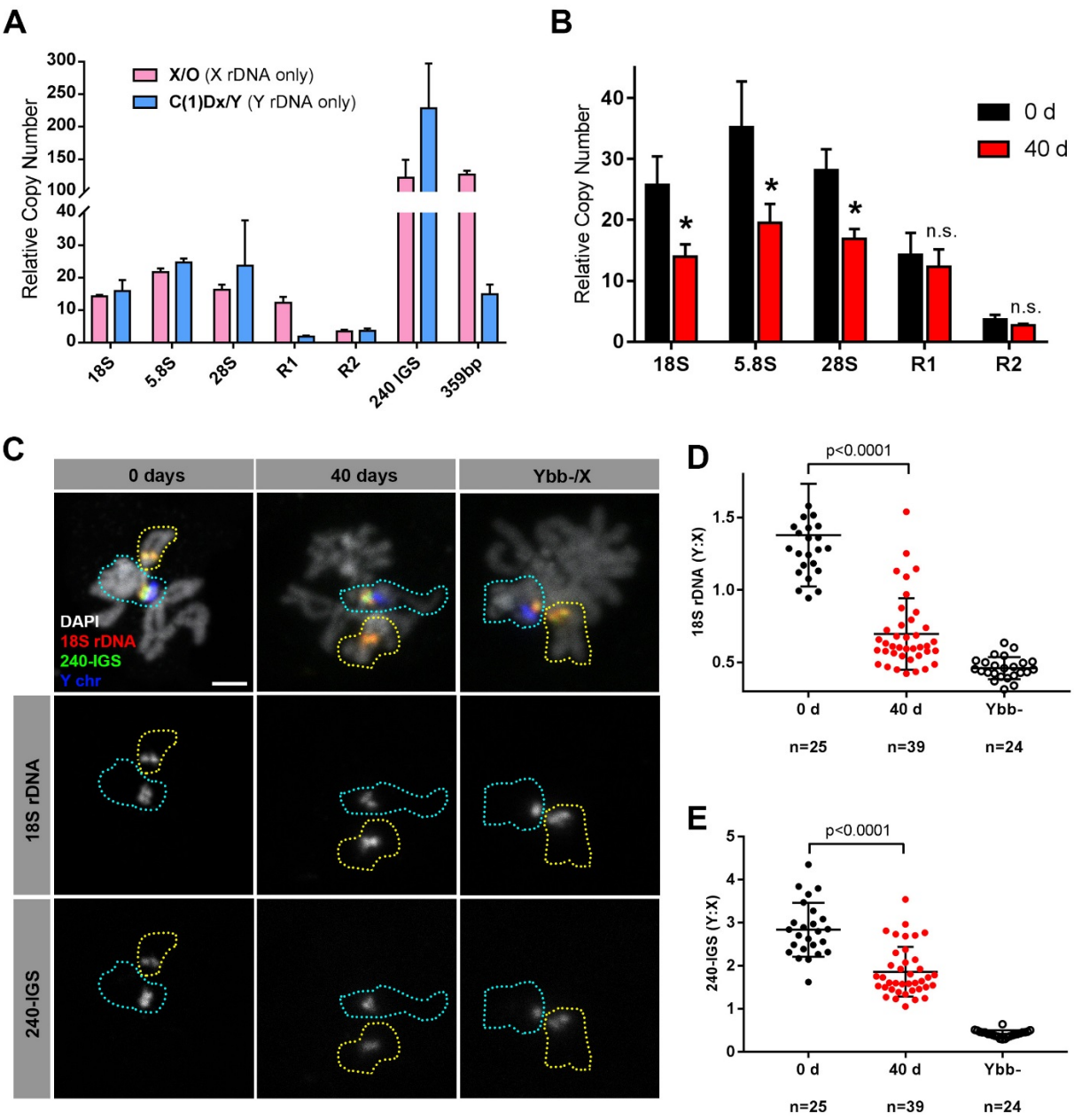


**Figure 4.7. rRNA gene copy number is lost in germ cells during aging**
**(A)** qPCR comparing features of the X and Y chromosome rDNA arrays. Mean ± SD. **(B)** rRNA gene copy number quantification by qPCR from 0 day and 40 day old testes (Mean ± SD, p-value * ≤0.05 t-test). **(C)** Chromosome spreads from mitotic spermatogonia. X chromosome (yellow outline), Y chromosome (cyan outline). DAPI (white), 18S rDNA (red), 240-bp IGS (green), $(AATAAAC)_n$ (blue). Bar: 2.5 µm. **(D)** Relative Y:X signal intensity for the 18S rDNA. Mean ± SD, t-test. **(E)** Relative Y:X signal intensity for the 240-bp IGS. Mean ± SD, t-test.

### 4.3.5 GSC nucleolar morphology and rDNA loss is heritable

If gametogenesis is completed unimpaired, then large-scale changes in genomic rDNA content in germ cells during aging should be inherited in the next generation. To test this, we aged flies until they were 40 days old and allowed them to mate, collecting their progeny (the new $F_1$ generation, derived from old parents) (**Figure 4.8A**). qPCR on testes genomic DNA collected from newly-eclosed $F_1$ flies showed a significant reduction in the copy number of mature rRNA genes encoded for in the 45S cistron when compared to newly-eclosed flies from the previous $P_0$ generation (**Figure 4.8B**). The number of R1 and R2-inserted gene copies was not reduced. When comparing the 0 day old $F_1$ rDNA content to the 40 day old $P_0$ which were their parents, there was no significant difference. This suggests that the bulk germ cells that experience reduction of rDNA copy number in old flies complete gametogenesis, and this copy number reduction is heritable.

Nucleolar morphology in $F_1$ GSCs at 0 days is also perturbed, with only 59.1% of GSCs displaying normal nucleolar morphology (**Figure 4.8C**). Compared to $P_0$ GSCs at 0 days (89.1% normal) this is a significant four-fold increase in GSCs with abnormal nucleolar morphology at the same age. However, distribution of GSC nucleolar morphologies in newly-eclosed $F_1$ and their 40 day old parents was nearly identical. X rRNA transcription in $P_0$ and $F_1$ GSCs by SNP-FISH recapitulated what was seen by nucleolar morphology (**Figure 4.8D**). Surprisingly though, as $F_1$ flies were aged, their GSCs underwent an unexpected recovery of nucleolar morphology between 0 and 10 days before starting to worsen again (**Figure 4.8E**). By 40 days, nucleolar morphology in $F_1$ GSCs is comparable to their appearance at 0 days ($p = 0.599$). These results show that GSC nucleolar morphology and rDNA copy number in germ cells are both heritable, and $F_1$ progeny from 40 day old parents resemble their parents in both reduced rDNA quantity and perturbed GSC nucleolar morphology and X rDNA activation.

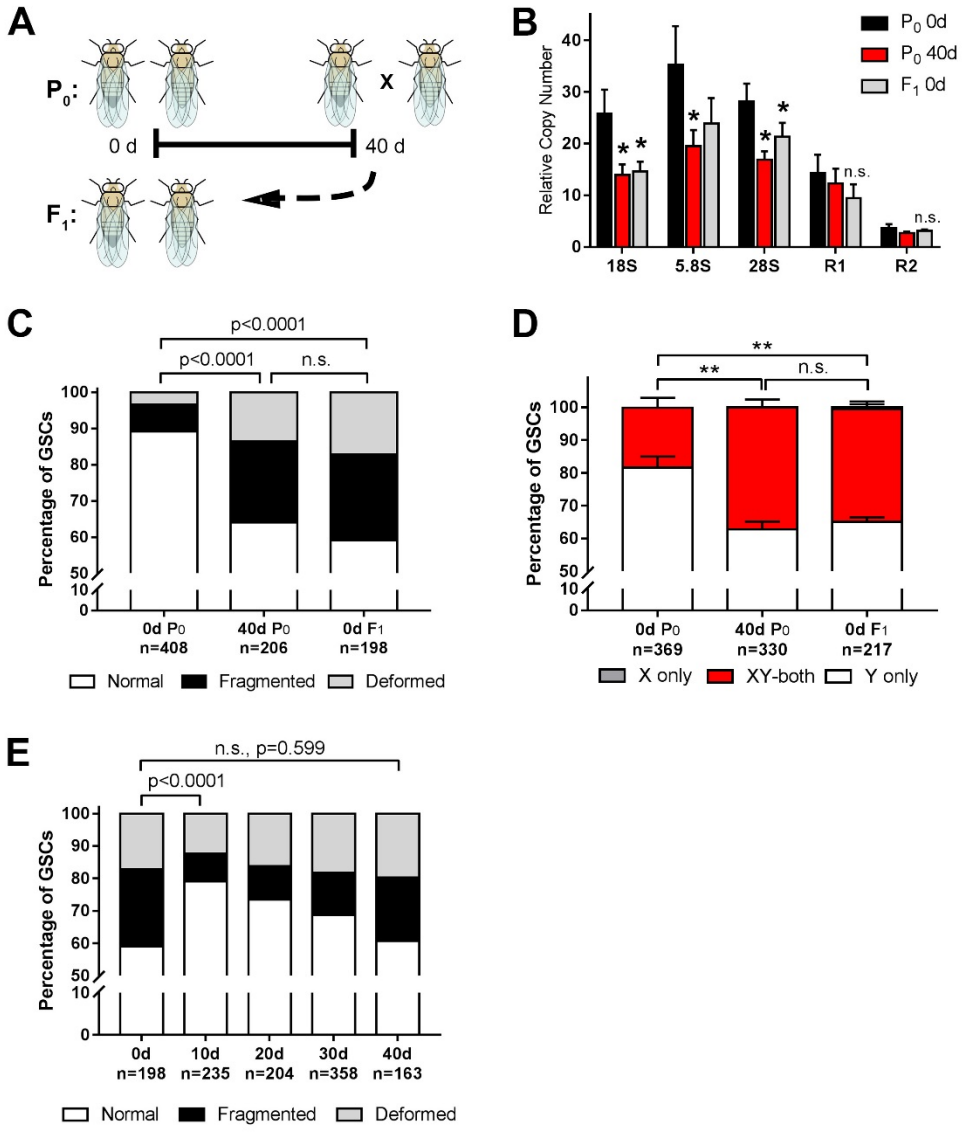


**Figure 4.8. GSC nucleolar morphology and rRNA gene copy loss is heritable**
**(A)** Scheme for aging of flies and collection of $F_1$ progeny from old parents. **(B)** rDNA quantification by qPCR in 0 day $P_0$, 40 day $P_0$, and 0 day $F_1$. Mean ± SD, * ≤ 0.05, t-test. **(C)** GSC nucleolar morphology in newly-eclosed $F_1$ flies is comparable to that of old $P_0$. Chi-squared test, * ≤ 0.05. **(D)** rRNA transcription by SNP-FISH. Mean ± SD, * ≤0.05, t-test. **(E) D**istribution of $F_1$ GSC nucleolar morphology during aging, graphed as a percentage of total GSCs scored (n listed underneath time point). For purposes of statistical analysis, values within the distribution were retained as whole counts to compare by chi-squared test (see methods), p-values listed.

## 4.4 Discussion

Here we show at both the single cell and whole tissue level that rDNA loss occurs in *Drosophila* male germ cells during aging. To the best of our knowledge, this is the first time such changes have been shown to occur, and provides the first direct evidence for a role for rDNA instability during aging in a multicellular organism.

In germline stem cells, we showed that nucleolar fragmentation occurs during aging like it does in yeast. However the nature of this nucleolar fragmentation seems to be inherently different, reflecting activation of dormant nucleolar organizers on the X chromosome rDNA rather than the formation of extrachromosomal rDNA, which is thought to underlie fragmentation in yeast. It is possible that extrachromosomal circles of rDNA are also "looped out" in GSCs, but it is currently impossible to specifically collect enough GSCs for biochemical verification. In addition, any experiments involving GSCs are technically limited to those that maintain the testis tissue architecture, which is necessary for identifying GSCs from their daughter cells. However, we imagine that the fundamental cause of nucleolar fragmentation is likely still the same: the inherent instability of the tandem repetitive rDNA array.

Our data suggests that this rDNA instability is primarily occurring with the Y chromosome rDNA, as the ratio of Y:X 18S rDNA drops significantly in spermatogonia with age and reflects the loss in total rRNA gene copy number in bulk germ cells. However, why the Y chromosome rDNA is affected moreso than the X chromosome is an unanswered question. The rDNA is known to be a difficult genomic region to replicate, owing to its repetitive nature and high rate of transcription. Collisions between the replication and transcription machinery can result in DNA double strand breaks and chromosome instability[241]. In yeast, a replication fork block protein, Fob1, exists to ensure that rDNA replication is unidirectional and in the same direction as

transcription to minimize the likelihood of these collisions occurring[108,242,243]. However, no Fob1 homolog appears to exist in *Drosophila* and it is unknown whether alternative methods of protecting against replication-transcription conflicts have evolved. Therefore, it is conceivable that the preferential loss of Y rDNA is linked to the fact that it is the actively transcribed array in *Drosophila*, opening it up to potential replication-transcription conflicts during S-phase. Thus we can imagine a "use it and lose it" scenario when it comes to rDNA in GSCs and germ cells with age. Also, since the number of genes with inserted R1 and R2 retrotransposable elements does not decrease while the total rRNA gene copies do, that means the relative fraction of inserted genes increases with age, which is likely to have important implications.

While we have shown that large-scale changes in rDNA quantity occur in germ cells during aging and corresponds to alterations in rRNA transcription, it is possible that existing rDNA is being modified or controlled epigenetically as well. In fact, it is known that silencing of individual rRNA genes in *Drosophila* is epigenetically controlled by a combination of heterochromatin-mediated repression and RNA interference[129]. Though it is unclear whether individual rRNA gene silencing and chromosome-wide repression of rDNA (nucleolar dominance) are established using the same mechanisms, it is almost certain that activation of the X rDNA during aging involves changes in its epigenetic state. While we propose that the impetus for these epigenetic changes is a reduction in functional rDNA on the Y chromosome, it is also possible that X rDNA activation simply reflects a global loss of constitutive heterochromatin that has been observed in aging/senescent cells, including in pericentromeric satellite DNA similar to the types of sequences that flank the rDNA[244–246]. Whether activation of the X rDNA is selectively carried out or simply a byproduct of global changes to chromatin structure during aging is a question that requires further study.

A fascinating and unexpected discovery was the apparent recovery in nucleolar morphology in GSCs from $F_1$ flies that start with a reduced quantity of rDNA (**Figure 4.8E**). What that suggests is that the activated X rDNA is re-repressed in GSCs, and it is tempting to speculate that this is because at least partial recovery of the Y rDNA has occurred. In fact, amplification of deficient rDNA arrays has been observed to occur in the pre-meiotic population of the *Drosophila* male germline from classical genetics studies[247–249]. More specifically, the mechanism of this rDNA amplification has been thought to be unequal mitotic sister chromatid exchange[249], which is the exact mode by which rRNA gene copy number is increased in *S. cerevesiae*[110–113,250]. Thus it is conceivable that rDNA magnification and unequal sister chromatid exchange is occurring at the level of the GSC. In fact, our lab has previously shown that GSCs selectively retain one sister chromatid of the X and Y chromosomes during cell division[251], and it is possible the choice of which sister chromatid is retained has to do with the rDNA. The asymmetry in nucleolar morphology between GSCs and GBs is certainly suggestive of asymmetric segregation of rDNA quantity/rDNA stability between the two (**Figure 4.2**). However, single-cell rDNA quantification must be achieved in GSCs and GBs before definitive conclusions can be drawn.

The unique genomic organization and structure of the rDNA has been remarkably conserved between eukaryotes, but these unique features are also known to present challenges and are a notoriously fragile chromosomal site[252]. The changes that occur in the rDNA in yeast during aging due to this fragility have been well-documented, and now we present evidence for similar dynamicity in the rDNA of *Drosophila* male germline stem cells and germ cells, suggesting that the role that rDNA instability plays during replicative aging may have been conserved as well. This has an important implication for organismal aging of multicellular organisms, where some of the longest-lived and mitotically-capable cells are tissue stem cells. Perturbations in nucleolar

morphology, decondensation of rDNA foci, and accumulation of double strand break markers within nucleoli were observed in old hematopoietic stem cells from mice[253]. In human peripheral white blood cells, which are derived from HSCs, wide variation in rDNA copy number was observed within individuals[218]. Thus we speculate that rDNA instability during aging might occur in adult tissue stem cells from any multicellular organism that has organized its rRNA genes into tandem arrays. It awaits future studies to determine whether this rDNA instability is a direct cause of cellular senescence like it is in yeast, and contributes to organismal aging.

# Chapter 5

# Conclusions and Future Directions

The results described in this dissertation provide insights into germ cell biology from two very different viewpoints. The first is a role for germ cell connectivity in sensitizing the germline to DNA damage, allowing for sharing of a death-promoting signal between members of an interconnected germ cell cyst when a cell is damaged. This result offers that two broadly observed but unexplained features of germ cells in most organisms, interconnected germ cells and a greater sensitivity to DNA damage in the germline than the soma, may actually provide reasons for one another. This idea assigns a new function for why such robust conservation of connectivity has occurred, and explains it in a way that potentially applies to all sexes instead of just in females that use oocyte nursing. The way in which this question was conceived revolves around the idea that if something is conserved (germ cell connectivity), *why* is it conserved in the first place?

The second insight contained in this dissertation is that the rDNA is a dynamic genomic element in *Drosophila* germ cells, experiencing changes in transcription, chromosome-wide silencing, and genomic quantity during aging. rDNA instability had been well-documented in replicative aging in yeast, but had never been thoroughly explored in multicellular organisms. My work suggests that rDNA instability may be a conserved feature of replicative aging in eukaryotes, with particular relevance to stem cell aging. In this case, evolution was used as a hint to frame our question: if one thing is conserved (the genomic organization of the rDNA in eukaryotes), then are

the consequences of it also conserved (rDNA instability)? Or have alternative ways to compensate evolved?

The studies described in this dissertation have provided insight into what happens to the *Drosophila* male germline in response to various insults, like DNA damage and aging. More broadly, though, they are based on conserved phenomenon across eukaryotic species and therefore have implications for more than just *Drosophila*. At the same time, there are many questions left to be answered that can be addressed in the experimental system. In this chapter, I will outline what I see as outstanding questions stemming from this work and important opportunities for future studies.

## 5.1 Identification of proteins trafficked between germ cells

As briefly described in Chapter 1.2.2, germ cell connectivity likely serves many functions beyond oocyte nursing. The propagation of a death-promoting signal via the fusome in response to DNA damage is an example of a previously unidentified role for connectivity, but the other functions that connectivity provide have yet to be elucidated. At the same time, propagation of death between interconnected germ cells also illustrates another intriguing subject for future study: determining what is and is not transmitted between connected germ cells, and through what means.

I showed in Chapter 3 that propagation of the death-promoting signal between connected germ cells is achieved through the fusome, and that the presence of ring canals alone (the physical openings/bridges between the germ cells) was insufficient to mediate synchronized all-or-none death. This is consistent with reports of how the fusome facilitates cell cycle synchronization within a cyst in the *Drosophila* ovary, sharing cell cycle regulators[71]. Because cytoplasmic connections in the form of ring canals are insufficient to allow for cell cycle synchronization or

all-or-none death, these data suggest that the fusome not only supports germ cell connectivity, but may actually increase the efficiency of sharing of the signals it does allow through. On the other hand, the fusome runs through the openings provided by the ring canals and likely also acts as a selective barrier; organelles like mitochondria and centrosomes from nurse cells cannot migrate into the developing oocyte until the fusome disintegrates[75,76]. These examples highlight the need for further studies to determine what is and is not shared between interconnected germ cells, and what is specifically allowed by the fusome versus ring canals. Determining what is communicated between germ cells will also provide us hints as to what other purposes germ cell connectivity serve.

The advantage of the *Drosophila* system is that germline-specific components of the fusome and ring canals exist, like the Ovhts protein produced from the *hu-li tai shao* gene which is cleaved to Hts-Fus/Hts-RC (see Chapter 2). While expression of *hu-li tai shao* can be found in muscle, central nervous, and other tissues of the adult fly, Ovhts is restricted to the ovary[254,255]. Several studies of other proteins in somatic tissues have identified Hts/Adducin (not the Ovhts isoform) as an interacting partner by mass spectrometry and biochemical methods[256,257], but there has been no systematic study looking for Hts-interactors in the germline that could identify candidate proteins that associate with the fusome. The *Drosophila* ovary would be an ideal system to do this in, because the fusome (and Hts-Fus) is only present in the germarium and mitotic cystocytes, while Hts-RC on ring canals is the only *hts* gene product in later egg chambers. However, many proteins that localize to the fusome have been seen to do in a cell-cycle dependent manner; cyclin A accumulates on the fusome in the cystocytes during G2[71] and the centrosomes and mitotic spindles orient towards the fusome in spermatogonia specifically during metaphase[258]. These examples simply illustrate the need to confirm spatial and temporal localization of potential

fusome and ring canal interacting proteins following identification by large-scale methods. The possibility also exists that some fusome/ring canal-associated proteins may differ between males and females, and almost certainly between developmental stages during gametogenesis. However, the reagents needed to carry out these studies are excellent and readily-available.

By and large, the most definitive experiments showing whether a protein is trafficked between germ cells have not been done. These would certainly involve live tissue imaging of germ cell cysts in conjunction with fluorescently-labeled or photoactivatably-tagged candidate proteins. The principle has been demonstrated to work in the *Drosophila* ovary, where PA-GFP was shown to be able to diffuse to sister cells within a stem cell cyst under conditions of delayed abscission between the GSC and the cystoblast[72,259].

All of these lines of study would provide pieces toward attempting to answer a more fundamental question: if germ cell connectivity exists to share things between germ cells, why must it be shared in the first place? Or in other words, what is it about synchronization (of cell cycle, meiotic entry, etc.) or equalization (levels of certain proteins, signaling) amongst a cyst that is needed so badly that promotes the conservation of germ cell connectivity? Germ cell cysts form almost universally during the pre-meiotic stages of gametogenesis, and connectivity is maintained through meiosis in males but broken down in females[186]. Based on this, it is not unreasonable to suspect that the fundamentally "germ cell" reason for the existence of syncytial germ cell cysts is in these pre-meiotic stages, and its maintenance through male meiosis is reflective of a male-specific need (like haploid genome complementation in spermatids[77]) rather than a universal role for all germ cells. An interesting idea to think about is that, while all germ cells within a cyst are thought to be genetically identical, genomic content is only one of many factors that could contribute to a gamete's overall fitness. Likewise, each round of genome replication that occurs

during germ cell expansion presents an opportunity for the genetic equivalence of cyst members to diverge. Remaining connected during the proliferative mitotic phases of gametogenesis could ensure that no sister cell gets too far ahead of the others, essentially leveling the playing field amongst siblings. This could reduce the ability of a spontaneous germline mutation to gain an early competitive advantage and propagate. Furthermore, because fusome mutants in *Drosophila* and TEX14 mutant male mice are all sterile[41,260], it implies that germ cell connectivity plays a role in normal gametogenesis that is completely indispensable. Regardless, why germ cells are connected to one another remains an interesting question and provides direction for future studies.

## 5.2 Outstanding questions regarding the rDNA in *Drosophila* male germ cells

I showed in Chapter 4 that nucleolar fragmentation and X rDNA activation occurs in germline stem cells during aging, and that rDNA quantity is decreased in differentiating germ cells. Because of that, I speculated that rDNA instability and loss was occurring in aging GSCs, which is the underlying reason why X rDNA was being activated in GSCs and total rDNA quantity was seen to decrease in spermatogonia. However, at least two direct questions arise from the results presented and offer evident topics to be addressed in the immediate future.

The first question that arises is the classic discrimination between correlation and causation; a decrease in Y chromosome rDNA is observed in germ cells and I speculated but did not definitively show that this is why the X chromosome rDNA is activated in GSCs, likely as a compensatory response to this loss. Thus, to close the gap in this scientific logic, it becomes important to show that by reducing Y rDNA quantity, X rDNA activation and nucleolar fragmentation can be directly induced in GSCs. In *S. cerevisiae*, homologous recombination is much more efficient than in complex eukaryotes and is capable of readily inserting reporters and

other elements into the rDNA[149,250,261], which could potentially allow for inducible deletions. However, in *Drosophila* it is much harder to selectively target a repetitive region for specific insertions or deletions, which has been one longstanding obstacle to studying the biology of rDNA and other repetitive genomic elements. However, one of the most powerful aspects of *Drosophila* as a system is its assembly of genetic tools, and historical collection of Y chromosomes with complete or partial rDNA deletions have been previously generated by ionizing radiation-induced deletions and rearrangements. Experiments are already underway to introduce the same Y rDNA partial deletion chromosome as in **Figure 4.7** to our wild-type X chromosome to see if nucleolar fragmentation and X rDNA activation in GSCs is increased. Thus a Y chromosome with specific disruption of rDNA reminiscent of what is seen in old germ cells can be introduced into a young background, while eliminating other possible extrinsic contributors like age-associated decline in niche signaling[262,263] or intrinsic cellular changes[264]. These experiments are already underway. However, the ideal scenario to test for the role of rDNA instability in aging of GSCs would involve being able to inducibly delete or destabilize rDNA in clones in the testis, creating a mosaic tissue where nucleolar fragmentation and X rDNA activation can be compared as well as other metrics of "stem cell function" like division and maintenance with age.

The second question that arises from the observation of large-scale rDNA changes in germ cells during aging is what the transgenerational outcomes are. In yeast, activation of the meiotic program has been shown to renew replicative lifespan in aging mother cells, thought to be caused by rDNA instability[161]. However, we observed that this may not be the case in *Drosophila* males, since progeny produced from old parents still have reduced rDNA quantity and unusual rRNA transcription patterns (**Figure 4.8**). However, nucleolar morphology is seen to transiently recover in the same $F_1$ implying re-repression of the X rDNA, which begs the question to be asked why

this is the case. The logical conclusion would be that the Y chromosome rDNA is reestablishing its nucleolar dominance because it has corrected whatever insult (i.e. decrease of functional rRNA gene numbers) that induced the change during aging of its parents.

As mentioned in Chapter 4.4, this brings to mind the historically-observed phenomenon of "rDNA magnification" in *Drosophila* stocks that were originally deficient for rDNA but were found to recover within one or two generations. Combining this historical observation with the data presented in this dissertation, it is not farfetched to suspect that this "rDNA magnification" may be occurring at the level of the stem cell, and is reflected in the $F_1$ recovery of nucleolar morphology. We can imagine three possible scenarios for how this could happen in the GSC: 1) chromosomal exchange between the X and Y chromosome rDNA arrays 2) unequal sister chromatid exchange among the Y chromosome, resulting in rDNA expansion in one chromatid and contraction in the other, or 3) expansion of the Y rDNA array during genome replication. Unequal sister chromatid exchange and inheritance of GSC rDNA array length would suggest the stem cell has a mechanism for selectively identifying sister chromatids with more or less rDNA, and is interesting to think about when taking into consideration the finding that GSCs non-randomly segregate sister chromatids from the X and Y chromosomes[251]. In yeast, substantial evidence exists to support unequal sister chromatid exchange as the primary mode of increasing rRNA gene copy number[113,114,250], but at the same time there is only one chromosomal rDNA array in yeast so interchromosomal exchange is not an option. In humans, frequent recombination between chromosomal arrays is suspected to occur between the five acrocentromeric chromosomes based on sequence similarity in the regions flanking the rDNA[93]. If interchromosomal exchange is happening between the X and Y rDNA in *Drosophila* GSCs, that presents an intriguing scenario where homogenization is occurring between the two arrays over evolutionary time. In *Drosophila*

*melanogaster*, one of the few known differences between the X and Y rDNA is the heavier transposable element burden within the X rDNA[230–232] . What would the effect of equalizing transposon burden be on genomic stability? Alternatively, what if interchromosomal recombination between the X and Y chromosomes at the rDNA are a normal and necessary occurrence in *Drosophila,* and rDNA magnification is simply a side effect? For example, it is known that the rDNA (and specifically the intergenic spacer region) is needed for proper meiotic pairing of the sex chromosomes[239,240]. Regular exchange between rDNA arrays could ensure that these loci retain adequate similarity. Studies designed to address the nature of GSC nucleolar morphology recovery promise to reveal insights into the nature of rDNA array plasticity. And because flies are multicellular organisms with rDNA arrays on multiple chromosomes, findings would more readily extrapolate to higher eukaryotes like humans and mice than previous research in yeast.

## 5.3 Lessons from rDNA instability: A paradigm for other repetitive genomic regions?

It has been well-established that the rDNA in *S. cerevisiae* is a fragile genomic site owing to its tandem repetitive nature, and likely exacerbated by its high transcriptional activity. However, the *S. cerevisiae* genome is also relatively devoid of repetitive DNA other than the rDNA, with all other repetitive sequences accounting for approximately 1% of the genome, with all of it appearing to be dispensable[265]. On the other hand, it has been known for decades that the bulk of the genomes in most higher eukaryotes consists of repetitive DNA[266], which is thought to account for the majority of the diversity in eukaryotic genome sizes[267]. For example, over half of the human genome is believed to be comprised of various kinds of repetitive DNA sequences[268,269]. The

smallest autosome, chromosome 21, consists of annotated sequences on only 26.2% of its length, and the rest of it (including the rDNA on the acrocentric short arm) is considered "genomic dark matter"[270]. If the tandem repetitive nature of the rDNA is largely responsible for its genomic instability, it stands to reason that other repetitive regions of the genome could face similar challenges.

In *Drosophila*, the rDNA accounts for approximately 2-3% of the genome. On the other hand, satellite DNAs (simple sequence tandem repeats) have been estimated to comprise over 20% of the genome, with many unique satellites present on multiple chromosome[224,271]. While most of the repetitive DNA is thought to be located in constitutive heterochromatin, transcription of many of these satellites has been observed to occur in embryos by microarray, with some of them being transcribed at extremely high levels[272]. Thus, the two primary factors thought to contribute to the instability of the rDNA, its repetitive nature and transcriptional activity, may be shared by other repetitive elements in the genome. While the work in this dissertation has specifically focused on the rDNA because of the body of literature in yeast and its clearly-established cell biological role (organization of the nucleolus), the possibility should be considered that age-related destabilization of repeats could occur on a genome-wide scale. In fact, accumulation of extrachromosomal circles of satellite DNAs have been observed in *Drosophila*[156], suggesting that intrachromosomal recombination (**Figure 4.1B**) can readily occur. This is analogous to the formation of ERCs in yeast. If age-related destabilization of repetitive regions extends beyond the rDNA, it is conceivable these changes may have been previously missed or neglected due to the lack of a well-established readout of function (like nucleolar organization for the rDNA). On the other hand, if age-related destabilization *does not* apply to other genomic repeats, it points towards the

uniqueness of the role the rDNA plays in aging. But then the question that begs to be asked is what is it about the rDNA that confers its unique role in aging?

An aspect of the rDNA that is beginning to become clearer is that the coding rRNA genes are not the only residents of the rDNA, and that a plethora of functional non-coding elements exist within the array itself. In yeast, a bidirectional non-coding promoter exists within the rRNA coding sequence whose transcription is thought to dissociate cohesin molecules holding sister chromatids together, allowing for recombination between sister chromatids at the rDNA array[114,273]. In mice, a non-coding RNA derived from the rRNA promoter is believed to recruit DNMT3b and NoRC to actively silence other genes[274,275]. A similar promoter-associated non-coding transcript has been found to be transcribed in a subset of human cancer cells[276]. Possibly related, it has been observed that large scale rearrangements and recombination events occurring at the rDNA is a feature of many solid tumors[122]. However, little is known about potential functional non-coding elements in the human rDNA outside of the rRNA genes. If it becomes apparent that the rDNA occupies a special position relative to other repetitive DNA in its age-related destabilization, the key to understanding why may be derived from the discovery of more of the unique elements that exist within the rDNA.

In summary, much remains to be understood about the repetitive genome in higher eukaryotes. Studies in *S. cerevisiae* have focused on rDNA instability, but most eukaryotic organisms contain other types of repetitive DNA that are many times more abundant. Based on our understanding of what contributes to rDNA instability during aging, other repetitive portions of the genome should suffer similar insults. The results presented in this dissertation on rDNA instability in germline stem cells and germ cells during aging could present a paradigm for genomic

stability that has implications beyond the rDNA itself. Proper investigation could determine if the rDNA's role in aging is unique, or if principles extend to the entirety of the repeatome.

# References


1. Spradling, A., Fuller, M. T., Braun, R. E. & Yoshida, S. Germline stem cells. *Cold Spring Harb. Perspect. Biol.* **3,** a002642 (2011).
2. Fuller, M. T. & Spradling, A. C. Male and female Drosophila germline stem cells: two versions of immortality. *Science* **316,** 402–4 (2007).
3. López-Otín, C., Blasco, M. A., Partridge, L., Serrano, M. & Kroemer, G. The hallmarks of aging. *Cell* **153,** 1194–217 (2013).
4. Li, L. & Xie, T. STEM CELL NICHE: Structure and Function. *Annu. Rev. Cell Dev. Biol.* **21,** 605–631 (2005).
5. Yamashita, Y. M., Fuller, M. T. & Jones, D. L. Signaling in stem cell niches: lessons from the Drosophila germline. *J. Cell Sci.* **118,** 665–72 (2005).
6. Ohlstein, B., Kai, T., Decotto, E. & Spradling, A. The stem cell niche: theme and variations. *Curr. Opin. Cell Biol.* **16,** 693–699 (2004).
7. Fuller, M. T. in *The Development of Drosophila melanogaster* **1,** 71–147 (New York: Cold Spring Harbor Laboratory Press, 1993).
8. de Cuevas, M. & Matunis, E. L. The stem cell niche: lessons from the Drosophila testis. *Development* **138,** 2861–9 (2011).
9. Hardy, R. W., Tokuyasu, K. T., Lindsley, D. L. & Garavito, M. The germinal proliferation center in the testis of Drosophila melanogaster. *J. Ultrastruct. Res.* **69,** 180–90 (1979).
10. Yamashita, Y. M., Jones, D. L. & Fuller, M. T. Orientation of Asymmetric Stem Cell Division by the APC Tumor Suppressor and Centrosome. *Science (80-. ).* **301,** 1547–1550

(2003).

11. Yamashita, Y. M., Mahowald, A. P., Perlin, J. R. & Fuller, M. T. Asymmetric Inheritance of Mother Versus Daughter Centrosome in Stem Cell Division. *Science (80-. ).* **315,** 518–521 (2007).

12. de Cuevas, M. & Spradling, A. C. Morphogenesis of the Drosophila fusome and its implications for oocyte specification. *Development* **125,** 2781–9 (1998).

13. Hsu, H.-J., LaFever, L. & Drummond-Barbosa, D. Diet controls normal and tumorous germline stem cells via insulin-dependent and -independent mechanisms in Drosophila. *Dev. Biol.* **313,** 700–712 (2008).

14. Yuan, H., Chiang, C.-Y. A., Cheng, J., Salzmann, V. & Yamashita, Y. M. Regulation of cyclin A localization downstream of Par-1 function is critical for the centrosome orientation checkpoint in Drosophila male germline stem cells. *Dev. Biol.* **361,** 57–67 (2012).

15. Salzmann, V. *et al.* Centrosome-dependent asymmetric inheritance of the midbody ring in Drosophila germline stem cell division. *Mol. Biol. Cell* **25,** 267–275 (2014).

16. Sheng, X. R. & Matunis, E. Live imaging of the *Drosophila* spermatogonial stem cell niche reveals novel mechanisms regulating germline stem cell output. *Development* **138,** 3367–3376 (2011).

17. Hime, G. R., Brill, J. A. & Fuller, M. T. Assembly of ring canals in the male germ line from structural components of the contractile ring. *J. Cell Sci.* 2779–88 (1996).

18. Lindsley, D. L. & Tokuyasu, K. T. in *Genetics and biology of Drosophila* (eds. Ashburner, M. & Wright, T. R.) 225–294 (Academic Press, New York, 1980).

19. Decotto, E. & Spradling, A. C. The Drosophila Ovarian and Testis Stem Cell Niches:

Similar Somatic Stem Cells and Signals. *Dev. Cell* **9,** 501–510 (2005).

20. DiNardo, S., Tran, J. & Brenner, T. J. Somatic control over the germline stem cell lineage during Drosophila spermatogenesis. *Nature* **407,** 754–757 (2000).

21. Gönczy, P., Matunis, E. & DiNardo, S. bag-of-marbles and benign gonial cell neoplasm act in the germline to restrict proliferation during Drosophila spermatogenesis. *Development* **124,** 4361–71 (1997).

22. Stanley, H. P., Bowman, J. T., Romrell, L. J., Reed, S. C. & Wilkinson, R. F. Fine structure of normal spermatid differentiation in Drosophila melanogaster. *J. Ultrastruct. Res.* **41,** 433–66 (1972).

23. Fabian, L. & Brill, J. A. Drosophila spermiogenesis: Big things come from little packages. *Spermatogenesis* **2,** 197–212 (2012).

24. Greenbaum, M. P., Iwamori, T., Buchold, G. M. & Matzuk, M. M. Germ cell intercellular bridges. *Cold Spring Harb. Perspect. Biol.* **3,** a005850 (2011).

25. FAWCETT, D. W., ITO, S. & SLAUTTERBACK, D. The occurrence of intercellular bridges in groups of cells exhibiting synchronous differentiation. *J. Biophys. Biochem. Cytol.* **5,** 453–60 (1959).

26. Haglund, K., Nezis, I. P. & Stenmark, H. Structure and functions of stable intercellular bridges formed by incomplete cytokinesis during development. *Commun. Integr. Biol.* **4,** 1–9 (2011).

27. Koch, E. A. & King, R. C. The origin and early differentiation of the egg chamber ofDrosophila melanogaster. *J. Morphol.* **119,** 283–303 (1966).

28. Spradling, A. C. in *The Development of Drosophila melanogaster* 1–70 (Cold Spring Harbor Laboratory Press, 1993).

29. Cooley, L. Drosophila ring canal growth requires Src and Tec kinases. *Cell* **93,** 913–5 (1998).

30. Robinson, D. N. & Cooley, L. Stable intercellular bridges in development: the cytoskeleton lining the tunnel. *Trends Cell Biol.* **6,** 474–9 (1996).

31. Robinson, D. N. & Cooley, L. Drosophila kelch is an oligomeric ring canal actin organizer. *J. Cell Biol.* **138,** 799–810 (1997).

32. Hudson, A. M. & Cooley, L. *Drosophila* Kelch functions with Cullin-3 to organize the ring canal actin cytoskeleton. *J. Cell Biol.* **188,** 29–37 (2010).

33. Hudson, A. M., Mannix, K. M. & Cooley, L. Actin Cytoskeletal Organization in Drosophila Germline Ring Canals Depends on Kelch Function in a Cullin-RING E3 Ligase. *Genetics* **201,** 1117–1131 (2015).

34. Kelso, R. J., Hudson, A. M. & Cooley, L. Drosophila Kelch regulates actin organization via Src64-dependent tyrosine phosphorylation. *J. Cell Biol.* **156,** 703–13 (2002).

35. Eikenes, Å. H., Brech, A., Stenmark, H. & Haglund, K. Spatiotemporal control of Cindr at ring canals during incomplete cytokinesis in the Drosophila male germline. *Dev. Biol.* **377,** 9–20 (2013).

36. McLaren, A. Primordial germ cells in the mouse. *Dev. Biol.* **262,** 1–15 (2003).

37. Pepling, M. E. & Spradling, A. C. Female mouse germ cells form synchronously dividing cysts. *Development* **125,** 3323–8 (1998).

38. Lei, L. & Spradling, A. C. Mouse primordial germ cells produce cysts that partially fragment prior to meiosis. *Development* **140,** 2075–2081 (2013).

39. Hara, K. *et al.* Mouse spermatogenic stem cells continually interconvert between equipotent singly isolated and syncytial states. *Cell Stem Cell* **14,** 658–72 (2014).

40. Greenbaum, M. P., Ma, L. & Matzuk, M. M. Conversion of midbodies into germ cell intercellular bridges. *Dev. Biol.* **305,** 389–96 (2007).

41. Greenbaum, M. P. *et al.* TEX14 is essential for intercellular bridges and fertility in male mice. *Proc. Natl. Acad. Sci.* **103,** 4982–4987 (2006).

42. Iwamori, T., Lin, Y.-N., Ma, L., Iwamori, N. & Matzuk, M. M. Identification and Characterization of RBM44 as a Novel Intercellular Bridge Protein. *PLoS One* **6,** e17066 (2011).

43. Iwamori, T. *et al.* TEX14 Interacts with CEP55 To Block Cell Abscission. *Mol. Cell. Biol.* **30,** 2280–2292 (2010).

44. Snapp, E. L., Iida, T., Frescas, D., Lippincott-Schwartz, J. & Lilly, M. A. The fusome mediates intercellular endoplasmic reticulum connectivity in Drosophila ovarian cysts. *Mol. Biol. Cell* **15,** 4512–21 (2004).

45. Lin, H., Yue, L. & Spradling, A. C. The Drosophila fusome, a germline-specific organelle, contains membrane skeletal proteins and functions in cyst formation. *Development* **120,** 947–56 (1994).

46. de Cuevas, M., Lee, J. K. & Spradling, A. C. alpha-spectrin is required for germline cell division and differentiation in the Drosophila ovary. *Development* **122,** (1996).

47. Yue, L. & Spradling, A. C. hu-li tai shao, a gene required for ring canal formation during Drosophila oogenesis, encodes a homolog of adducin. *Genes Dev.* **6,** 2443–54 (1992).

48. Kloc, M., Bilinski, S., Dougherty, M. T., Brey, E. M. & Etkin, L. D. Formation, architecture and polarity of female germline cyst in Xenopus. *Dev. Biol.* **266,** 43–61 (2004).

49. Loppion, G., Crespel, A., Martinez, A.-S., Auvray, P. & Sourdaine, P. Study of the

potential spermatogonial stem cell compartment in dogfish testis, Scyliorhinus canicula L. *Cell Tissue Res.* **332,** 533–542 (2008).

50. Haglund, K. *et al.* Cindr Interacts with Anillin to Control Cytokinesis in Drosophila melanogaster. *Curr. Biol.* **20,** 944–950 (2010).

51. Field, C. M. & Alberts, B. M. Anillin, a contractile ring protein that cycles from the nucleus to the cell cortex. *J. Cell Biol.* **131,** 165–78 (1995).

52. Minestrini, G., Máthé, E. & Glover, D. M. Domains of the Pavarotti kinesin-like protein that direct its subcellular distribution: effects of mislocalisation on the tubulin and actin cytoskeleton during Drosophila oogenesis. *J. Cell Sci.* **115,** 725–36 (2002).

53. Kramerova, I. A. & Kramerov, A. A. Mucinoprotein is a universal constituent of stable intercellular bridges inDrosophila melanogaster germ line and somatic cells. *Dev. Dyn.* **216,** 349–360 (1999).

54. Sokol, N. S. & Cooley, L. Drosophila filamin encoded by the cheerio locus is a component of ovarian ring canals. *Curr. Biol.* **9,** 1221–30 (1999).

55. Roulier, E. M., Panzer, S. & Beckendorf, S. K. The Tec29 tyrosine kinase is required during Drosophila embryogenesis and interacts with Src64 in ring canal development. *Mol. Cell* **1,** 819–29 (1998).

56. Lu, N., Guarnieri, D. J. & Simon, M. A. Localization of Tec29 to ring canals is mediated by Src64 and PtdIns(3,4,5)P3-dependent mechanisms. *EMBO J.* **23,** 1089–1100 (2004).

57. Greenbaum, M. P., Iwamori, N., Agno, J. E. & Matzuk, M. M. Mouse TEX14 Is Required for Embryonic Germ Cell Intercellular Bridges but Not Female Fertility1. *Biol. Reprod.* **80,** 449–457 (2009).

58. Zamboni, L. & Gondos, B. Intercellular bridges and synchronization of germ cell

differentiation during oogenesis in the rabbit. *J. Cell Biol.* **36,** 276–82 (1968).

59. Gondos, B., Bhiraleus, P. & Hobel, C. J. Ultrastructural observations on germ cells in human fetal ovaries. *Am. J. Obstet. Gynecol.* **110,** 644–52 (1971).

60. Brill, J. A., Hime, G. R., Scharer-Schuksz, M. & Fuller, M. T. A phospholipid kinase regulates actin organization and intercellular bridge formation during germline cytokinesis. *Development* **127,** 3855–64 (2000).

61. Carmena, M. *et al.* Drosophila polo kinase is required for cytokinesis. *J. Cell Biol.* **143,** 659–71 (1998).

62. Giansanti, M. G., Bonaccorsi, S. & Gatti, M. The role of anillin in meiotic cytokinesis of Drosophila males. *J. Cell Sci.* **112 ( Pt 14),** 2323–34 (1999).

63. BURGOS, M. H. & FAWCETT, D. W. Studies on the fine structure of the mammalian testis. I. Differentiation of the spermatids in the cat (Felis domestica). *J. Biophys. Biochem. Cytol.* **1,** 287–300 (1955).

64. Ventela, S., Toppari, J. & Parvinen, M. Intercellular Organelle Traffic through Cytoplasmic Bridges in Early Spermatids of the Rat: Mechanisms of Haploid Gene Product Sharing. *Mol. Biol. Cell* **14,** 2768–2780 (2003).

65. Russell, L. D., Vogl, A. W. & Weber, J. E. Actin localization in male germ cell intercellular bridges in the rat and ground squirrel and disruption of bridges by cytochalasin D. *Am. J. Anat.* **180,** 25–40 (1987).

66. Gondos, B. & Hobel, C. J. Ultrastructure of germ cell development in the human fetal testis. *Z. Zellforsch. Mikrosk. Anat.* **119,** 1–20 (1971).

67. Bastock, R. & St Johnston, D. Drosophila oogenesis. *Curr. Biol.* **18,** R1082–R1087 (2008).

68. Lehmann, R. Germ Plasm Biogenesis--An Oskar-Centric Perspective. *Curr. Top. Dev. Biol.* **116,** 679–707 (2016).

69. Lei, L. & Spradling, A. C. Mouse oocytes differentiate through organelle enrichment from sister cyst germ cells. *Science (80-. ).* **352,** 95–99 (2016).

70. Ruby, J. R., Dyer, R. F. & Skalko, R. G. The occurrence of intercellular bridges during oogenesis in the mouse. *J. Morphol.* **127,** 307–39 (1969).

71. Lilly, M. A., de Cuevas, M. & Spradling, A. C. Cyclin A Associates with the Fusome during Germline Cyst Formation in the Drosophila Ovary. *Dev. Biol.* **218,** 53–63 (2000).

72. Mathieu, J. *et al.* Aurora B and Cyclin B Have Opposite Effects on the Timing of Cytokinesis Abscission in Drosophila Germ Cells and in Vertebrate Somatic Cells. *Dev. Cell* **26,** 250–265 (2013).

73. Ohlmeyer, J. T. & Schüpbach, T. Encore facilitates SCF-Ubiquitin-proteasome-dependent proteolysis during Drosophila oogenesis. *Development* **130,** 6339–49 (2003).

74. Varadarajan, R., Ayeni, J., Jin, Z., Homola, E. & Campbell, S. D. Myt1 inhibition of Cyclin A/Cdk1 is essential for fusome integrity and premeiotic centriole engagement in Drosophila spermatocytes. *Mol. Biol. Cell* **27,** 2051–63 (2016).

75. Cox, R. T. & Spradling, A. C. A Balbiani body and the fusome mediate mitochondrial inheritance during Drosophila oogenesis. *Development* **130,** 1579–1590 (2003).

76. Mahowald, A. P. & Strassheim, J. M. Intercellular migration of centrioles in the germarium of Drosophila melanogaster. An electron microscopic study. *J. Cell Biol.* **45,** 306–20 (1970).

77. Braun, R. E., Behringer, R. R., Peschon, J. J., Brinster, R. L. & Palmiter, R. D. Genetically haploid spermatids are phenotypically diploid. *Nature* **337,** 373–6 (1989).

78. Telfer, W. H. Development and physiology of the oocyte-nurse cell syncytium [Insects]. *Advances in insect physiology* **v. 1975, 1,** (1975).

79. Gottanka, J. & Büning, J. Oocytes develop from interconnected cystocytes in the panoistic ovary of Nemoura sp. (Pictet) (Plecoptera : Nemouridae). *Int. J. Insect Morphol. Embryol.* **19,** 219–225 (1990).

80. Buning, J. Germ cell cluster formation in insect ovaries. *Int. J. Insect Morphol. Embryol.* **22,** 237–253 (1993).

81. Burnett, A. L., Davis, L. E. & Ruffing, F. E. A histological and ultrastructural study of germinal differentiation of interstitial cells arising from gland cells in Hydra viridis. *J. Morphol.* **120,** 1–8 (1966).

82. Nishimiya-Fujisawa, C. & Kobayashi, S. Germline stem cells and sex determination in Hydra. *Int. J. Dev. Biol.* **56,** 499–508 (2012).

83. Barthel, D. & Detmer, A. The spermatogenesis of Halichondria panicea (Porifera, Demospongiae). *Zoomorphology* **110,** 9–5 (1990).

84. Lanna, E. & Klautau, M. Oogenesis and spermatogenesis in Paraleucilla magna (Porifera, Calcarea). doi:10.1007/s00435-010-0117-5

85. Douzery, E. J. P., Snell, E. A., Bapteste, E., Delsuc, F. & Philippe, H. The timing of eukaryotic evolution: does a relaxed molecular clock reconcile proteins and fossils? *Proc. Natl. Acad. Sci. U. S. A.* **101,** 15386–91 (2004).

86. Fairclough, S. R., Dayel, M. J. & King, N. Multicellular development in a choanoflagellate. *Curr. Biol.* **20,** R875-6 (2010).

87. Dayel, M. J. *et al.* Cell differentiation and morphogenesis in the colony-forming choanoflagellate Salpingoeca rosetta. *Dev. Biol.* **357,** 73–82 (2011).

88. Long, E. O. & Dawid, I. B. Repeated Genes in Eukaryotes. *Annu. Rev. Biochem.* **49,** 727–764 (1980).

89. Srivastava, A. K. & Schlessinger, D. Structure and organization of ribosomal DNA. *Biochimie* **73,** 631–638 (1991).

90. McClintock, B. The relation of a particular chromosomal element to the development of the nucleoli in Zea mays. *Zeitschrift f**r Zellforsch. und Mikroskopische Anat.* **21,** 294–326 (1934).

91. Boisvert, F.-M., van Koningsbruggen, S., Navascués, J. & Lamond, A. I. The multifunctional nucleolus. *Nat. Rev. Mol. Cell Biol.* **8,** 574–85 (2007).

92. Pederson, T. The nucleolus. *Cold Spring Harb. Perspect. Biol.* **3,** a000638 (2011).

93. Floutsakou, I. *et al.* The shared genomic architecture of human nucleolar organizer regions. *Genome Res.* **23,** 2003–12 (2013).

94. Henderson, A. S., Warburton, D. & Atwood, K. C. Location of ribosomal DNA in the human chromosome complement. *Proc. Natl. Acad. Sci. U. S. A.* **69,** 3394–8 (1972).

95. Ritossa, F. M., Atwood, K. C., Lindsley, D. L. & Spiegelman, S. On the chromosomal distribution of DNA complementary to ribosomal and soluble RNA. *Natl. Cancer Inst. Monogr.* **23,** 449–72 (1966).

96. Pardue, M. Lou, Gerbi, S. A., Eckhardt, R. A. & Gall, J. G. Cytological localization of DNA complementary to ribosomal RNA in polytene chromosomes of Diptera. *Chromosoma* **29,** 268–290 (1970).

97. Ritossa, F. M. & Spiegelman, S. LOCALIZATION OF DNA COMPLEMENTARY TO RIBOSOMAL RNA IN THE NUCLEOLUS ORGANIZER REGION OF DROSOPHILA MELANOGASTER. *Proc. Natl. Acad. Sci. U. S. A.* **53,** 737–45 (1965).

98. Lodish, H. *et al.* Processing of rRNA and tRNA. (2000).

99. Goodfellow, S. J. & Zomerdijk, J. C. B. M. in *Sub-cellular biochemistry* **61,** 211–236 (2013).

100. Russell, J. & Zomerdijk, J. C. B. M. RNA-polymerase-I-directed rDNA transcription, life and works. *Trends Biochem. Sci.* **30,** 87–96 (2005).

101. Sylvester, J. E. *et al.* The human ribosomal RNA genes: structure and organization of the complete repeating unit. *Hum. Genet.* **73,** 193–8 (1986).

102. Gerbi, S. A. The evolution of eukaryotic ribosomal DNA. *Biosystems* **19,** 247–258 (1986).

103. Gonzalez, I. L. & Schmickel, R. D. The human 18S ribosomal RNA gene: evolution and stability. *Am. J. Hum. Genet.* **38,** 419–27 (1986).

104. Heix, J. & Grummt, I. Species specificity of transcription by RNA polymerase I. *Curr. Opin. Genet. Dev.* **5,** 652–6 (1995).

105. McStay, B. Nucleolar dominance: a model for rRNA gene silencing. *Genes Dev.* **20,** 1207–14 (2006).

106. Stage, D. E. & Eickbush, T. H. Sequence variation within the rRNA gene loci of 12 Drosophila species. *Genome Res.* **17,** 1888–97 (2007).

107. Zhang, W. *et al.* Engineering the ribosomal DNA in a megabase synthetic chromosome. *Science (80-. ).* **355,** eaaf3981 (2017).

108. Brewer, B. J. & Fangman, W. L. A replication fork barrier at the 3' end of yeast ribosomal RNA genes. *Cell* **55,** 637–43 (1988).

109. Brewer, B. J., Lockshon, D. & Fangman, W. L. The arrest of replication forks in the rDNA of yeast occurs independently of transcription. *Cell* **71,** 267–76 (1992).

110. Weitao, T., Budd, M., Hoopes, L. L. M. & Campbell, J. L. Dna2 helicase/nuclease causes

replicative fork stalling and double-strand breaks in the ribosomal DNA of Saccharomyces cerevisiae. *J. Biol. Chem.* **278,** 22513–22 (2003).

111. Burkhalter, M. D. & Sogo, J. M. rDNA Enhancer Affects Replication Initiation and Mitotic Recombination. *Mol. Cell* **15,** 409–421 (2004).

112. Kobayashi, T., Horiuchi, T., Tongaonkar, P., Vu, L. & Nomura, M. SIR2 regulates recombination between different rDNA repeats, but not recombination within individual rRNA genes in yeast. *Cell* **117,** 441–53 (2004).

113. Kobayashi, T., Heck, D. J., Nomura, M. & Horiuchi, T. Expansion and contraction of ribosomal DNA repeats in Saccharomyces cerevisiae: requirement of replication fork blocking (Fob1) protein and the role of RNA polymerase I. *Genes Dev.* **12,** 3821–30 (1998).

114. Kobayashi, T. & Ganley, A. R. D. Recombination Regulation by Transcription-Induced Cohesin Dissociation in rDNA Repeats. *Science (80-. ).* **309,** 1581–1584 (2005).

115. Akamatsu, Y. & Kobayashi, T. The Human RNA Polymerase I Transcription Terminator Complex Acts as a Replication Fork Barrier That Coordinates the Progress of Replication with rRNA Transcription Activity. *Mol. Cell. Biol.* **35,** 1871–81 (2015).

116. Kwan, E. X., Wang, X. S., Amemiya, H. M., Brewer, B. J. & Raghuraman, M. K. rDNA Copy Number Variants Are Frequent Passenger Mutations in *Saccharomyces cerevisiae* Deletion Collections and *de Novo* Transformants. *G3: Genes|Genomes|Genetics* **6,** 2829–2838 (2016).

117. Takeuchi, Y., Horiuchi, T. & Kobayashi, T. Transcription-dependent recombination and the role of fork collision in yeast rDNA. *Genes Dev.* **17,** 1497–1506 (2003).

118. Paredes, S. & Maggert, K. A. Expression of I-CreI Endonuclease Generates Deletions

Within the rDNA of Drosophila. *Genetics* **181,** (2009).

119. McStay, B. & Grummt, I. The epigenetics of rRNA genes: from molecular to chromosome biology. *Annu. Rev. Cell Dev. Biol.* **24,** 131–57 (2008).

120. Kobayashi, T. Strategies to maintain the stability of the ribosomal RNA gene repeats--collaboration of recombination, cohesion, and condensation. *Genes Genet. Syst.* **81,** 155–61 (2006).

121. Kobayashi, T. A new role of the rDNA and nucleolus in the nucleus—rDNA instability maintains genome integrity. *BioEssays* **30,** 267–272 (2008).

122. Stults, D. M. *et al.* Human rRNA Gene Clusters Are Recombinational Hotspots in Cancer. *Cancer Res.* **69,** (2009).

123. Stancheva, I., Lucchini, R., Koller, T. & Sogo, J. M. Chromatin structure and methylation of rat rRNA genes studied by formaldehyde fixation and psoralen cross-linking. *Nucleic Acids Res.* **25,** 1727–1735 (1997).

124. Santoro, R. & Grummt, I. Molecular mechanisms mediating methylation-dependent silencing of ribosomal gene transcription. *Mol. Cell* **8,** 719–25 (2001).

125. Santoro, R., Li, J. & Grummt, I. The nucleolar remodeling complex NoRC mediates heterochromatin formation and silencing of ribosomal gene transcription. *Nat. Genet.* **32,** 393–396 (2002).

126. Zhou, Y. *et al.* The chromatin remodeling complex NoRC targets HDAC1 to the ribosomal gene promoter and represses RNA polymerase I transcription. *EMBO J.* **21,** 4632–40 (2002).

127. Santoro, R. & Grummt, I. Epigenetic mechanism of rRNA gene silencing: temporal order of NoRC-mediated histone modification, chromatin remodeling, and DNA methylation.

*Mol. Cell. Biol.* **25,** 2539–46 (2005).

128. Guetg, C. *et al.* The NoRC complex mediates the heterochromatin formation and stability of silent rRNA genes and centromeric repeats. *EMBO J.* **29,** 2135–2146 (2010).

129. Peng, J. C. & Karpen, G. H. H3K9 methylation and RNA interference regulate nucleolar organization and repeated DNA stability. *Nat. Cell Biol.* **9,** 25–35 (2007).

130. Navashin, M. Chromosome Alterations Caused by Hybridization and Their Bearing upon Certain General Genetic Problems. *Cytologia (Tokyo).* **5,** 169–203 (1934).

131. Chen, Z. J. & Pikaard, C. S. Transcriptional analysis of nucleolar dominance in polyploid plants: biased expression/silencing of progenitor rRNA genes is developmentally regulated in Brassica. *Proc. Natl. Acad. Sci. U. S. A.* **94,** 3442–7 (1997).

132. Chen, Z. J., Comai, L. & Pikaard, C. S. Gene dosage and stochastic effects determine the severity and direction of uniparental ribosomal RNA gene silencing (nucleolar dominance) in Arabidopsis allopolyploids. *Proc. Natl. Acad. Sci. U. S. A.* **95,** 14891–6 (1998).

133. Preuss, S. & Pikaard, C. S. rRNA gene silencing and nucleolar dominance: insights into a chromosome-scale epigenetic on/off switch. *Biochim. Biophys. Acta* **1769,** 383–92

134. Lawrence, R. J. *et al.* A concerted DNA methylation/histone methylation switch regulates rRNA gene dosage control and nucleolar dominance. *Mol. Cell* **13,** 599–609 (2004).

135. Probst, A. V. *et al.* Arabidopsis Histone Deacetylase HDA6 Is Required for Maintenance of Transcriptional Gene Silencing and Determines Nuclear Organization of rDNA Repeats. *Plant Cell Online* **16,** (2004).

136. Earley, K. *et al.* Erasure of histone acetylation by Arabidopsis HDA6 mediates large-scale gene silencing in nucleolar dominance. *Genes Dev.* **20,** 1283–93 (2006).

137. Durica, D. S. & Krider, H. M. Studies on the ribosomal RNA cistrons in interspecific Drosophila hybrids. *Dev. Biol.* **59,** 62–74 (1977).

138. Honjo, T. & Reeder, R. H. Preferential transcription of Xenopus laevis ribosomal RNA in interspecies hybrids between Xenopus laevis and Xenopus mulleri. *J. Mol. Biol.* **80,** 217–28 (1973).

139. Eliceiri, G. L. & Green, H. Ribosomal RNA synthesis in human-mouse hybrid cells. *J. Mol. Biol.* **41,** 253–60 (1969).

140. Croce, C. M., Talavera, A., Basilico, C. & Miller, O. J. Suppression of production of mouse 28S ribosomal RNA in mouse-human hybrids segregating mouse chromosomes. *Proc. Natl. Acad. Sci. U. S. A.* **74,** 694–7 (1977).

141. Smirnov, E. *et al.* NORs and their transcription competence during the cell cycle. *Folia Biol. (Praha).* **52,** 59–70 (2006).

142. Kalmárová, M. *et al.* Positioning of NORs and NOR-bearing chromosomes in relation to nucleoli. *J. Struct. Biol.* **160,** 49–56 (2007).

143. Zhou, J. *et al.* Y chromosome mediates ribosomal DNA silencing and modulates the chromatin state in Drosophila. *Proc. Natl. Acad. Sci.* **109,** 9941–9946 (2012).

144. Greil, F. & Ahmad, K. Nucleolar dominance of the Y chromosome in Drosophila melanogaster. *Genetics* **191,** 1119–28 (2012).

145. Ganley, A. R. D. & Kobayashi, T. Ribosomal DNA and cellular senescence: new evidence supporting the connection between rDNA and aging. *FEMS Yeast Res.* **14,** 49–59 (2014).

146. Kaeberlein, M. Lessons on longevity from budding yeast. *Nature* **464,** 513–519 (2010).

147. Egilmez, N. K. & Jazwinski, S. M. Evidence for the involvement of a cytoplasmic factor in the aging of the yeast Saccharomyces cerevisiae. *J. Bacteriol.* **171,** 37–42 (1989).

148. Kennedy, B. K., Austriaco, N. R. & Guarente, L. Daughter cells of Saccharomyces cerevisiae from old mothers display a reduced life span. *J. Cell Biol.* **127,** 1985–93 (1994).

149. Sinclair, D. A. & Guarente, L. Extrachromosomal rDNA circles--a cause of aging in yeast. *Cell* **91,** 1033–42 (1997).

150. Shcheprova, Z., Baldi, S., Frei, S. B., Gonnet, G. & Barral, Y. A mechanism for asymmetric segregation of age during yeast budding. *Nature* **454,** 728–34 (2008).

151. Steinkraus, K. A., Kaeberlein, M. & Kennedy, B. K. Replicative Aging in Yeast: The Means to the End. *Annu. Rev. Cell Dev. Biol.* **24,** 29–54 (2008).

152. Sinclair, D. A., Mills, K. & Guarente, L. Accelerated aging and nucleolar fragmentation in yeast sgs1 mutants. *Science* **277,** 1313–6 (1997).

153. Kennedy, B. K. *et al.* Redistribution of silencing proteins from telomeres to the nucleolus is associated with extension of life span in S. cerevisiae. *Cell* **89,** 381–91 (1997).

154. Kaeberlein, M., McVey, M. & Guarente, L. The SIR2/3/4 complex and SIR2 alone promote longevity in Saccharomyces cerevisiae by two different mechanisms. *Genes Dev.* **13,** 2570–80 (1999).

155. Longo, V. D. & Kennedy, B. K. Sirtuins in Aging and Age-Related Disease. *Cell* **126,** 257–268 (2006).

156. Cohen, S., Yacobi, K. & Segal, D. Extrachromosomal circular DNA of tandemly repeated genomic sequences in Drosophila. *Genome Res.* **13,** 1133–45 (2003).

157. Cohen, S., Agmon, N., Sobol, O. & Segal, D. Extrachromosomal circles of satellite repeats and 5S ribosomal DNA in human cells. *Mob. DNA* **1,** 11 (2010).

158. Merker, R. J. & Klein, H. L. hpr1Delta affects ribosomal DNA recombination and cell life span in Saccharomyces cerevisiae. *Mol. Cell. Biol.* **22,** 421–9 (2002).

159. Heo, S. J. *et al.* Bloom's syndrome gene suppresses premature ageing caused by Sgs1 deficiency in yeast. *Genes Cells* **4,** 619–25 (1999).

160. Ganley, A. R. D., Ide, S., Saka, K. & Kobayashi, T. The effect of replication initiation on gene amplification in the rDNA and its relationship to aging. *Mol. Cell* **35,** 683–93 (2009).

161. Unal, E., Kinde, B. & Amon, A. Gametogenesis eliminates age-induced cellular damage and resets life span in yeast. *Science* **332,** 1554–7 (2011).

162. Tsang, C. K., Li, H. & Zheng, X. S. Nutrient starvation promotes condensin loading to maintain rDNA stability. *EMBO J.* **26,** 448–458 (2007).

163. Ha, C. W. & Huh, W.-K. Rapamycin increases rDNA stability by enhancing association of Sir2 with rDNA in Saccharomyces cerevisiae. *Nucleic Acids Res.* **39,** 1336–1350 (2011).

164. Smith Jr, D. L. *et al.* Calorie restriction effects on silencing and recombination at the yeast rDNA. *Aging Cell* **8,** 633–642 (2009).

165. Riesen, M. & Morgan, A. Calorie restriction reduces rDNA recombination independently of rDNA silencing. *Aging Cell* **8,** 624–632 (2009).

166. Medvedik, O., Lamming, D. W., Kim, K. D. & Sinclair, D. A. MSN2 and MSN4 Link Calorie Restriction and TOR to Sirtuin-Mediated Lifespan Extension in Saccharomyces cerevisiae. *PLoS Biol.* **5,** e261 (2007).

167. Cornu, M., Albert, V. & Hall, M. N. mTOR in aging, metabolism, and cancer. *Curr. Opin. Genet. Dev.* **23,** 53–62 (2013).

168. Kennedy, B. K. & Lamming, D. W. The Mechanistic Target of Rapamycin: The Grand ConducTOR of Metabolism and Aging. *Cell Metab.* **23,** 990–1003 (2016).

169. Van Doren, M., Williamson, A. L. & Lehmann, R. *Regulation of zygotic gene expression*

*in Drosophila primordial germ cells*. *Current Biology* **8,** (1998).

170. Deluca, S. Z. Z. & O'Farrell, P. H. H. Barriers to Male Transmission of Mitochondrial DNA in Sperm Development. *Dev. Cell* **22,** 660–668 (2012).

171. Wichmann, A., Jaklevic, B. & Su, T. T. Ionizing radiation induces caspase-dependent but Chk2- and p53-independent cell death in Drosophila melanogaster. *Proc. Natl. Acad. Sci. U. S. A.* **103,** 9952–7 (2006).

172. Xie, H. B. & Golic, K. G. Gene deletions by ends-in targeting in Drosophila melanogaster. *Genetics* **168,** 1477–89 (2004).

173. Wylie, A. *et al.* p53 activity is selectively licensed in the *Drosophila* stem cell compartment. *Elife* **3,** e01530 (2014).

174. Tain, L. S. *et al.* Drosophila HtrA2 is dispensable for apoptosis but acts downstream of PINK1 independently from Parkin. *Cell Death Differ.* **16,** 1118–1125 (2009).

175. Yacobi-Sharon, K., Namdar, Y. & Arama, E. Alternative germ cell death pathway in Drosophila involves HtrA2/Omi, lysosomes, and a caspase-9 counterpart. *Dev. Cell* **25,** 29–42 (2013).

176. Takada, S., Kelkar, A. & Theurkauf, W. E. Drosophila Checkpoint Kinase 2 Couples Centrosome Function and Spindle Assembly to Genomic Integrity. *Cell* **113,** 87–99 (2003).

177. Cheng, J. *et al.* Centrosome misorientation reduces stem cell division during ageing. *Nature* **456,** 599–604 (2008).

178. Chiang, A. C.-Y., Yang, H. & Yamashita, Y. M. spict, a cyst cell-specific gene, regulates starvation-induced spermatogonial cell death in the Drosophila testis. *Sci. Rep.* **7,** 40245 (2017).

179. Fu, K. K., Phillips, T. L., Heilbron, D. C., Ross, G. & Kane, L. J. Relative Biological Effectiveness of Low- and High-LET Radiotherapy Beams for Jejunal Crypt Cell Survival at Low Doses Per Fraction. *Radiology* **132,** 205–209 (1979).

180. Novitski, E. THE COMPOUND X CHROMOSOMES I N DROSOPHILA1.

181. McCain, J., Danzy, L., Hamdi, A., Dellafosse, O. & DiMario, P. Tracking nucleolar dynamics with GFP-Nopp140 during Drosophila oogenesis and embryogenesis. *Cell Tissue Res.* **323,** 105–15 (2006).

182. Aldrich, J. C., Maggert, K. A., Grainger, R. M., Eickbush, T. & Hartl, D. Transgenerational Inheritance of Diet-Induced Genome Rearrangements in Drosophila. *PLOS Genet.* **11,** e1005148 (2015).

183. Paredes, S. & Maggert, K. A. Ribosomal DNA contributes to global chromatin regulation. *Proc. Natl. Acad. Sci.* **106,** 17829–17834 (2009).

184. Aldrich, J. C. & Maggert, K. A. Simple quantitative PCR approach to reveal naturally occurring and mutation-induced repetitive sequence variation on the Drosophila Y chromosome. *PLoS One* **9,** e109906 (2014).

185. Larracuente, A. M. & Ferree, P. M. Simple Method for Fluorescence DNA <em>In Situ</em> Hybridization to Squashed Chromosomes. *J. Vis. Exp.* 52288 (2015). doi:10.3791/52288

186. Pepling, M. E., de Cuevas, M. & Spradling, A. C. Germline cysts: a conserved phase of germ cell development? *Trends Cell Biol.* **9,** 257–62 (1999).

187. de Cuevas, M., Lilly, M. & Spradling, A. GERMLINE CYST FORMATION IN DROSOPHILA. *Annu. Rev. Genet.* **31,** 405–428 (1997).

188. Huynh, J.-R. & St Johnston, D. The Origin of Asymmetry: Early Polarisation of the

Drosophila Germline Cyst and Oocyte. *Curr. Biol.* **14,** R438–R449 (2004).

189. Yoshida, S. From cyst to tubule: innovations in vertebrate spermatogenesis. *Wiley Interdiscip. Rev. Dev. Biol.* **5,** 119–131 (2016).

190. Arnon, J., Meirow, D., Lewis-Roness, H. & Ornoy, A. Genetic and teratogenic effects of cancer treatments on gametes and embryos. *Hum. Reprod. Update* **7,** 394–403 (2001).

191. Meistrich, M. L. Effects of chemotherapy and radiotherapy on spermatogenesis in humans. *Fertil. Steril.* **100,** 1180–1186 (2013).

192. Oakberg, E. F. Sensitivity and Time of Degeneration of Spermatogenic Cells Irradiated in Various Stages of Maturation in the Mouse Sensitivity and Time of Degeneration of Spermatogenic Cells Irradiated in Various Stages of Maturation in the Mouse"'2. *Source Radiat. Res.* **2,** 369–391 (1955).

193. Gunes, S., Al-Sadaan, M. & Agarwal, A. Spermatogenesis, DNA damage and DNA repair mechanisms in male infertility. *Reprod. Biomed. Online* **31,** 309–319 (2015).

194. Yang, H. & Yamashita, Y. M. The regulated elimination of transit-amplifying cells preserves tissue homeostasis during protein starvation in Drosophila testis. *Development* **142,** 1756–66 (2015).

195. Fairchild, M. J., Smendziuk, C. M. & Tanentzapf, G. A somatic permeability barrier around the germline is essential for Drosophila spermatogenesis. *Development* **142,** 268–281 (2015).

196. Lim, J. G. Y. & Fuller, M. T. Somatic cell lineage is required for differentiation and not maintenance of germline stem cells in Drosophila testes. *Proc. Natl. Acad. Sci.* **109,** 18477–18481 (2012).

197. Madigan, J. P., Chotkowski, H. L. & Glaser, R. L. DNA double-strand break-induced

phosphorylation of Drosophila histone variant H2Av helps prevent radiation-induced apoptosis. *Nucleic Acids Res.* **30,** 3698–705 (2002).

198. Ulsh, B. A. CHECKING THE FOUNDATION: RECENT RADIOBIOLOGY AND THE LINEAR NO-THRESHOLD THEORY. *Health Phys.* **99,** 747–758 (2010).

199. McLean, P. F. & Cooley, L. Protein Equilibration Through Somatic Ring Canals in Drosophila. *Science (80-. ).* **340,** 1445–1447 (2013).

200. Igaki, T. *et al.* Evolution of mitochondrial cell death pathway: Proapoptotic role of HtrA2/Omi in Drosophila. *Biochem. Biophys. Res. Commun.* **356,** 993–997 (2007).

201. Khan, F. S. *et al.* The interaction of DIAP1 with dOmi/HtrA2 regulates cell death in Drosophila. *Cell Death Differ.* **15,** 1073–83 (2008).

202. Vande Walle, L., Lamkanfi, M. & Vandenabeele, P. The mitochondrial serine protease HtrA2/Omi: an overview. *Cell Death Differ.* **15,** 453–460 (2008).

203. Widlak, P. & Garrard, W. T. Discovery, regulation, and action of the major apoptotic nucleases DFF40/CAD and endonuclease G. *J. Cell. Biochem.* **94,** 1078–87 (2005).

204. Song, Y.-H. Drosophila melanogaster: a model for the study of DNA damage checkpoint response. *Mol. Cells* **19,** 167–79 (2005).

205. Ciccia, A. & Elledge, S. J. The DNA Damage Response: Making It Safe to Play with Knives. *Mol. Cell* **40,** 179–204 (2010).

206. Brodsky, M. H. *et al.* Drosophila melanogaster MNK/Chk2 and p53 regulate multiple DNA repair and apoptotic pathways following DNA damage. *Mol. Cell. Biol.* **24,** 1219–31 (2004).

207. Peters, M. *et al.* Chk2 regulates irradiation-induced, p53-mediated apoptosis in Drosophila. *Proc. Natl. Acad. Sci. U. S. A.* **99,** 11305–10 (2002).

208. Takada, S., Collins, E. R. & Kurahashi, K. The FHA domain determines Drosophila Chk2/Mnk localization to key mitotic structures and is essential for early embryonic DNA damage responses. *Mol. Biol. Cell* **26,** 1811–28 (2015).

209. Lettre, G. *et al.* Genome-wide RNAi identifies p53-dependent and -independent regulators of germ cell apoptosis in C. elegans. *Cell Death Differ.* **11,** 1198–1203 (2004).

210. Fritze, C. E., Verschueren, K., Strich, R. & Easton Esposito, R. Direct evidence for SIR2 modulation of chromatin structure in yeast rDNA. *EMBO J.* **16,** 6495–6509 (1997).

211. Li, C., Mueller, J. E. & Bryk, M. Sir2 represses endogenous polymerase II transcription units in the ribosomal DNA nontranscribed spacer. *Mol. Biol. Cell* **17,** 3848–59 (2006).

212. Michel, A. H., Kornmann, B., Dubrana, K. & Shore, D. Spontaneous rDNA copy number variation modulates Sir2 levels and epigenetic gene silencing. *Genes Dev.* **19,** 1199–1210 (2005).

213. Kobayashi, T. Regulation of ribosomal RNA gene copy number and its role in modulating genome integrity and evolutionary adaptability in yeast. *Cell. Mol. Life Sci.* **68,** 1395–1403 (2011).

214. Jack, C. V. *et al.* Regulation of ribosomal DNA amplification by the TOR pathway. *Proc. Natl. Acad. Sci.* **112,** 9674–9679 (2015).

215. MEHTA, I. S., FIGGITT, M., CLEMENTS, C. S., KILL, I. R. & BRIDGER, J. M. Alterations to Nuclear Architecture and Genome Behavior in Senescent Cells. *Ann. N. Y. Acad. Sci.* **1100,** 250–263 (2007).

216. Gibbons, J. G., Branco, A. T., Godinho, S. A., Yu, S. & Lemos, B. Concerted copy number variation balances ribosomal DNA dosage in human and mouse genomes. **112,** (2015).

217. Weider, L. J. *et al.* The Functional Significance of Ribosomal (r)DNA Variation: Impacts on the Evolutionary Ecology of Organisms. *Annu. Rev. Ecol. Evol. Syst.* **36,** 219–242 (2005).

218. Stults, D. M., Killen, M. W., Pierce, H. H. & Pierce, A. J. Genomic architecture and inheritance of human ribosomal RNA gene clusters. *Genome Res.* **18,** 13–8 (2008).

219. Ochs, R. L., Lischwe, M. A., Spohn, W. H. & Busch, H. Fibrillarin: a new protein of the nucleolus identified by autoimmune sera. *Biol. cell* **54,** 123–33 (1985).

220. Tollervey, D., Lehtonen, H., Jansen, R., Kern, H. & Hurt, E. C. Temperature-sensitive mutations demonstrate roles for yeast fibrillarin in pre-rRNA processing, pre-rRNA methylation, and ribosome assembly. *Cell* **72,** 443–57 (1993).

221. Rose, M. R. Genetics of increased lifespan in drosophila. *BioEssays* **11,** 132–135 (1989).

222. Partridge, L., Piper, M. D. W. & Mair, W. Dietary restriction in Drosophila. *Mech. Ageing Dev.* **126,** 938–950 (2005).

223. Linford, N. J., Bilgir, C., Ro, J. & Pletcher, S. D. Measurement of lifespan in Drosophila melanogaster. *J. Vis. Exp.* (2013). doi:10.3791/50068

224. Lohe, A. R., Hilliker, A. J. & Roberts, P. A. Mapping simple repeated DNA sequences in heterochromatin of Drosophila melanogaster. *Genetics* **134,** 1149–74 (1993).

225. Levesque, M. J., Ginart, P., Wei, Y. & Raj, A. Visualizing SNVs to quantify allele-specific expression in single cells. *Nat. Methods* **10,** 865–7 (2013).

226. Waggener, J. M. & DiMario, P. J. Two Splice Variants of Nopp140 in Drosophila melanogaster. *Mol. Biol. Cell* **13,** 362–381 (2002).

227. Jakubczak, J. L., Xiong, Y. & Eickbush, T. H. Type I (R1) and type II (R2) ribosomal DNA insertions of Drosophila melanogaster are retrotransposable elements closely related

to those of Bombyx mori. *J. Mol. Biol.* **212,** 37–52 (1990).

228. Dawid, I. B. & Rebbert, M. L. Nucleotide sequences at the boundaries between gene and insertion regions in the rDNA of Drosophilia melanogaster. *Nucleic Acids Res.* **9,** 5011–20 (1981).

229. Roiha, H. & Glover, D. M. Chracterisation of complete type II insertions in cloned segments of ribosomal DNA from Drosophila melanogaster. *J. Mol. Biol.* **140,** 341–55 (1980).

230. Wellauer, P. K., Dawid, I. B. & Tartof, K. D. X and Y chromosomal ribosomal DNA of Drosophila: comparison of spacers and insertions. *Cell* **14,** 269–78 (1978).

231. Tartof, K. D. & Dawid, I. G. Similarities and differences in the structure of X and Y chromosome rRNA genes of Drosophila. *Nature* **263,** 27–30 (1976).

232. Pérez-González, C. E., Burke, W. D. & Eickbush, T. H. R1 and R2 retrotransposition and deletion in the rDNA loci on the X and Y chromosomes of Drosophila melanogaster. *Genetics* **165,** 675–85 (2003).

233. Chehrehasa, F., Meedeniya, A. C. B., Dwyer, P., Abrahamsen, G. & Mackay-Sim, A. EdU, a new thymidine analogue for labelling proliferating cells in the nervous system. *J. Neurosci. Methods* **177,** 122–130 (2009).

234. Salic, A. & Mitchison, T. J. A chemical method for fast and sensitive detection of DNA synthesis in vivo. *Proc. Natl. Acad. Sci. U. S. A.* **105,** 2415–20 (2008).

235. LIMA-DE-FARIA, A. & JAWORSKA, H. Late DNA Synthesis in Heterochromatin. *Nature* **217,** 138–142 (1968).

236. Berger, C., Horlebein, A., Gögel, E. & Grummt, F. Temporal order of replication of mouse ribosomal RNA genes during the cell cycle. *Chromosoma* **106,** 479–84 (1997).

237. Dimitrova, D. S. DNA replication initiation patterns and spatial dynamics of the human ribosomal RNA gene loci. *J. Cell Sci.* **124,** 2743–2752 (2011).

238. Eickbush, T. H. & Eickbush, D. G. Integration, Regulation, and Long-Term Stability of R2 Retrotransposons. *Microbiol. Spectr.* **3,** (2015).

239. McKee, B. D. & Karpen, G. H. Drosophila ribosomal RNA genes function as an X-Y pairing site during male meiosis. *Cell* **61,** 61–72 (1990).

240. Ren, X., Eisenhour, L., Hong, C., Lee, Y. & McKee, B. D. Roles of rDNA spacer and transcription unit-sequences in X-Y meiotic chromosome pairing in Drosophila melanogaster males. *Chromosoma* **106,** 29–36 (1997).

241. Helmrich, A., Ballarino, M., Nudler, E. & Tora, L. Transcription-replication encounters, consequences and genomic instability. *Nat. Struct. Mol. Biol.* **20,** 412–418 (2013).

242. Labib, K. & Hodgson, B. Replication fork barriers: pausing for a break or stalling for time? *EMBO Rep.* **8,** 346–53 (2007).

243. Linskens, M. H. & Huberman, J. A. Organization of replication of ribosomal DNA in Saccharomyces cerevisiae. *Mol. Cell. Biol.* **8,** 4927–35 (1988).

244. Larson, K. *et al.* Heterochromatin Formation Promotes Longevity and Represses Ribosomal RNA Synthesis. *PLoS Genet.* **8,** e1002473 (2012).

245. Tsurumi, A. & Li, W. Global heterochromatin loss. *Epigenetics* **7,** 680–688 (2012).

246. Swanson, E. C., Manning, B., Zhang, H. & Lawrence, J. B. Higher-order unfolding of satellite heterochromatin is a consistent and early event in cell senescence. *J. Cell Biol.* **203,** 929–42 (2013).

247. Boncinelli, E., Graziani, F., Polito, L., Malva, C. & Ritossa, F. rDNA magnification at the bobbed locus of the Y chromosome in Drosophila melanogaster. *Cell Differ.* **1,** 133–42

(1972).

248. Henderson, A. & Ritossa, F. On the inheritance of rDNA of magnified bobbed loci in D. melanogaster. *Genetics* **66,** 463–73 (1970).

249. Tartof, K. D. Unequal mitotic sister chromatin exchange as the mechanism of ribosomal RNA gene magnification. *Proc. Natl. Acad. Sci. U. S. A.* **71,** 1272–6 (1974).

250. Johzuka, K. & Horiuchi, T. Replication fork block protein, Fob1, acts as an rDNA region specific recombinator in S. cerevisiae. *Genes Cells* **7,** 99–113 (2002).

251. Yadlapalli, S. & Yamashita, Y. M. Chromosome-specific nonrandom sister chromatid segregation during stem-cell division. *Nature* **498,** 251–4 (2013).

252. Durkin, S. G. & Glover, T. W. Chromosome Fragile Sites. *Annu. Rev. Genet.* **41,** 169–192 (2007).

253. Flach, J. *et al.* Replication stress is a potent driver of functional decline in ageing haematopoietic stem cells. *Nature* **512,** 198–202 (2014).

254. Telonis-Scott, M., Kopp, A., Wayne, M. L., Nuzhdin, S. V. & McIntyre, L. M. Sex-Specific Splicing in Drosophila: Widespread Occurrence, Tissue Specificity and Evolutionary Conservation. *Genetics* **181,** 421–434 (2008).

255. Petrella, L. N., Smith-Leiker, T. & Cooley, L. The Ovhts polyprotein is cleaved to produce fusome and ring canal proteins required for Drosophila oogenesis. *Development* **134,** 703–712 (2007).

256. Wang, S. *et al.* Drosophila adducin regulates Dlg phosphorylation and targeting of Dlg to the synapse and epithelial membrane. *Dev. Biol.* **357,** 392–403 (2011).

257. Vinayagam, A. *et al.* An Integrative Analysis of the InR/PI3K/Akt Network Identifies the Dynamic Response to Insulin Signaling. *Cell Rep.* **16,** 3062–3074 (2016).

258. Venkei, Z. G. & Yamashita, Y. M. The centrosome orientation checkpoint is germline stem cell specific and operates prior to the spindle assembly checkpoint in Drosophila testis. *Development* **142,** (2014).

259. Patterson, G. H. & Lippincott-Schwartz, J. A Photoactivatable GFP for Selective Photolabeling of Proteins and Cells. *Science (80-. ).* **297,** (2002).

260. Wilson, P. G. Centrosome inheritance in the male germ line of Drosophila requires hu-li tai-shao function. *Cell Biol. Int.* **29,** 360–369 (2005).

261. Guarente, L., Imai, S., Armstrong, C. M. & Kaeberlein, M. Transcriptional silencing and longevity protein Sir2 is an NAD-dependenthistone deacetylase. *Nature* **403,** 795–800 (2000).

262. Boyle, M., Wong, C., Rocha, M. & Jones, D. L. Decline in self-renewal factors contributes to aging of the stem cell niche in the Drosophila testis. *Cell Stem Cell* **1,** 470–8 (2007).

263. Toledano, H., D'Alterio, C., Czech, B., Levine, E. & Jones, D. L. The let-7-Imp axis regulates ageing of the Drosophila testis stem-cell niche. *Nature* **485,** 605–10 (2012).

264. Jones, D. L. & Rando, T. A. Emerging models and paradigms for stem cell ageing. *Nat. Cell Biol.* **13,** 506–12 (2011).

265. Richardson, S. M. *et al.* Design of a synthetic yeast genome. *Science (80-. ).* **355,** 1040–1044 (2017).

266. Britten, R. J. & Kohne, D. E. Repeated Sequences in DNA. *Science (80-. ).* **161,** (1968).

267. Hartl, D. L. Molecular melodies in high and low C. *Nat. Rev. Genet.* **1,** 145–149 (2000).

268. Schmid, C. W. & Deininger, P. L. Sequence organization of the human genome. *Cell* **6,** 345–58 (1975).

269. de Koning, A. P. J., Gu, W., Castoe, T. A., Batzer, M. A. & Pollock, D. D. Repetitive Elements May Comprise Over Two-Thirds of the Human Genome. *PLoS Genet.* **7,** e1002384 (2011).

270. Sakaki, Y. *et al.* The DNA sequence of human chromosome 21. *Nature* **405,** 311–319 (2000).

271. Bosco, G., Campbell, P., Leiva-Neto, J. T. & Markow, T. A. Analysis of Drosophila Species Genome Size and Satellite DNA Content Reveals Significant Differences Among Strains as Well as Between Species. *Genetics* **177,** (2007).

272. He, B. *et al.* Mapping the pericentric heterochromatin by comparative genomic hybridization analysis and chromosome deletions in Drosophila melanogaster. *Genome Res.* **22,** 2507–2519 (2012).

273. Saka, K., Ide, S., Ganley, A. R. D. & Kobayashi, T. Cellular Senescence in Yeast Is Regulated by rDNA Noncoding Transcription. *Curr. Biol.* **23,** 1794–1798 (2013).

274. Santoro, R., Schmitz, K.-M., Sandoval, J. & Grummt, I. Intergenic transcripts originating from a subclass of ribosomal DNA repeats silence ribosomal RNA genes in trans. *EMBO Rep.* **11,** 52–58 (2010).

275. Schmitz, K.-M., Mayer, C., Postepska, A. & Grummt, I. Interaction of noncoding RNA with the rDNA promoter mediates recruitment of DNMT3b and silencing of rRNA genes. *Genes Dev.* **24,** 2264–9 (2010).

276. Shiao, Y.-H. *et al.* An Intergenic Non-Coding rRNA Correlated with Expression of the rRNA and Frequency of an rRNA Single Nucleotide Polymorphism in Lung Cancer Cells. *PLoS One* **4,** e7505 (2009).